SEMI-ANNUAL and Final REPORT

NASA CONTRACT NAS 5-31368

For
MODIS Team Member: Steven W. Running
Assoc. Team Member: Ramakrishna R. Nemani

15 July 2004

WORK ACCOMPLISHED

In the past half-year, we have finished following objects for our contract:

- Deliver the new version software for our MOD15 Leaf Area Index and Fraction Absorbed Photosynthetically Active Radiation, and our MOD17 terrestrial gross and net primary product.

- Generated and delivered 684GB of the improved MOD17 data set at our FTP site.

- Cutout 7 by 7 subset of MODIS data for validation work at flux tower network.

- Validate MOD15 LAI and MOD17 GPP at flux sites.

- Test the accuracy of meteorological data sets to MOD17 and its impact on MOD17.

- Develop MODIS applications products for natural resource management.

- Develop Surface Observation Gridded System (SOGS) for generation of higher spatial resolution daily meteorological data set. The data set can greatly enhance the accuracy of terrestrial variables estimated by ecosystem models at local and regional scale.

The NTSG lab currently employs:
Dr. Steven Running, Director and Professor,
Dr. Ramakrishina Nemani, Assist Director and Research Professor
Dr. John Kimball, Postdoctoral Research Associate
Dr. Faith Ann Heinsch, Postdoctoral Research Associate
Dr. Qiaozhen Mu, Postdoctoral Research Associate
Dr. Maosheng Zhao, Postdoctoral Research Associate
Mr. Andrew Neuschwander, Programmer/Sys Admin
Mr. Joshua Compbell, Assistant programmer

Mr. Saxon Holbrook, Computer Systems Engineer
Mr. Matt Reeves, PhD student
Mr. W. Matt Jolly, PhD student
Ms. Pat Andrews, PhD student
Ms. Rachel Loehman, PhD student
Ms. Alana Oakins, Research Assistant
Ms. Youngee Cho, Office Manager

All of these members contribute to certain aspects of our MODIS work.

ACTIVITIES of Steven W. Running, Principal Investigator

Along with the normal array of conference presentations, I am working on two NRC committee reports concerning the evolution of EOS science in the future NPOESS environment. These reports will be out in 2004. I also spent a lot of time writing text for the North American Carbon Program Science Implementation Strategy. This draft document has not yet been finalized and publicly released.

I published a major overview paper for Bioscience on the MODIS Gross Primary Production/Net Primary Production dataset.

Running S. W., R. R. Nemani1, F. A. Heinsch, M. Zhao, M. Reeves, H. Hashimoto. (2004). A continuous Satellite-derived measure of global terrestrial primary productivity: Future science and applications. *Bioscience*. 56(6): 547-560.

Jolly W. M., Graham J. M., A. Michaelis, R. R. Nemani and S. W. Running. (2004) A flexible integrated system for generating meteorological surface derived from point source across multiple geographic scales. *Environmental modeling & Softwrae*. (in press)

Jolly W. M., R. R. Nemani and S. W. Running. (2004) Enhancement of understory productivity by asynchronous phenology with overstory competitors in a temperature deciduous forest. *Tree Physiology*. 24:1069-1071.

Jolly W. M., R. R. Nemani and S. W. Running. (2004) Effects of precipitation and soil water potential on drought deciduous phonology in the Kalahari. *Global Change Biology*. 10(3):303-308.

Other Research Activity, Invited Conference Attendance:

MODIS Science Team meeting, Washington DC, July 2004
The State of the Nation's Ecosystems project – The Heinz Center, Woods Hole, MA, June 2004
US Interagency Working Group on Earth Observations (IWGEO) Experts Meeting, June 2004
Mountain Climate Science Symposium Meeting, Reno, NV, May 2004
Carbon Cycle Science Steering Group Meeting, Washington DC, May 2004
International Conference on Modeling Forest Production, Vienna, Austria, April 2004
Integrated Regional Studies for Global Sustainability, Auburn, AL, March 2004
19^{th} IGBP-SC Meeting, Moscow, Russia, February 2004
Ecosystem Interagency Working Group CCSP/Ecosystem Workshop, Silver Spring, MD, February 2004
Carbon Data Assimilation Modeling (CDMA)/ACME Joint Project meeting, Boulder, CO, February 2004
Big Sky Institute – Community Education Programs, Bozeman, MT, January 2004
Symposium at Society for Range Management, Salt Lake City, UT, January 2004

ACTIVITIES OF R. Nemani (MODIS Associate Team Member)

MODIS Net primary production (MOD17)

I presented the results from our Science paper to a panel of experts at the United Nations Environmental Program/Global Environmental Outlook 2003 in Paris, France. As a result, GEO Year Book 2003 includes a highlight on the "apparent greening of the biosphere". In February 2004, When U.N formally released the GEO document in Seoul, Korea, it highlighted the fact that world is getting greener for a variety of reasons including changes in climate. http://www.unep.org/geo/yearbook/box7a.htm

The US Global Change Research Program also highlighted our study in their "changing planet" 2004-2005 summarizing recent knowledge and future plans for climate change research in the United States. http://www.usgcrp.gov/usgcrp/ProgramElements/recent/carbonrecent.htm

Our study was also chosen as a Hot New Paper to highlight in ISI/Essential Science Indicators. Our paper ranked among the top 10 for citations in the last two years in the field of geosciences. http://www.esi-topics.com/nhp/2004/september-04-RamakrishnaNemani.html

NASA chose to highlight our study in their annual accomplishments for 2003 as part of their report to Congress.

A brief summary of the paper along with a figure that appeared in a number of publications is given below.

Climate-Driven Increases in Global Terrestrial Net Primary Production from 1982 to 1999.
Ramakrishna R. Nemani, Charles D. Keeling, Hirofumi Hashimoto, William M. Jolly, Stephen C. Piper, Compton J. Tucker, Ranga B. Myneni, Steven W. Running. Science, 300, 1560, 2003 (June 6th)

Recent climatic changes have enhanced plant growth in northern mid-latitudes and high latitudes. However, a comprehensive analysis of the impact of global climatic changes on vegetation productivity has not before been expressed in the context of variable limiting factors to plant growth. We present a global investigation of vegetation responses to climatic changes by analyzing 18 years (1982 to 1999) of both climatic data and satellite observations of vegetation activity. Our results indicate that global changes in climate have eased several critical climatic constraints to plant growth, such that net primary production increased 6% (3.4 petagrams of carbon over 18 years) globally. The largest increase was in tropical ecosystems. Amazon rain forests accounted for 42% of the global increase in net primary production, owing mainly to decreased cloud cover and the resulting increase in solar radiation.

Fig 1: Spatial distribution of changes in NPP between 1982 and 1999.

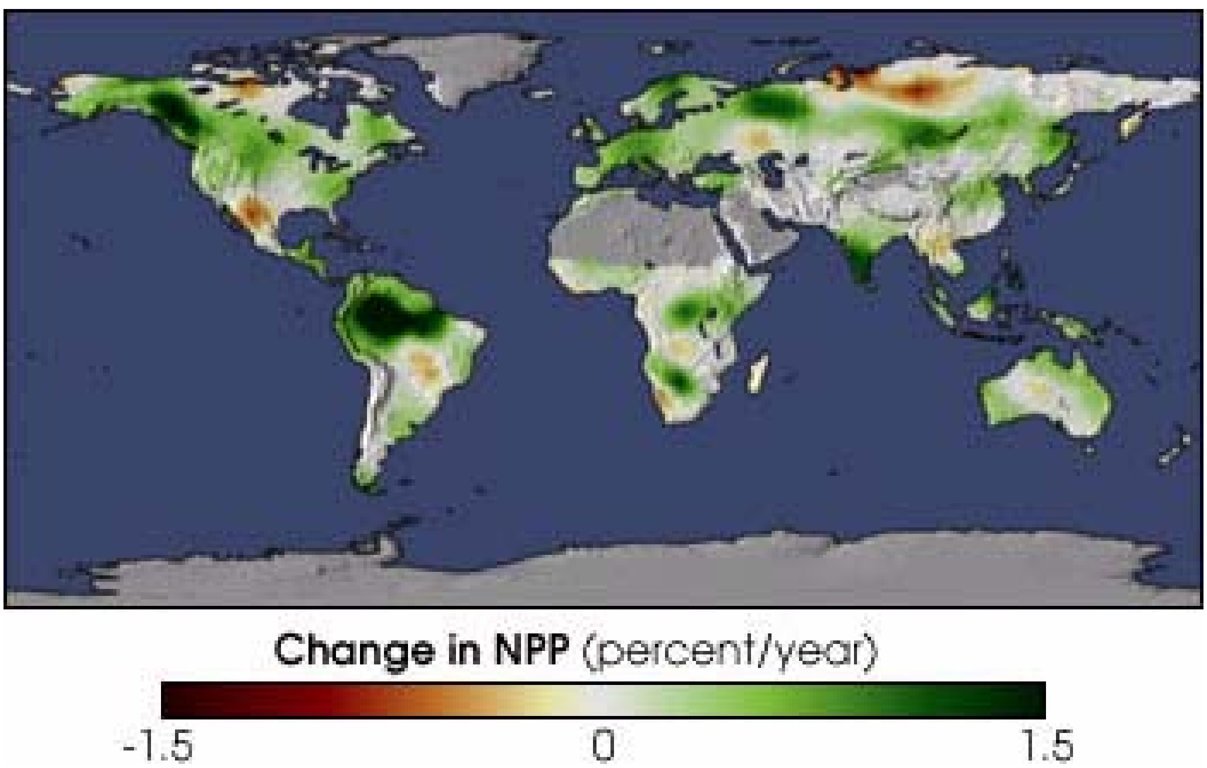

Outreach Activities:

PRESS

- **Global Garden Grows Greener**

  - **TV**
    - CNN
    - KBCITV (Idaho-USA)
    - BBC
    - The Weather Channel
    - KECI (Missoula, MT)

  - **Radio**
    - BBC
    - NPR
    - KUHF Radio (Houston Public Radio, Texas)
    - VOA--Enviornment Report (Download MP3)

  - **News Agencies**
    - Eureka Alert
    - Bloomberg

  - **News Papers**
    - Folha de S. Paulo (Brazil)
    - O Globo Online (Brazil)
    - Globe and Mail (Canada)
    - Le Figaro (France)
    - Berliner Morgenpost (Germany)
    - Bietigheimer Zeitung (Germany)
    - Die Stimme (Germany)
    - Fraenkischer Tag (Germany)
    - Frankfurter Rundschau (Germany)
    - Leipziger Volkszeitung (Germany)
    - Nuertinger Zeitung (Germany)
    - Oberhessische Presse (Germany)
    - Offenbach Post (Germany)
    - Osnabruecker Zeitung (Germany)
    - The Daily Telegrams (India)
    - Indian Express (India)
    - Corriere Della Sera (Italy)
    - Il Giornale Ideale - Scienze (Italy)
    - Lithuanian-American Weekly (Lithuania)
    - De Telegraaf (Netherlands)

- Pravda (Russia)
- Basler Zeitung (Switzerland)
- Daily Telegraph (UK)
- Financial Times (UK)
- The Independent (UK)
- Mirror (UK)
- Baltimore Sun (USA)
- Billings Gazette (USA)
- Christian Science Monitor (USA)
- Montana Tracker News (USA)
- The Missoulian (USA)
- The Arizona Republic (USA)

- **Magazines**

  - Science Magazine
  - Die Spiegel (Germany)
  - Newsweek International

- **Front Pages**

  - CNN Science & Space
  - Google News
  - NASA
  - NASA ESE
  - NASA GSFC Earth Sciences Directorate

- **Web Stories**

  - Amazon Daily
  - BBS News
  - Bright Surf
  - Center for the Study of Carbon Dioxide and Global Change
  - Environment News Service
  - Environmental Data Interactive Exchange
  - Environment News Network
  - Goddard Space Flight Center
  - MSNBC News
  - National Geographic News
  - Globalwarming.org
  - NASA News
  - NASA GSFC Top Story
  - NASA GSFC Earth Sciences Directorate
  - NASA Earth Observatory (News)
  - NASA Earth Observatory (Features)
  - OregonLive.com

- Physlink
- Research at Boston University
- Space.com
- Space Daily
- Space Ref
- Science Daily
- Sci-Fi Today
- Techno Scan
- The Week That Was
- Frizz (Brazil)
- Monologo Virtual (Brazil)
- Campbell River's News Online (Canada)
- Canada.com (Canada)
- Capital University of Medical Sciences(China)
- Novinky (Czech Republic)
- Uno EE (Estonia)
- Baden24 (Germany)
- Die Presse (Germany)
- Die Stimme (Germany)
- Markt-Lippe (Germany)
- Yahoo Deutschland Nachrichten (Germany)
- Solar Contact (Germany)
- Innovations Report (Germany)
- VDI Nachrichten dot com (Germany)
- Physics 4 U (Greece)
- Gradpula (Hungary)
- Iskon Online(Hungary)
- Deepika Global (India)
- Focus.it (Italy)
- Fresh Eye (Japan)
- Forum Fok (Netherlands)
- NietNormaal (Netherlands)
- Gazeta (Poland)
- Noticias Del Espacio (Spain)
- 20min.com (Switzerland)
- Vietnam Web Site (Vietnam)
- Sarajevo-x dot com (Yugoslavia)

- **Internet Chat on This Story**

- Forseti
- Dobermann
- Nature.Net

MEETINGS ATTENDED

United Nations Environmental Program/Global Environmental Outlook, Paris 10/03
U.S. Arctic Commission, Seatle, 11/03
American Geophysical Union, SFO, 12/03
Intelligent Data Understanding, Dana Point. 2/04
ORNL User Advisory Group, Fort Collins, 5/04
U.S. Arctic Commission, MBL, 5/04
U.S-India Cooperation in High Technology, space and Science, Bangalore, 6/04
EOS/MODIS, Washington, D.C, 7/04
MODIS VEG II, Missoula, MT 8/04
MODIS LAI meeting Missoula, MT, 8/04
NACP meeting Missoula, MT, 8/04
AIAA San Diego, 9/04

PUBLICATIONS:

Hashimoto, H. R. Nemani, M. White, W. Jolly, S.C. Piper, C.D. Keeling, R. Myneni and S.W. Running. ENSO induced variability in terrestrial carbon cycling. Journal of Geophysical Research-Atmospheres (in press).

Jolly, M., R Nemani and S. Running. 2004. Enhancement of understory productivity by asynchronous phenology with overstory competitors in a temperate deciduous forest, Tree Physiology, 24: 1069-1071.

Jolly, M., J.M. Graham, A. Michaelis, R.R. Nemani, S.W. Running. 2004. A flexible,integrated system for generating meteorological surfaces derived from point sources across multiple geographic scales. Environmental Modeling and Software (in press).

Elvidge, C.D, C. Milesi, J. Dietz, B. Tuttle, P.C. Sutton, R. Nemani and J.E. Vogelmann. U.S. constructed area approaches the size of Ohio. EOS Transactions, 85(24): 233-240.

Running et al., Nemani, R. R., Heinsch, F. A., Zhao, M., Reeves, M., Jolly, M. (2004). A continuous Satellite-derived measure of global terrestrial primary productivity. *Bioscience*, 54(6): 547-560.

White, M.A. and R. R. Nemani. 2004. Soil water forecasting in the continental U.S., Canadian J. Remote Sensing, 30(5): 1-14.

ACTIVITIES OF Faith Ann Heinsch (Postdoctoral Researcher)

Summary:

It is important to determine the accuracy of the MOD17A2 (GPP) algorithm at the local scale as well as the global scale. Therefore, we are collaborating with AmeriFlux researchers at fifteen sites throughout the USA and Canada (http://public.ornl.gov/ameriflux/Participants/Sites/Map/index.cfm) covering a wide range of climate and biome types. Researchers have provided us with 36 site-years of eddy covariance flux tower-based gross primary production (GPP) estimates and meteorological data for 2000-2003. Comparisons are then made with the 8-day and annual GPP calculated using an off-line version of the MODIS algorithm (Version 4.5) in combination with Collection 3 MOD12Q1 (Land Cover), Collection 4 MOD15A2 (LAI/FPAR), and DAO meteorological data (GEOS402). This version of the MOD17A2 algorithm contains a revised Biome-Properties Look-Up Table (BPLUT) that provides reasonable estimates of GPP at the global scale. Use of the standard DAO meteorology with the GPP algorithm indicates that the algorithm tends to overestimate GPP over a 7 x 7 km grid surrounding each tower site by a relative error of 19% (Figure 1a, r^2 = 0.65). Use of tower meteorology with the MOD17A2 algorithm removes the bias of the GPP algorithm (relative error = -2%), but increases the spread of the results (Figure 1b, r^2 = 0.57). it is difficult to attribute error solely to the MODIS Product, however, as flux towers tend to underestimate GPP by 10-20% or more. The analysis indicates that much of the error that can be associated with the algorithm comes from the use of coarse resolution meteorological data (27% ±45%). We hypothesize that this is largely due to discrepancies in the vapor pressure deficit (VPD) as shown for a wet site at Niwot Ridge ,CO (Figure 2a) and a dry site at Tonzi Ranch, CA (Figure 2b). The DAO input data consistently underestimate actual VPD in drier regions, resulting in the overestimation of GPP in these areas. Additional error is associated with MOD15A2 LAI/FPAR inputs, resulting primarily from cloud contamination. This issue is been currently resolved by using the most rigorous possible quality control of the MOD15A2 data, and filling missing periods via linear interpolation. Unfortunately, in cloudy areas, these missing periods can be substantial. In addition, the LAI/FPAR from MODIS tends to overestimate site LAI (Figure 3), although many of the estimates are within the specification of the algorithm (±0.5 m^2 m^{-2}). Land cover classification does not appear to have a significant impact on site estimates of GPP at this time. Future research will focus on several intensive site-specific evaluations of all inputs into the algorithm to better elucidate reasons for discrepancies between tower and MODIS GPP estimates.

Conference Presentations (since last report):

IBFRA 12th Annual Scientific Conference, Fairbanks, AK 3 – 6 May 2004.Heinsch, FA, JS Kimball, M Zhao and SW Running. "Verification of Satellite Gross and Net Primary Production Estimates at Several Boreal Sites"

ChEAS Annual Meeting, Minoqua, WI 23 – 25 July 2004. Heinsch, FA, JS Kimball, M Zhao, SW and Running. "Update on MODIS and BIOME-BGC results for ChEAS"

MODIS Vegetation Workshop II 17 – 19 August 2004. Zhao, M, FA Heinsch, and S.W. Running. "Improvements and Uncertainties of the Global Terrestrial Primary Productivity Dataset (MOD17)

AmeriFlux Science Meeting, Boulder, CO 5 – 7 October 2004. Heinsch, FA, M Zhao, SW Running, and JS Kimball. "Modification and Validation of the MODIS GPP and NPP Products"

Publications:

Heinsch, F.A. et al., Submitted. Evaluation of remote sensing based terrestrial productivity from MODIS using regional tower eddy flux network observations. IEEE Transactions on Geoscience and Remote Sensing.

Figures:

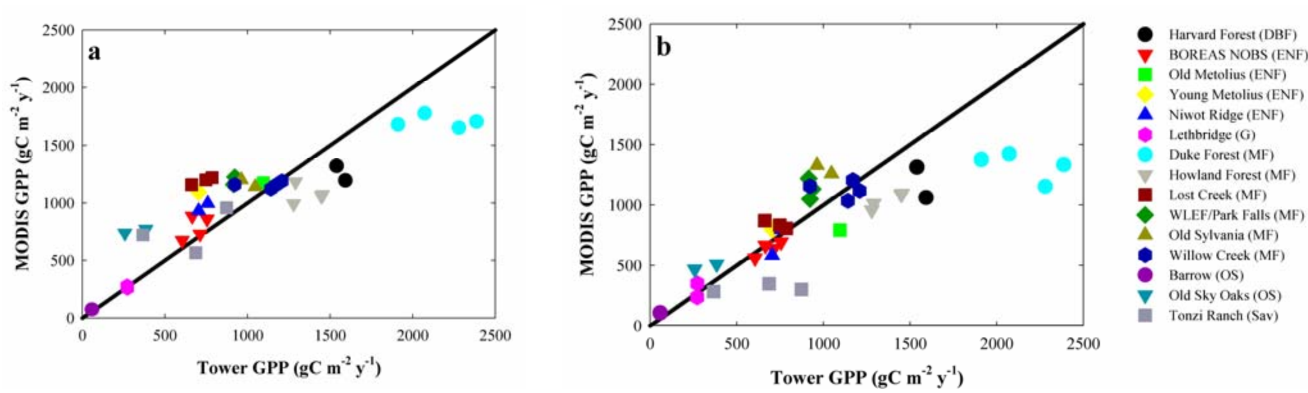

Figure 1. Comparison of MODIS GPP estimates from the MOD17A2 algorithm with flux tower estimates of GPP using the official MOD15A2 (Collection 4) algorithm with (a) DAO (GEOS402) and (b) tower-specific meteorology inputs.

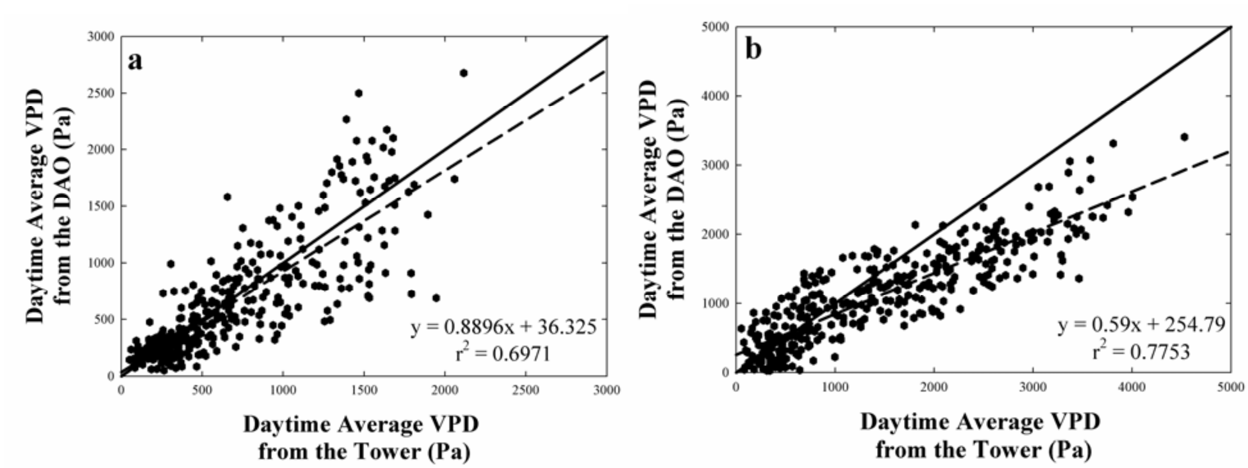

Figure 2. Comparison of the vapor pressure deficit (VPD) measured at the tower site and that estimated by the global DAO meteorology for 2002. Sites with both (a) low daytime average VPD and (b) high daytime average VPD are shown.

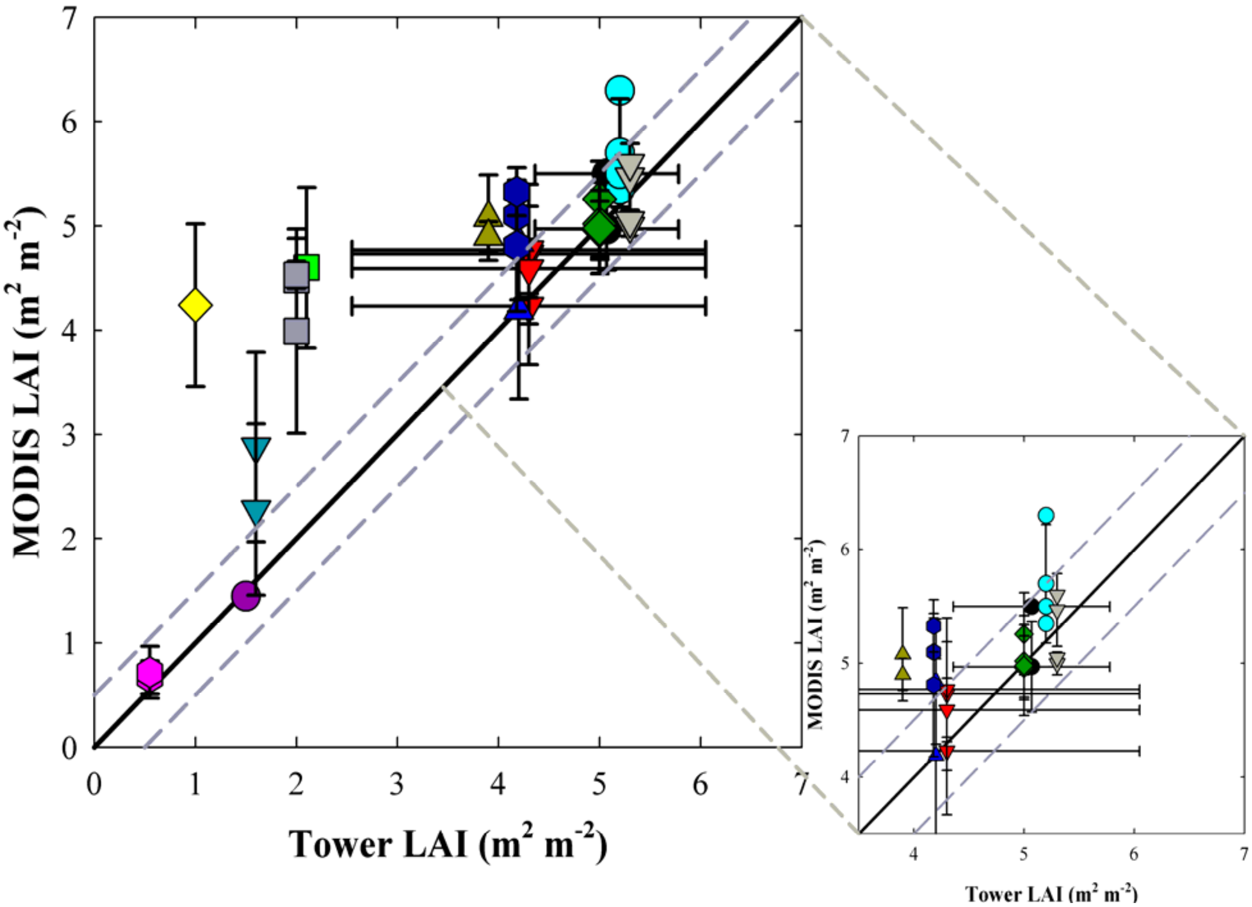

Figure 3. The average maximum leaf area index (LAI) estimated for the tower pixel from the MOD15 algorithm (Collection 4) as compared with site-specific measurements of LAI.

ACTIVITIES OF Maosheng Zhao (Postdoctoral Researcher)

1. Improve MOD17 products for collection5

MODIS primary production products (MOD17) are the first regular, near-real-time data sets for repeated monitoring of vegetation primary production on vegetated land at 1-km resolution at an 8-day interval. But both the inconsistent spatial resolution between the gridded meteorological data and MODIS pixels, and the cloud-contaminated MODIS FPAR/LAI (MOD15A2) retrievals can introduce considerable errors to Collection4 primary production (denoted as C4 MOD17) results. Here, we aim to rectify these problems through reprocessing key inputs to MODIS primary vegetation productivity algorithm, resulting in improved Collection5 MOD17 (here denoted as C5 MOD17) estimates.

This was accomplished by spatial interpolation of the coarse resolution meteorological data input and with temporal filling of cloud-contaminated MOD15A2 data. Furthermore, we modified the Biome Parameter Look-Up Table (BPLUT) based on recent synthesized NPP data and some observed GPP derived from some flux tower measurements to keep up with the improvements in upstream inputs. Because MOD17 is one of the down-stream MODIS land products, the performance of the algorithm can be largely influenced by the uncertainties from upstream inputs, such as land cover, FPAR/LAI, the meteorological data, and algorithm itself. MODIS GPP fits well with GPP derived from 12 flux towers over North America.

Globally, the 3-year MOD17 NPP is comparable to the Ecosystem Model-Data Intercomparison (EMDI) NPP data set, and global total MODIS GPP and NPP are inversely related to the observed atmospheric CO_2 growth rates, and MEI index, indicating MOD17 are reliable products. From 2001 to 2003, mean global GPP and NPP estimated by MODIS are 109.29 PgC/y and 56.02 PgC/y, respectively. Based on this research, the improved global MODIS primary production data set is now ready for monitoring ecological conditions, natural resources and environmental changes.

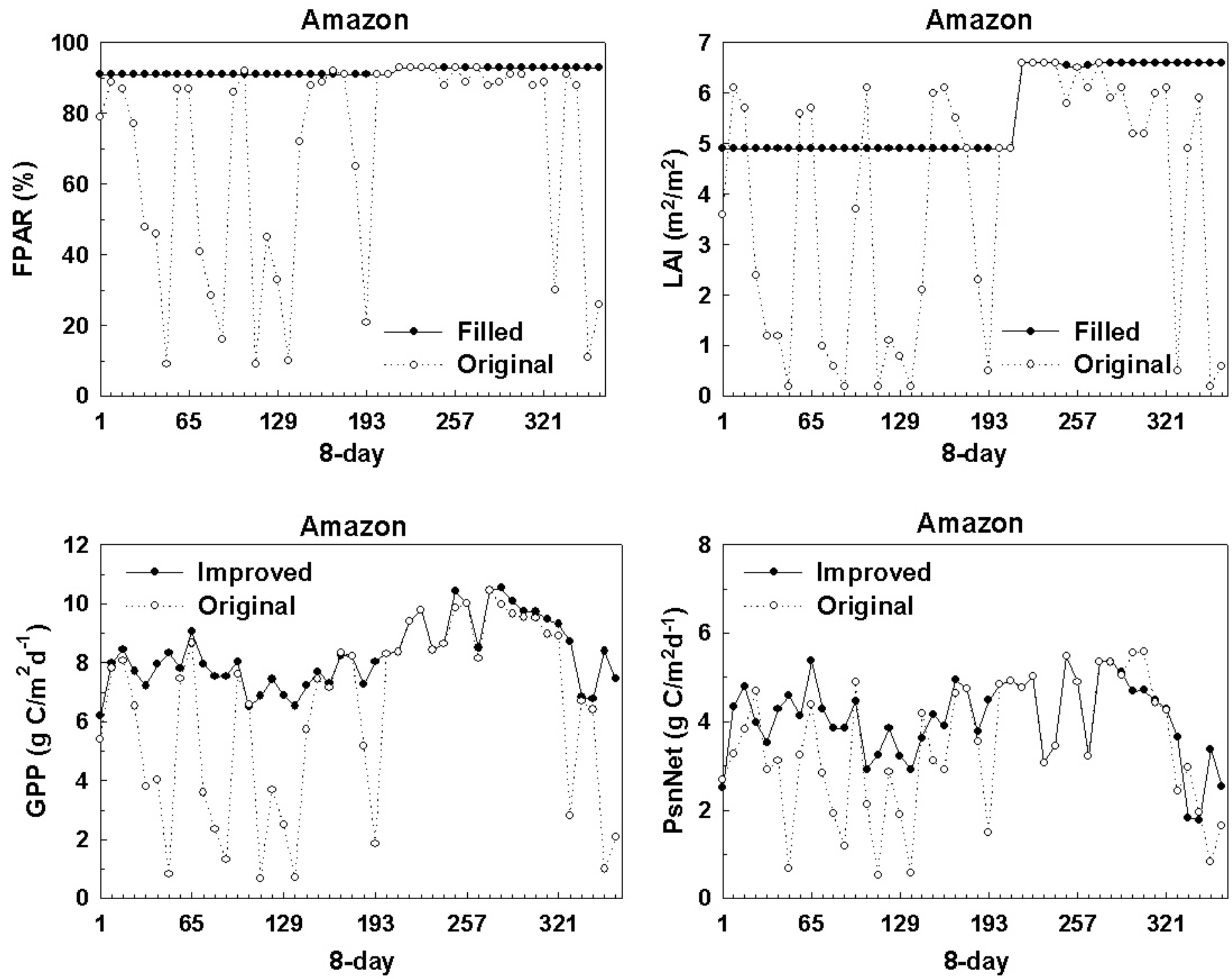

Figure 1. An example on how temporal filling cloud-contaminated 8-day FPAR and LAI, and thereafter improved 8-day GPP and PsnNet for one MODIS 1-km pixel located in Amazon (AMZN) basin (lat = -5.0, lon= -65.0). MODIS land cover for AMZN is evergreen broadleaf forest (EBF). In 2002, the improved annual GPP and NPP are 2759 g C/m2y-1 and 914 g C/m2y-1, respectively, in comparison to corresponding original annual GPP and NPP of 2252 g C/m2y-1 and 871 g C/m2y-1.

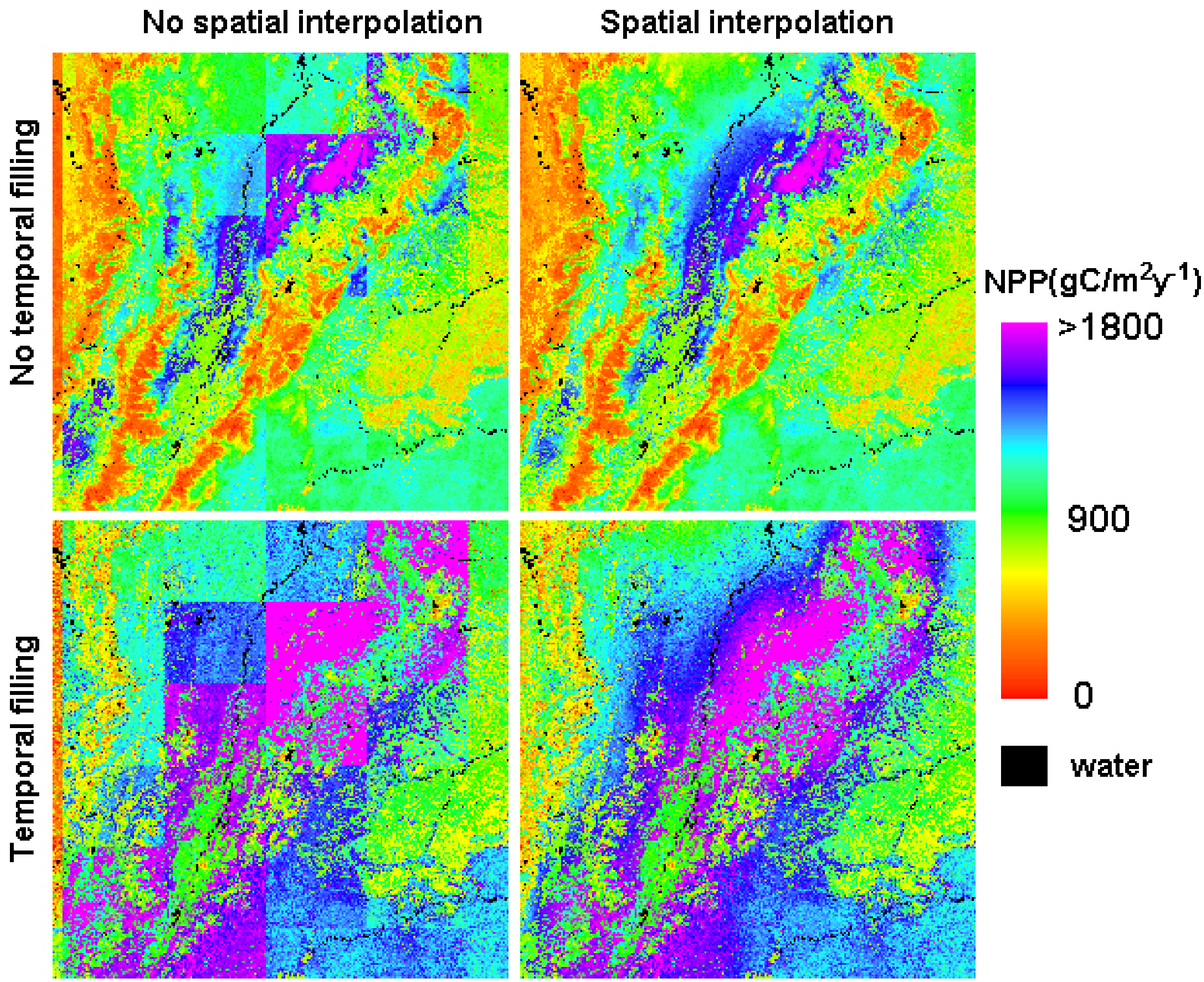

Figure 2. An example of the influence of spatial interpolation/non-interpolation, and temporal filling/non-filling MOD15A2 on MODIS NPP. The region is part of MODIS 10-degree tile H10V08 located near the Amazon basin and has been reprojected to geographical projection. The dominant MODIS land cover for the region is evergreen broadleaf forest and woody savannas.

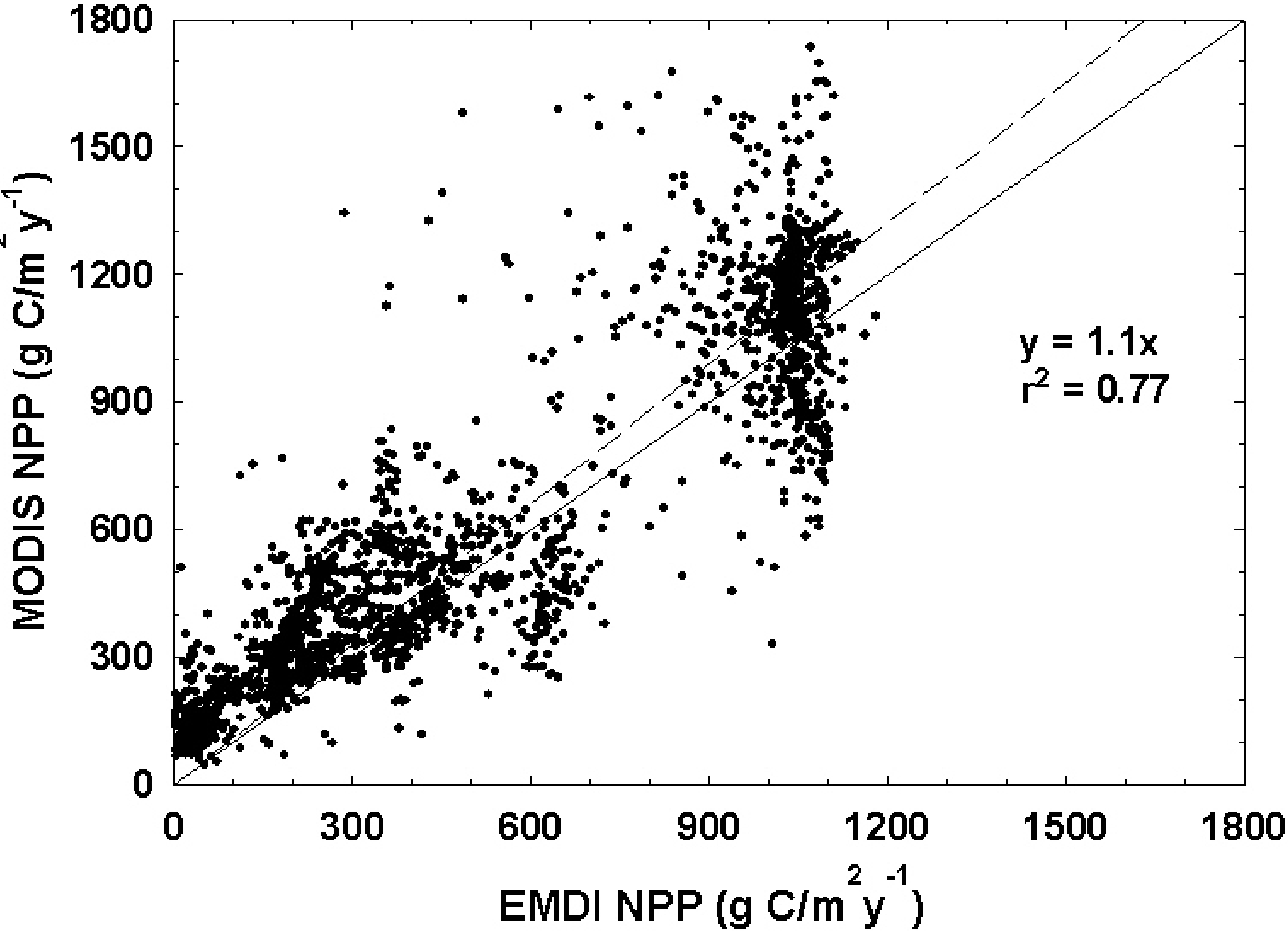

Figure 3. Validation of MODIS mean annual NPP with the Ecosystem Model-Data Intercomparison (EMDI) NPP data set.

2. Study the accuracy of meteorological data sets and its Impact on MOD17 products

The near real-time MOD17 requires regularly daily gridded assimilation meteorological data set as input, and the accuracy of the existing meteorological data sets show marked difference spatially and temporally. This study compares the three main assimilation and reanalysis global surface meteorological data sets – Data Assimilation Office (DAO) GEOS402, ECMWF 40 (ERA-40), NCEP-NCAR reanalysis 1(NCEP) with, the data from Climate Research Unit of University of East Anglia (CRU) and NASA Surface meteorology and Solar Energy (SSE) for vegetated land area – to assess the sensitivity of MODIS global terrestrial primary production to the uncertainties of meteorological inputs.

Compared with SSE and CRU, NCEP tends to overestimate surface solar radiation, underestimate temperature and Vapor Pressure Deficit (VPD), and ERA-40 is closer to SSE and CRU, but its radiation tend to lower in tropical region. DAO is closer to ERA-40, which suggests its magnitude may be closer to real value. Global daily observations from WMO weather stations also are used to directly compare with DAO, NCEP and ERA-40. The larger discrepancies among different meteorological data sets occur in low latitude region. Global total GPP and NPP driven by DAO, NCEP and ERA-40 show large differences, and spatially, large difference occurs in tropical region due to higher production, larger vegetated areas and higher uncertainties in meteorological data sets in tropics.

MOD17 driven by DAO, NCEP and ECMWF also are compared with it driven by observed surface meteorological data set with solar radiation from over 300 weather stations across USA, respectively. The results demonstrate the need for improving the accuracy of global surface meteorological data set, especially for tropical regions, to better understand and predict global carbon cycle under changing climate.

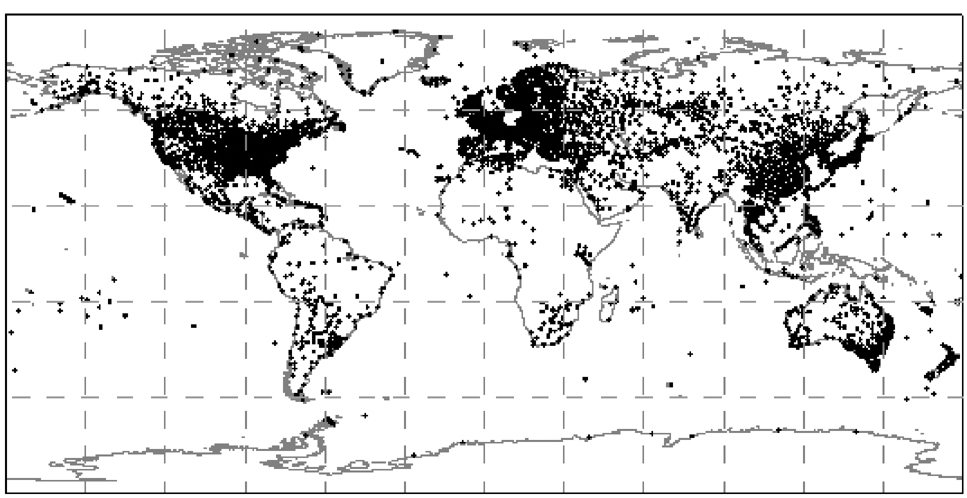

Figure 4. The distribution of weather stations with daily solar radiation observations over USA (n=327), and of World Meteorological Organization (WMO) weather stations (n > 5,000) for validation DAO, NCEP and ECMWF data sets.

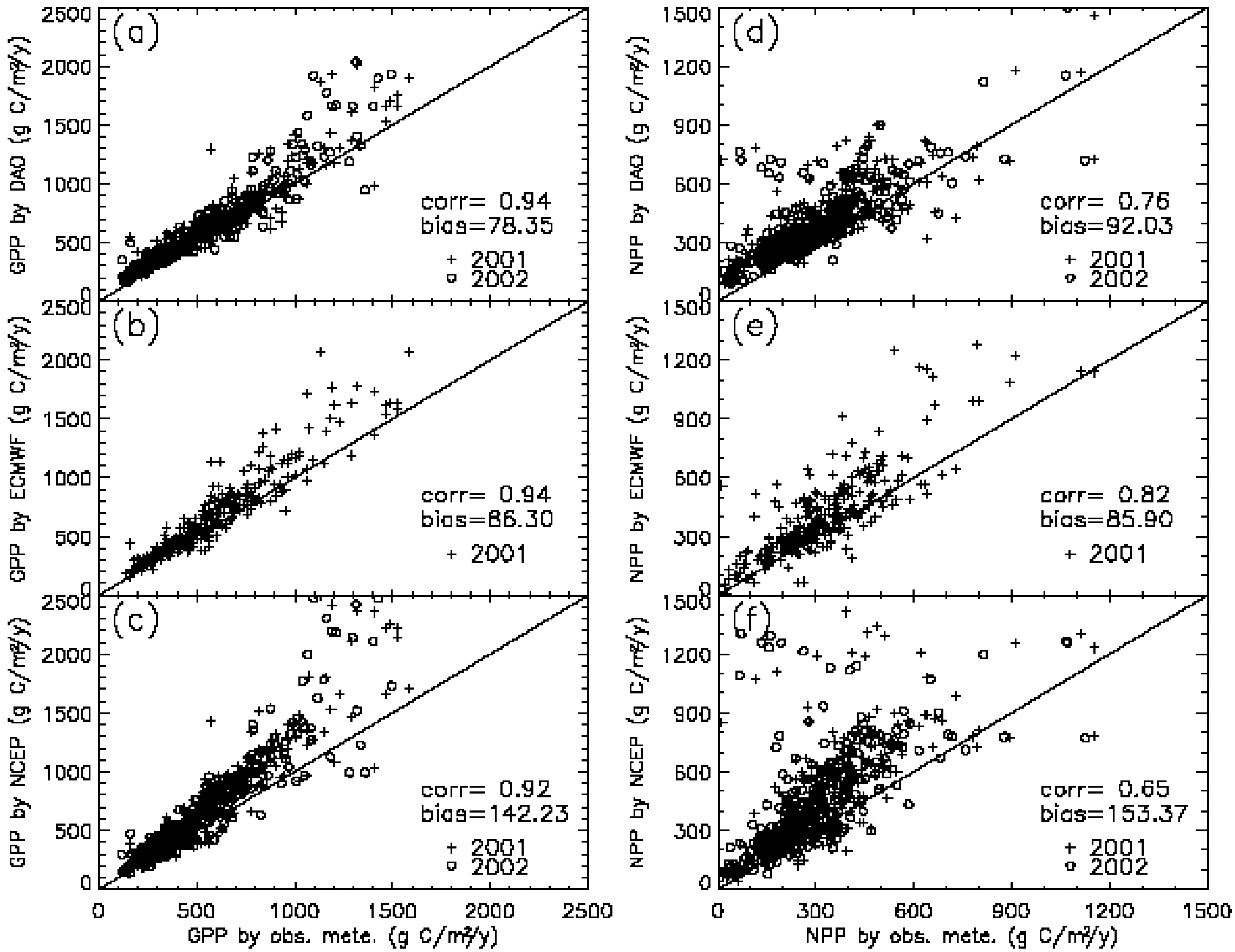

Figure 5. Comparison of total GPP/NPP driven by DAO, ECMWF and NCEP with them driven by observed meteorological data from USA weather stations. It shows that, first NPP has less accuracy than GPP, and secondly, ECMWF has higher accuracy than both DAO and NCEP, NCEP have the least accuracy.

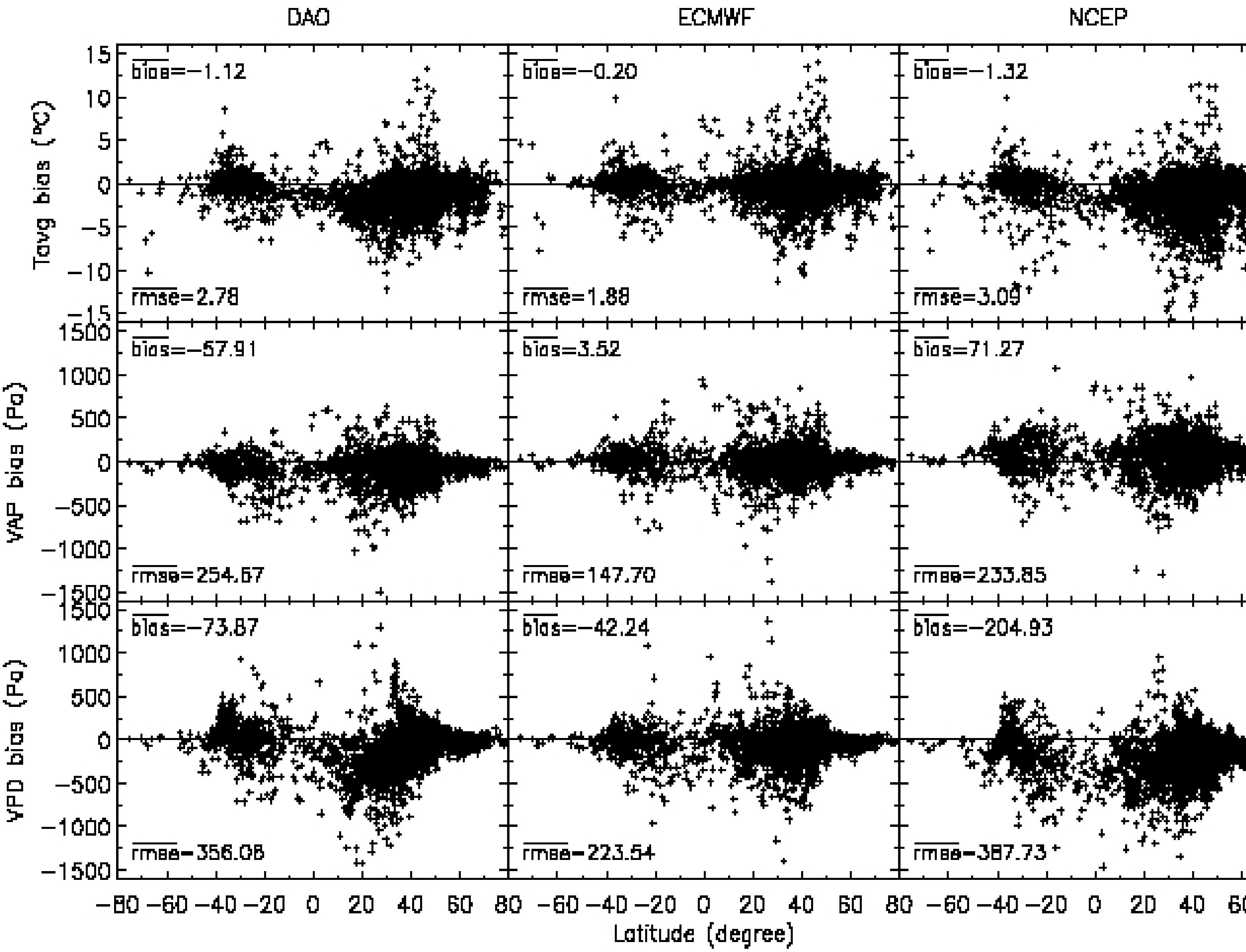

Figure 6. Comparison of three daily meteorological variables (Tavg, VAP and VPD) bias from WMO observations along latitude for DAO, ECMWF and NCEP from 2000 to 2001. It reveals that, first the accuracy of these meteorological data sets reduced from higher latitudes to low latitudes, and secondly, ECMWF has the highest accuracy.

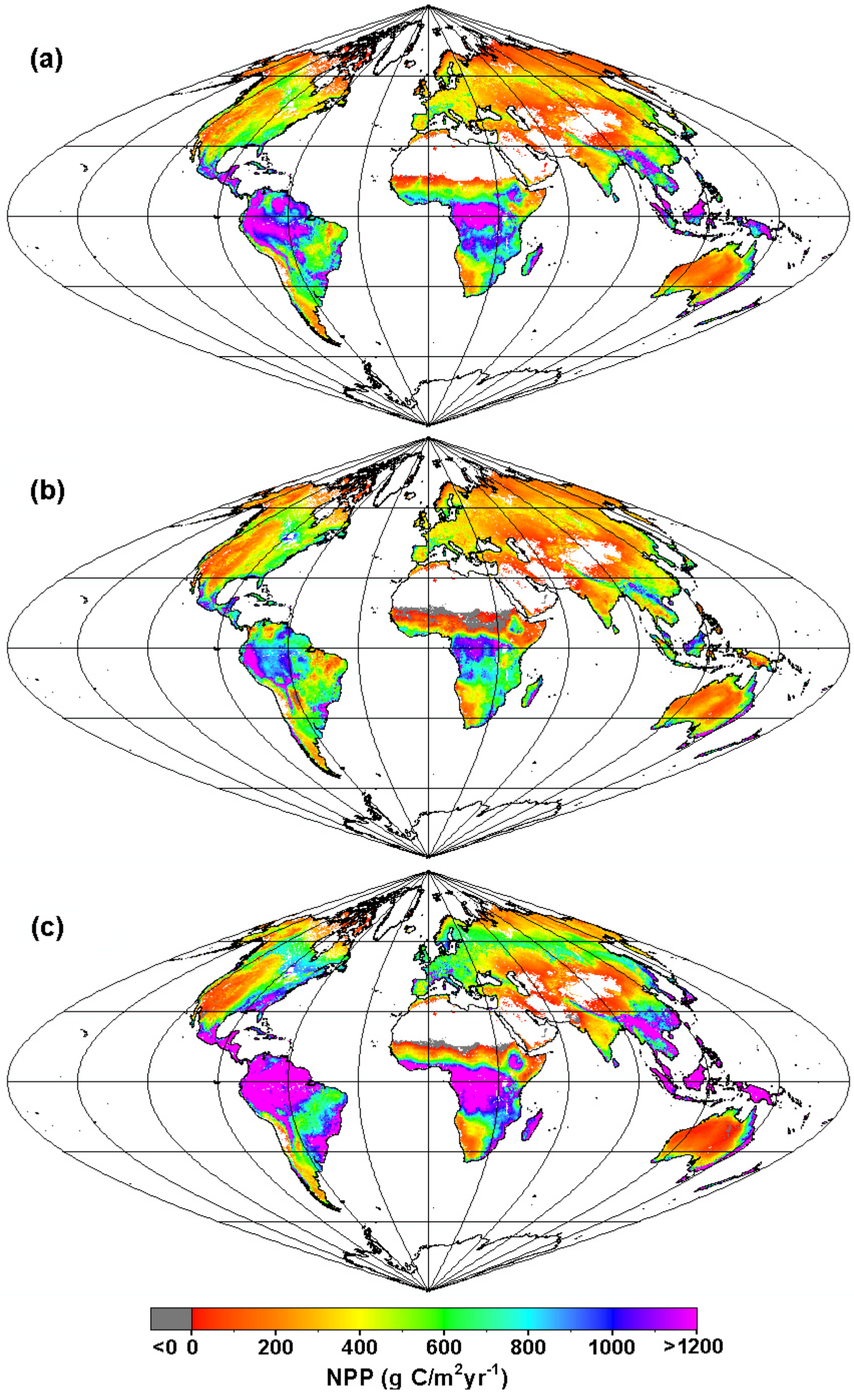

Figure 7. Comparison of annual 1-km MODIS NPP run by DAO (a), ECMWF (b) and NCEP (c), respectively. Generally, NCEP has higher estimations than DAO and ECMWF. ECMWF tend to underestimate NPP over tropical areas.

Year		2000	2001	2002	2003
DAO	**GPP (Pg C)**	**108.42**	**110.76**	**107.82**	**107.50**
	NPP (Pg C)	**56.06**	**57.74**	**55.53**	**54.80**
ECMWF	**GPP (Pg C)**	**101.79**	**102.71**	**N/A***	**N/A***
	NPP (Pg C)	**46.71**	**46.59**	**N/A***	**N/A***
NCEP	**GPP (Pg C)**	**124.82**	**125.75**	**123.40**	**123.72**
	NPP (Pg C)	**73.80**	**73.73**	**72.22**	**72.29**

* ECMWF reanalysis data (ERA-40) are not available past Aug. 31, 2002.

Table 1. Comparison of global total MODIS GPP & NPP forced by different meteorological data sets from 2000 to 2003.

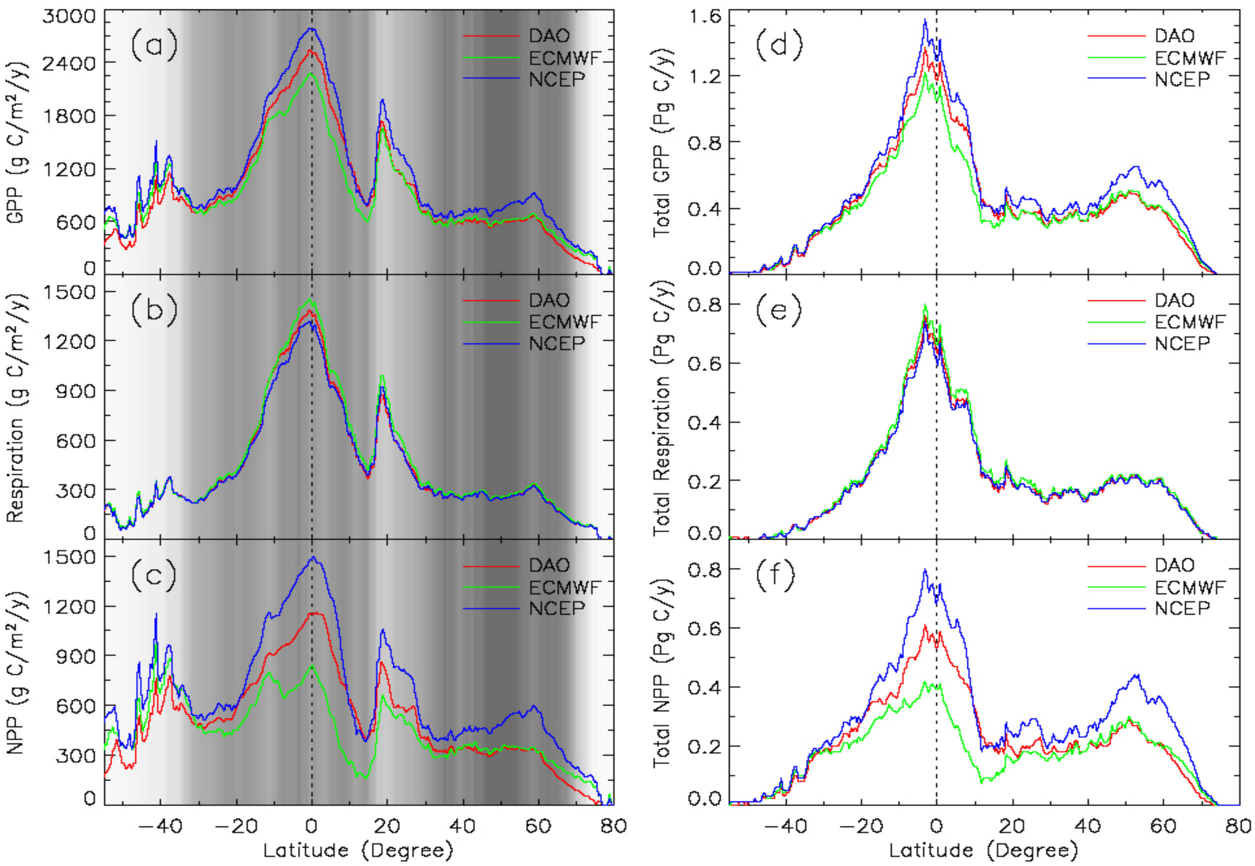

Figure 8. The annual zonal mean of GPP, respiration and NPP, and corresponding zonal total values. The vegetated land area is shown in gray scale, where darker shades represent higher vegetated area. It shows that difference in GPP is mainly responsible for the discrepancy in NPP. In the end, lager uncertainties in VPD (caused by uncertainties in Tavg, not shown here) and solar radiation are responsible for these differences.

3. Apply MOD17 algorithm to Pan-Arctic region

Based on historical AVHRR driven FPAR/LAI data set from 1982-2000, we run MOD17 algorithm with NCEP data sets as meteorological inputs to detect recent NPP trend in the region and the underlying mechanisms responsible for the change. Our study shows that advances in the growing season induced by warming trend mainly contribute to the increased NPP in this region.

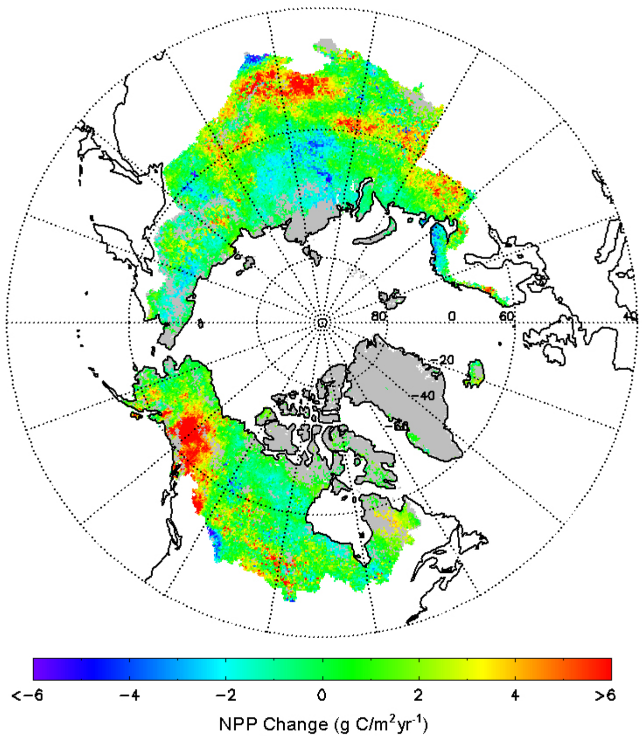

Figure 9. Recent NPP change for Pan-Arctic region and Alaska from 1982-2000.

4. Cooperate with BIGFOOT project to validate MOD17

We provide MODIS data as Bigfoot request to validate MOD17. The feedbacks between flux tower validation group and our lad are critical for refinement of MODIS algorithm, and improvement its usefulness to scientific and natural resource management communities.

Conferences:

MODIS Science Team Meeting, Baltimore, MD, July 2004.

Maosheng Zhao, Faith Ann Heinsch, and Steven W. Running. "Improvement, validation and uncertainties of MODIS terrestrial GPP/NPP (MOD17A2,A3)" (Poster)

MODIS Vegetation Workshop II, Missoula, MT, Aug. 2004.

Zhao, M, FA Heinsch, and SW Running. "Improvements and Uncertainties of the Global Terrestrial Primary Productivity Dataset (MOD17)" (Presentation)

Publications:

Running S. W., R. R. Nemani, F. A. Heinsch, **M. Zhao**, M. Reeves, H. Hashimoto. 2004. A continuous Satellite-derived measure of global terrestrial primary productivity: Future science and applications. *Bioscience*. 56(6): 547-560.

McDonald K., J. Kimball, E. Njoku, R. Zimmermann, **M. Zhao**. 2004. Variability in Springtime Thaw in the Terrestrial High Latitudes: Monitoring a Major Control on the Biospheric Assimilation of Atmospheric CO_2 with Spaceborne Microwave Remote Sensing. *Earth Interactions*. (In Press).

Zhao M., F. A. Heinsch, R. R. Nemani, S. W. Running. 2004. Improvements of the MODIS terrestrial gross and net primary production global dataset. *Remote Sensing of Environment* (In review).

Turner D. P., W. Ritts, W. B. Cohen, T. Maeirsperger, S. T. Gower, A. Kirschbaum, S. W. Running, **M. Zhao**, S. Wofsy, A. Dunn, B. Law, J. Campbell, W. Oechel, H. J. Kwon, T. Meyers, E. Small, S. Kurc, J. Gamon. 2004. Site-level Evaluation of Satellite-based Global GPP and NPP Monitoring. *Global Change Biology*. (in review).

Kimball J., **M. Zhao**, K. McDonald, F. A. Heinsch, and S.W. Running. 2004. Satellite Remote Sensing of Terrestrial Net Primary Production for the Pan-Arctic Basin and Alaska. *Mitigation and Adaptation Strategies for Global Change*. (submitted).

Heinsch, F. A., **M. Zhao,** S.W. Running, J. Kimball and R. R. Nemani et al. 2004. Evaluation of Remote Sensing Based Terrestrial Productivity from MODIS Using Regional Tower Eddy Flux Network Observations. *IEEE Transactions on Geoscience and Remote Sensing*. (submitted).

Turner D. P., W. Ritts, **M. Zhao**, S. Kurc, A. Dunn, S. Wofsy, E. Small, S. W. Running. 2004. Assessing Interannual Variation in MODIS-based Estimates of Gross Primary Production. *IEEE Transactions on Geoscience and Remote Sensing*. (submitted).

Kimball J., **M. Zhao**, K. McDonald, F. A. Heinsch, and S.W. Running. 2004. Satellite observations of annual variability in terrestrial carbon cycles and seasonal growing seasons at high northern latitudes. *Proceedings of the Fourth International Asia-Pacific Environmental Remote Sensing Symposium* (SPIE). (submitted).

Zhao M., R. R. Nemani, S. W. Running. 2004. Sensitivity Of MODIS Global Terrestrial Primary Production To The Accuracy Of Daily Meteorological Data Sets (In preparation)

ACTIVITIES OF Qiaozhen MU (Postdoctoral Researcher)

1. I modified point Biome-BGC to grid Biome-BGC with the help of Andrew Neuschwander. The input meteorological data can be in binary format files. There is one file for each year of each variable. And the other ancil files can be in ascii or binary files, such as USA_0.5_LC.asc (vegetation types), rockdepm_0.5.asc (effective soil depth), sand_0.5.asc (sand percentage), silt_0.5.asc (silt percentage), clay_0.5.asc (clay percentage), mask.asc (land/sea mask), us_0.5_dem.short (elevation). The output are binary files, outputting only the results where land locates, where model can integrate. One ascii file contains the columns and rows where Biome-BGC can't integrate.

2. Qiaozhen Mu, Maosheng Zhao, Steven W. Running made a poster on "Terrestrial Productivity in USA derived by A Biogeochemical Model and Remote Sensing Products from 1982 to 1997" for the MODIS vegetation workshop II.

In conterminous USA, Biome-BGC uses the 1980-1997 meteorology data, STATSGO soil texture data for sand/silt/clay percentages and effective soil depth, MOD12Q1 land cover type 5, and elevation data from GTOPO30 aggregated to 8 km resolution as the input data. MOD 17 algorithms use remotely sensed AVHRR, FPAR, LAI and DAYMET meteorology data as the input. GPP/NPP mean and NPP std simulated by Biome-BGC and MOD 17 have the similar patterns in conterminous USA, with Biome-BGC results lower in the middle from north to south during 1982-1997.

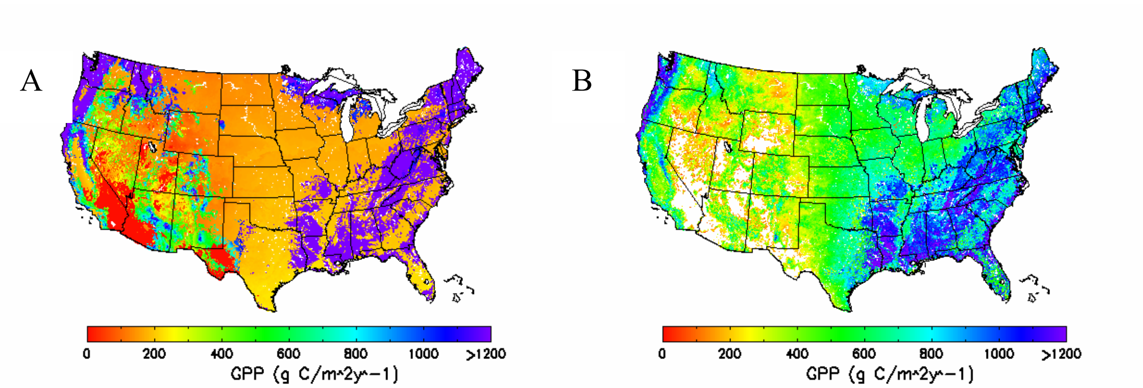

Fig. 1 GPP mean in conterminous USA A) by Biome-BGC B) by remotely sensing

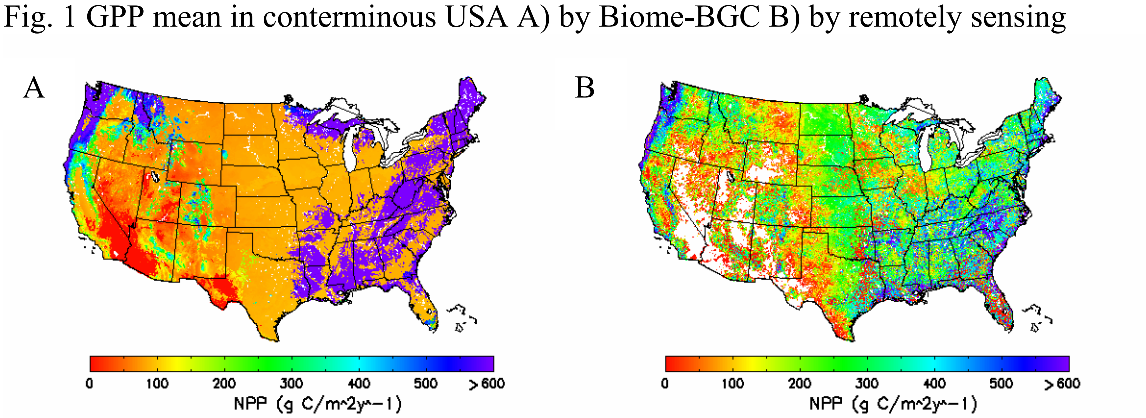

Fig. 2 NPP mean in conterminous USA A) by Biome-BGC B) by remotely sensing

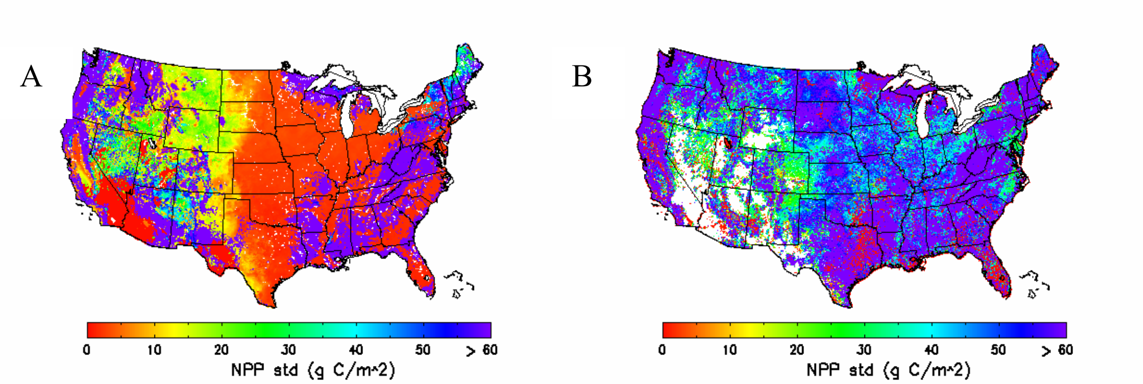

Fig. 3 NPP STD in conterminous USA A) by Biome-BGC B) by remotely sensing

GPP/NPP mean and NPP std simulated by Biome-BGC and MOD 17 have the similar patterns in conterminous USA, with Biome-BGC results lower in the middle from north to south during 1982-1997.

For the annual average over conterminous USA, solar radiation (SRAD) affects GPP/NPP the most, precipitation the second and VPD the third. The relationships between GPP, NPP and mean temperature are not significant.

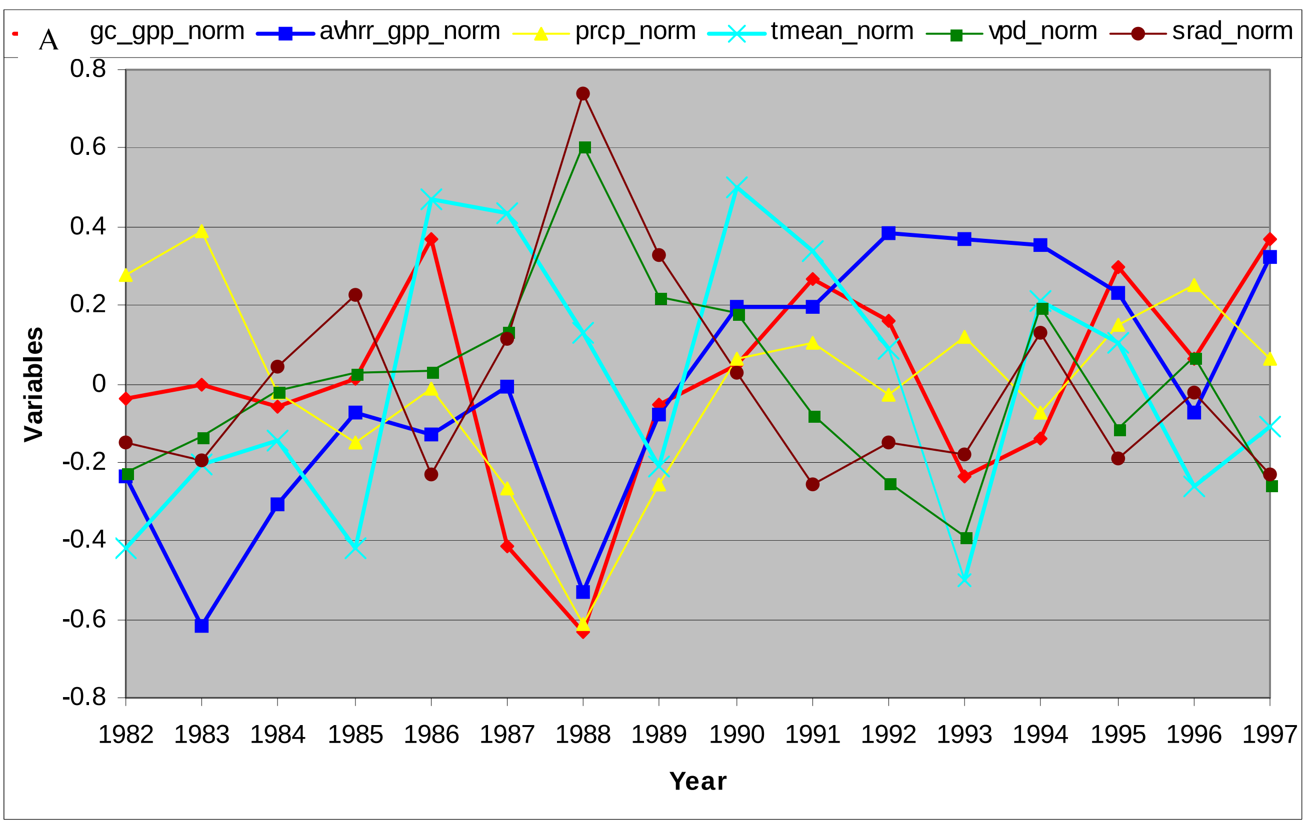

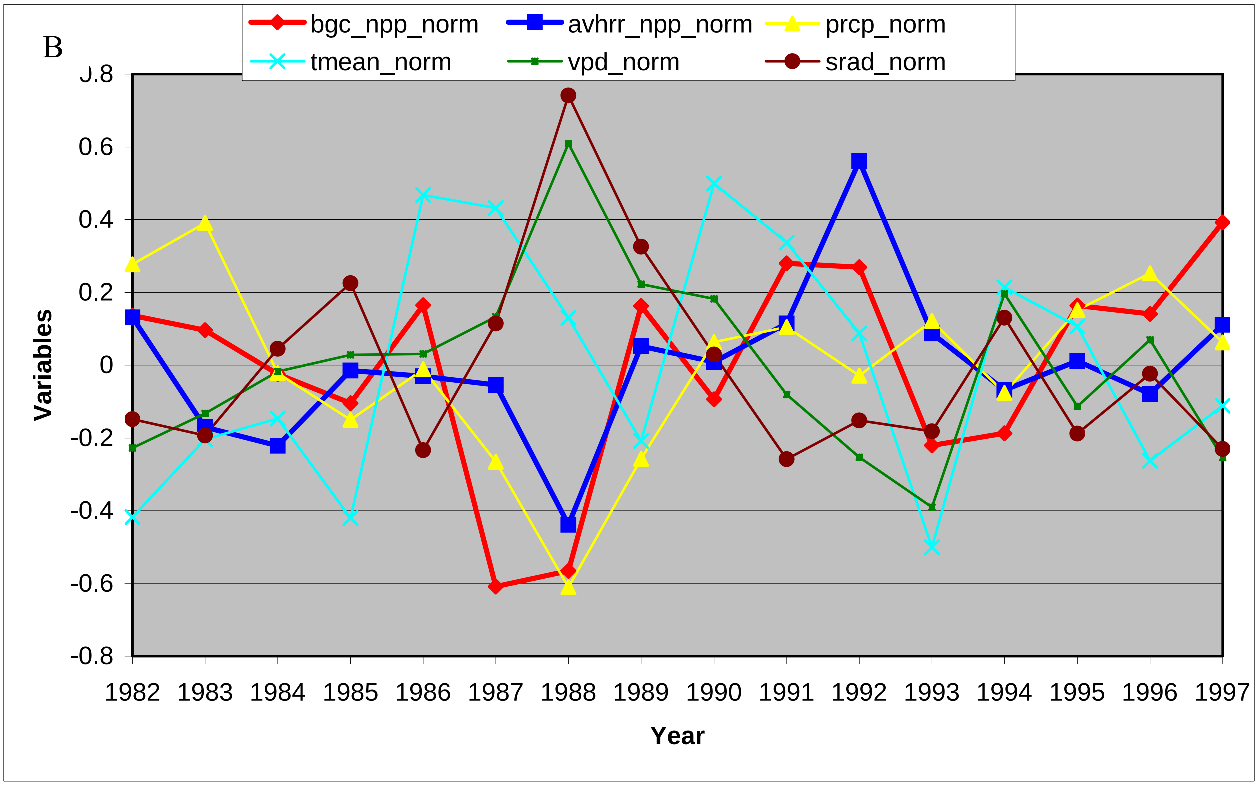

Fig. 4 annual A) GPP B) NPP by Biome-BGC and remotely sensing, annual meteorology variables averaged over conterminous USA

For the spatial results, the annual mean temperature decreases in the middle and east part, increases in most of western part. The precipitation decreases in the western-southern and east part around the five-lake part, increases in the middle, western-northern and east parts of conterminous USA. VPD (vapor pressure deficit) has the similar change as temperature, increases mainly in the west-south part. For the Biome-BGC results, GPP/NPP decrease in the northern-eastern, middle and western-southern parts. For the meteorology variables trends, precipitation conflicts with NPP in the south-west, agrees with GPP/NPP in the middle and east.

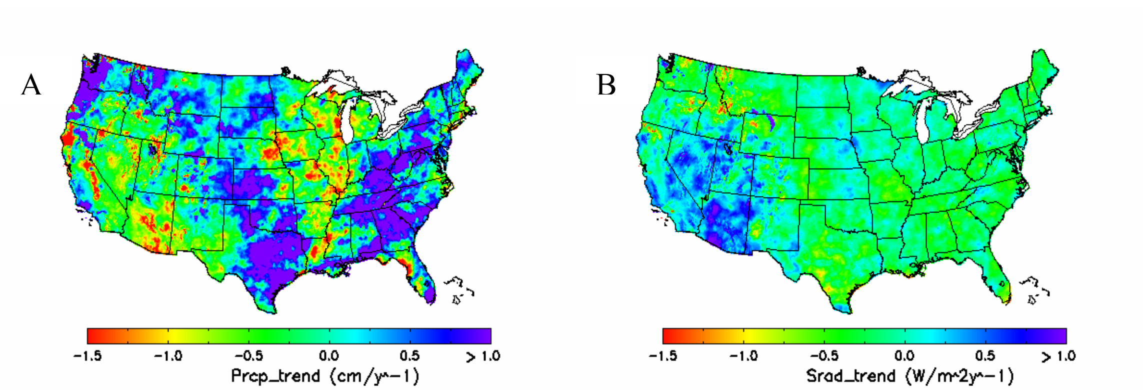

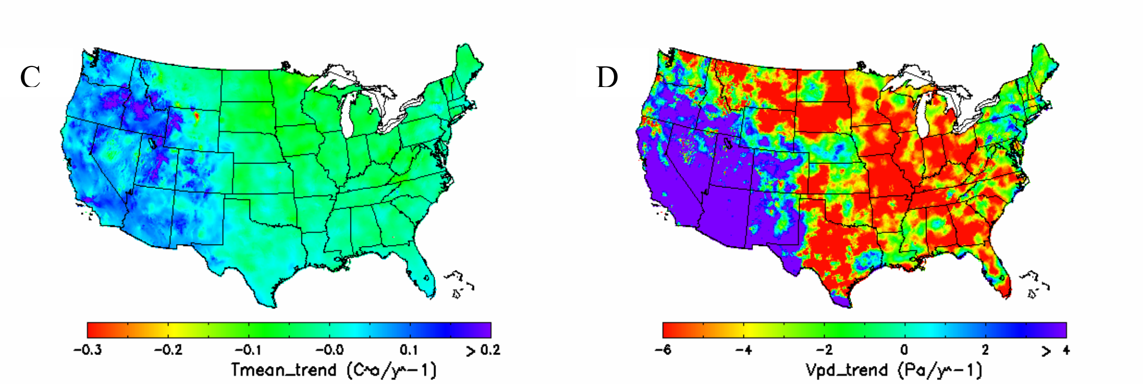

Fig.5 A) precipitation B) solar radiation C) mean temperature D) vapor pressure deficit trends in conterminous USA

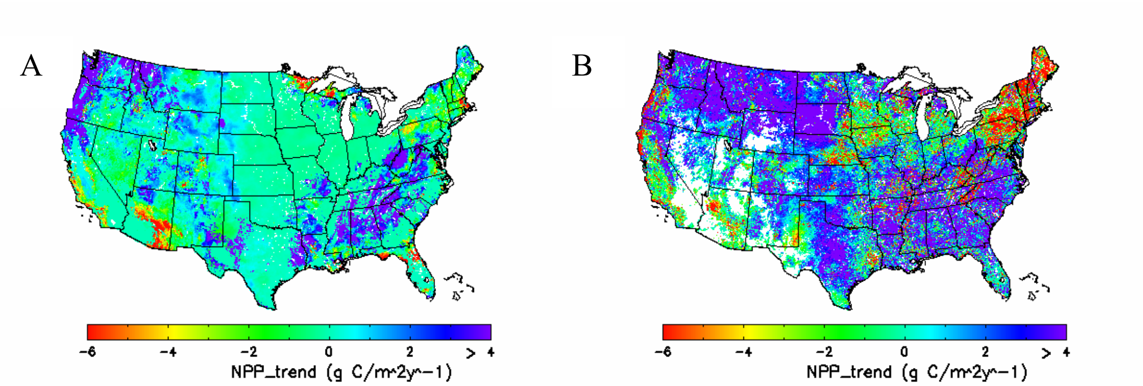

Fig. 6 NPP trends in conterminous USA A) by Biome-BGC B) by remotely sensing

In the future, we will use Biome-BGC and MOD17 algorithms to study the water effects on NPP/GPP and other physical processes.

3. I am writing the model codes for Evapotranspiration (ET) in Australia based on the paper “Land Surface Evaporation from Flux Towers and MODIS Remote Sensing" by Helen A. Cleugh, Ray Leuning and Steven W. Running”, using the Australian climate data and MOD11A2 (LST), MOD13A2 (NDVI), MOD15A2 (LAI/FPAR), MOD43B3 (Albedo) and MOD12Q1 (land vegetation type) data.

First, I get the max and min LAI and NDVI in the studying time period for each pixel using the files existing (for surface resistance). When calculating ET using the MODIS data, if one 8-day-period or 16-day-period file for one tile doesn't exist, I use the temporal interpolation method as Maosheng Zhao does in MOD17 algorithms. The Australia climate is in geographic coordination, the resolation is 0.5 degrees, for the MODIS data, the resolutions is 1KM. I use the spatial interpolation method to get the climate data for each pixel in one tile as Maosheng Zhao deals with DAO data for MOD17.

Second, the model calculates the latent heat of vaporization using MOD11A2 (LST) based on the equation (4.2.1) in Handbook of Hydrology, calculates aerodynamic_resistance (Ra) using the relationship between LAI and momentum roughness, and surface_resistance (Rs) using max, min of LAI, NDVI.

$$R_a = \frac{1}{k^2 U}\left[\ln\left(\frac{z-d}{z_{0H}}\right) - \psi_H\left(\frac{z-d}{L}\right)\right]\left[\ln\left(\frac{z-d}{z_0}\right) - \psi_M\left(\frac{z-d}{L}\right)\right]$$

$$f_c = \left[N^*{}_{DV\,I}\right]^2$$

$$N^*{}_{DVI} = \frac{N_{DVI} - N_{DVIx}}{N_{DVIx} - N_{DVIo}}$$

$$G_s = C_L \max\left[L_{ai0}, \left(f_c L_{aix}\right)\right]$$

$$R_s = 1/G_s$$

The model calculates net downward radiation using net shortwave radiation, air temperature provided by Australia climate data,

$$Rn = \left[S \downarrow (1-\alpha)\right] + \left|(\varepsilon_a - \varepsilon_s)\sigma T_a{}^4\right|$$

$$\varepsilon_a = 1 - 0.261\exp\left[-7.77 * 10^{-4}(273 - T_a)^2\right]$$

$$G = C_G R_n$$

$$A = R_n - G$$

The model calculates saturated vapor pressure (SVP), air density using air temperature and vapor pressure in Australia climate data.

$D_a = 2.3211 e^{\left(0.0815\overline{T_{DAO}}\right)}$, vapor pressure deficit

T_{DAO}: the DAO average air temperature

$$e_s - e_a \approx s(T_s - T_a) + D_a$$

$s = de^* / dT$, the slope of the curve relating saturation water vapor pressure to temperature.

Using all the variables got from the model or from the Australia climate data, ET is calculated using the Penman-Monteith equation.

$$\lambda E = \frac{sA + (\rho c_p D_a / R_a)}{s + \gamma(1 + R_s / R_a)}$$

4. I downloaded Land Information System (LIS) model source codes and data. Andrew Neuschwander helped me compile the model. We found a bug with the model to read the input parameter data files. I have sent them an email about the bug, they didn't respond yet.

Activities for Matt Reeves, PhD Student

Most of my time during this period was spent either preparing manuscripts or writing my dissertation. To this end, I have submitted two papers for publication. The first entitled "Applying Improved Estimates of MODIS Productivity to Characterize Grassland Vegetation Dynamics" was submitted to the Journal of Rangeland Ecology and Management on or about 30, April 2004. This paper was also delivered as a presentation at the Annual Meeting for the Society for Range Management in Salt Lake City, Utah. The second paper entitled "Usefulness and limits of MODIS GPP for estimating wheat yield" was accepted for publication in the International Journal of Remote Sensing. A third paper, nearly finished, entitled "Integrating MODIS vegetation data with a model of spring wheat growth and yield for Montana" will be submitted to Agronomy Journal by December 2004. My dissertation entitled "Derivation of wheat yield And Rangeland Productivity in the Northern Great Plains Using MODIS Algorithms was successfully completed on 29, August 2004. This research was conducted to answer four basic questions: To what extent does MODIS vegetation data emulate trends in rangeland vegetation dynamics? Can wheat yield be accurately estimated for entire regions using only the MODIS vegetation product suite? If not, what changes can be made to the modeling environment and input data stream to improve yield estimates? and, what is the appropriate spatial domain for characterizing regional rangeland productivity and wheat yield from MODIS data? Answers to these questions are summarized below.

To what extent do MODIS vegetation data emulate trends in rangeland vegetation dynamics?

MODIS data can be used for monitoring rangeland vegetation productivity with the following caveats: 1) Inter-annual variation can probably be more appropriately characterized than intra-annual differences 2) Intra-annual differences are more easily detected during years with favorable growing conditions and 3) progressive spatial aggregation from the pixel level to large regions will provide more precise and reliable estimates of productivity. Rangelands are often interspersed with agricultural land use, and in the Northern Great Plains, particularly wheat farming. Based on this observation, I devised a testing procedure for evaluating the suitability of MODIS GPP data for computing wheat yield.

Can wheat yield be accurately estimated for entire regions using only the MODIS vegetation product suite?

The relationship between predicted and observed wheat yield at the county level was the strongest ($r^2 = 0.46$) in 2001, which is also the year of the strongest relationship between MODIS PSN_{net} and observed above-ground green biomass in North Dakota (Figure 1). Subsequent aggregation to the state level produced wheat yield estimates which were never more than 5% different from observed yield (Table 1). These results, in part, answer the questions "Can wheat yield be accurately estimated for entire regions using only the MODIS vegetation product suite?" and "What is the appropriate spatial domain for characterizing regional wheat yield from MODIS vegetation data?".

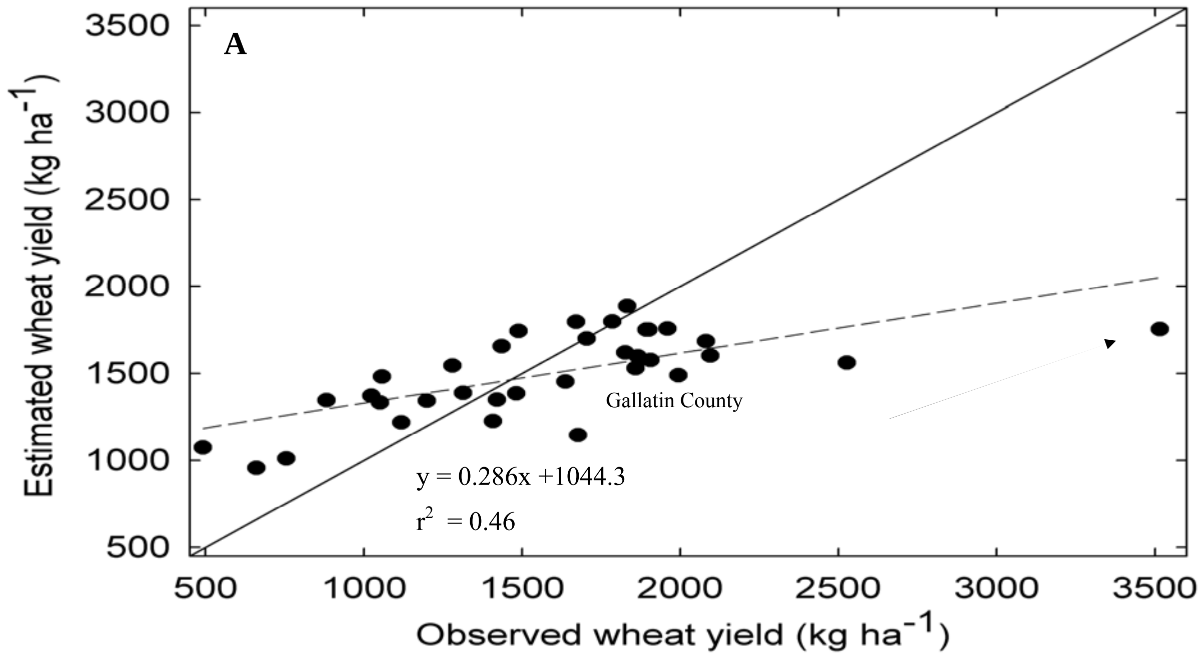

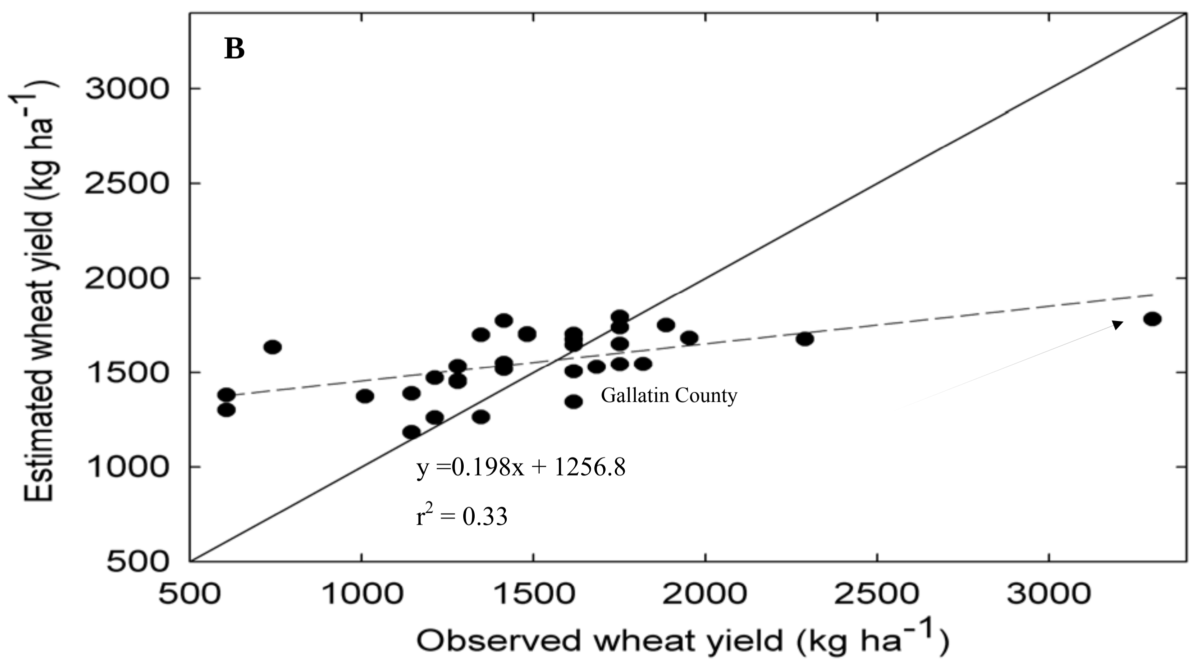

Figure 1. Observed versus estimated county level wheat yield (Kg ha^{-1}) for Montana in 2001 (A) and 2002 (B). The dashed line is a linear least – squares best fit regression analysis. Gallatin County is the notable outlier.

Table 1. Results of state level wheat yield estimates from MODIS GPP for Montana and North Dakota in 2001 and 2002.

State	Year	Estimated yield(SE) kg ha^{-1}	Observed yield(SE) kg ha^{-1}	% Difference estimated - observed	Apparent Growing Season*
MT	2001	1520.9± (62.6)	1500.1± (105.6)	1	81 - 208
MT	2002	1475.8± (70.9)	1410.0± (91.1)	5	81 - 225
ND	2001	2092.8± (67.0)	2188.8± (141.4)	-4	81 - 216
ND	2002	1640.1± (41.1)	1700.8± (161.2)	-4	81 - 225

*The apparent growing season that provided the best relationship between estimated and observed state level wheat yield for Montana and North Dakota.

The research provides evidence that, indeed, MODIS GPP estimates can be used to accurately estimate wheat yield, but only for large regions (states). The poor ability of MODIS GPP for estimating yield at the county level provided the impetus for improving data inputs and model logic. These suggested improvements were (1) implementation of more appropriate and regionally specific analysis masks to delineate wheat from other crops; (2) inclusion of localized, observed meteorological data and; (3) adaptation of crop physiological parameters in the current GPP algorithm to more closely emulate observed physiological characteristics of commonly grown wheat varieties in the region of interest. Chapter four focused on implementing these changes by adapting the wheat yield logic of (Amir and Sinclair 1991) (Figure 2).

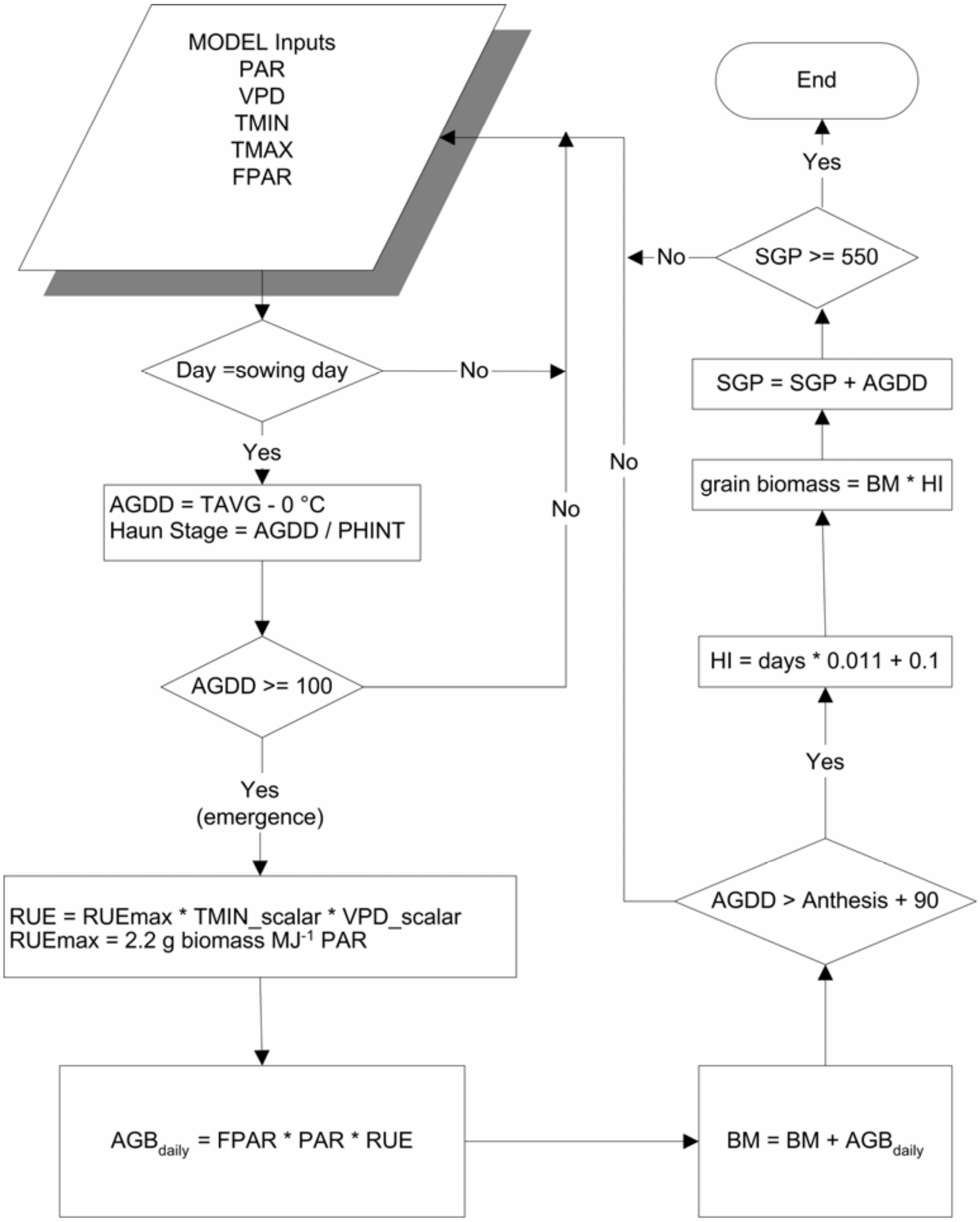

Abbreviations:
PAR = Photosynthetically active radiation
VPD = Vapor pressure deficit
TMIN = Minimum daily temperature
TMAX = Maximum daily temperature
FPAR = fraction of absorbed photosynthetically active radiation
TAVG = Average daily temperature
AGDD = Accumulated growing degree days
RUE = Radiation use efficiency
BM = Biomass
HI = Harvest index
AGBdaily = Above ground biomass(daily increment)

Figure 2. Flow diagram of the model adapted from (Amir and Sinclair 1991) including data processing, model input and output.

The adapted model, which relied on MODIS FPAR and meteorological observations, was run for Montana for the years 2001 to 2003. Implementing these changes improved county level wheat yield prediction. In addition, simulated state level wheat yield was never different ($P \leq 0.05$) than observed yield in any year of the study (Table 2).

Table 2. Variance, mean and associated F-ratio test parameters for demonstrating equality of variances ($P < 0.05$)[1].

Year	2001		2002		2003	
Parameter	Observed	Predicted	Observed	Predicted	Observed	Predicted
Mean	1483	1429	1138	1294	1275	1245
Variance	370118	374873	346271	481696	11642	63350
F	1.0128		1.391		1.841	
P(F<=f)	0.487		0.198		0.056	
$F_{critical}$	1.882		1.905		1.882	
Df	26		25		26	

[1]This was a two - tailed analysis.

Literature Cited

Amir, J. and T. R. Sinclair (1991). "A model of the temperature and solar-radiation effects on spring wheat growth and yield." Field Crops Research 28: 47-58.

ACTIVITIES OF Compute Service Team

Compute Service Team (CST), Manager Saxon Holbrook
Andrew Neuschwander, Andy Michaelis, Joshua Campbell

MODIS Related Activities:

- ESIP Federation Activities: S. Holbrook was an active member of the Constitution and Bylaws Committee, the Working Group for Peer Review and regularly participated in telephone conferences, the MODIS Cluster and ESTO Cluster.
- Managed day-to-day activities and projects of the CST. CST Members during this period: Andrew Neuschwander (Linux System Admin), Andy Michaelis (Student Programmer, Graduated December 2003), Joshua Campbell (Student Programmer, Hired August 2004)
- Participated in creation of MODIS Vegetation Workshop II Website.
- Supported technology needs during MODIS Vegetation Workshop II.
- Provided data management and programming support for MODIS research and production activities.
- Maintained NTSG Images gallery and FTP data distribution.
- Managed Software Environment and Licenses required for all activities.
- Managed Legato Backup and Restores of online & near online MODIS Data.
- Managed and optimized network. Monitored Abilene I2 connection to EDC & Goddard.
- Managed Windows Workstations and Linux Compute Environments.
- Maintained the DAYMET.org website.

MODIS Data Holdings and Data Distribution:

- MODIS data online exceeds 1.8 Terabytes
- MODIS data served by direct FTP access exceeds 684GB (Feb-July 2004)

Usage Statistics for FTP Downloads from ftp.ntsg.umt.edu

Summary Period: Last 12 Months
Generated 18-Oct-2004 04:02 MDT

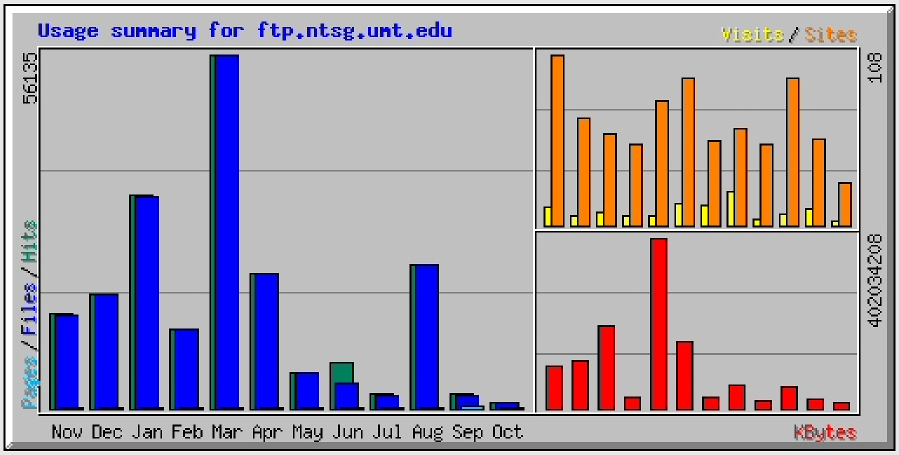

Summary by Month										
Month	Daily Avg				Monthly Totals					
	Hits	Files	Pages	Visits	Sites	KBytes	Visits	Pages	Files	Hits
Oct 2004	58	57	0	0	27	13411256	3	3	976	998
Sep 2004	74	72	11	0	55	21108683	10	346	2162	2243
Aug 2004	735	732	4	0	93	52252877	7	124	22715	22793
Jul 2004	71	70	0	0	51	18061172	4	6	2175	2229
Jun 2004	248	133	3	0	61	53375322	22	96	3996	7448
May 2004	183	179	2	0	53	25405640	13	77	5567	5690
Apr 2004	712	710	0	0	93	159562776	14	28	21301	21383
Mar 2004	1810	1808	0	0	79	402034208	6	14	56070	56135
Feb 2004	433	432	0	0	51	26439106	6	7	12547	12584
Jan 2004	1089	1087	4	0	58	193891093	8	130	33708	33765
Dec 2003	586	582	5	0	68	113277281	6	160	18066	18185
Nov 2003	498	497	1	0	108	100883352	12	42	14931	14963
Totals						**1179702766**	**111**	**1033**	**194214**	**198416**

Usage Statistics for images.ntsg.umt.edu

Summary Period: Last 12 Months
Generated 18-Oct-2004 04:02 MDT

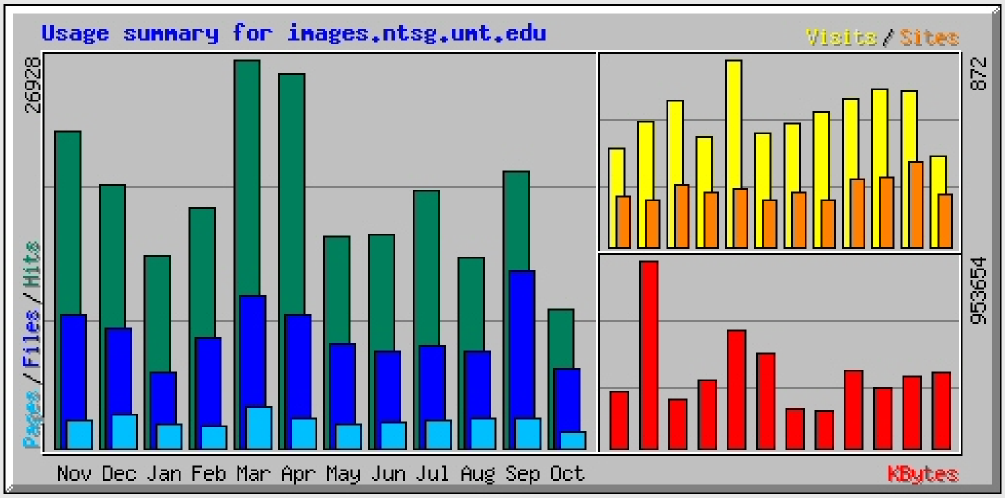

Summary by Month										
Month	Daily Avg				Monthly Totals					
	Hits	Files	Pages	Visits	Sites	KBytes	Visits	Pages	Files	Hits
Oct 2004	537	305	63	23	249	380490	424	1146	5500	9667
Sep 2004	639	411	69	24	395	361983	723	2077	12330	19196
Aug 2004	425	215	67	23	326	303148	737	2084	6695	13188
Jul 2004	576	229	63	22	312	398385	693	1962	7110	17870
Jun 2004	490	222	60	20	216	185528	629	1818	6666	14727
May 2004	472	231	52	18	252	203048	573	1612	7183	14654
Apr 2004	866	308	67	17	215	483860	531	2031	9241	25992
Mar 2004	868	339	90	28	274	594732	872	2819	10534	26928
Feb 2004	572	261	53	17	253	343970	512	1561	7569	16598
Jan 2004	430	169	52	21	285	252102	680	1631	5259	13353
Dec 2003	587	268	75	18	222	953654	583	2352	8323	18216
Nov 2003	731	306	63	15	237	290580	461	1912	9196	21949
Totals						**4751480**	**7418**	**23005**	**95606**	**212338**

- Enhanced MOD17 images served by Web access exceeds 2.2GB (Feb-July 2004)

MODIS project Publications from 1989 to 2004

Running S. W., R. R. Nemani1, F. A. Heinsch, M. Zhao, M. Reeves, H. Hashimoto. (2004). A continuous Satellite-derived measure of global terrestrial primary productivity: Future science and applications. *Bioscience*. 56(6): 547-560.

Jolly W. M., Graham J. M., A. Michaelis, R. R. Nemani and S. W. Running. (2004) A flexible integrated system for generating meteorological surface derived from point source across multiple geographic scales. *Environmental modeling & Softwrae*. (in press)

Jolly W. M., R. R. Nemani and S. W. Running. (2004) Enhancement of understory productivity by asynchronous phenology with overstory competitors in a temperature deciduous forest. *Tree Physiology*. 24:1069-1071.

Jolly W. M., R. R. Nemani and S. W. Running. (2004) Effects of precipitation and soil water potential on drought deciduous phonology in the Kalahari. *Global Change Biology*. 10(3):303-308.

Turner D. P., W. D. Ritts, W. B. Cohen, S. T. Gower, M. Zhao, S. W. Running, S. C. Wofsy, S. Urbanski, A. L. Dun, J. W. Munger. (2003). Scaling Gross Primary Production (GPP) over boreal and deciduous forest landscapes in support of MODIS GPP product validation. *Remote Sensing of Environment*. 88, 256-279.

Kang, S., S. Running, J. Lim, M. Zhao, C. Park, R. Loehman. (2003) A regional phenology model for detecting onset of greenness in temperate mixed forests, Korea: an application of MODIS leaf area index. *Remote Sensing of Environment*. 86: 232-242.

Nemani, R.R., C.D. Keeling, H. Hashimoto, W.M. Jolly, S.C. Piper, C.J. Tucker, R.B. Myneni and S.W. Running. (2003). Climate-Driven Increases in Global Terrestrial Net Primary Production from 1982 to 1999. *Science*.300: 060-1063.

Milesi, C., C. Elvidge, R. Nemani, S. Running. (2003) Assessing the impact of urban land development on net primary productivity in the southeastern United States. *Remote Sensing of Environment*. 86: 401-410

Nishida, K., Nemani, R. R., Running, S. W., Glassy, J. M. (2003):An operational remote sensing algorithm of land surface evaporation. *Journal of Geophysical Research*. 108(D9)doi:10.1029/2002JD002062.

Nishida, K., Nemani, R. R., Running, S. W., Glassy, J. M. (2003): Development of an evapotranspiration index from Aqua/MODIS for monitoring surface moisture status. *IEEE Transactions of Geoscience and Remote Sensing.* 41(2), 493-501.

Nemani, R., M. White, L. Pierce, P. Votava, J. Coughlan, S. Running. (2003) Biospheric Monitoring and Ecological Forecasting. *Earth Observation Magazine.* 12(2): 6-8.

Milesi, C., C. Elvidge, R. Nemani, S. Running. (2003) Assessing the environmental impacts of human settlements using satellite data. *Management of Environmental Quality.* 14(1): 99-107.

Whited, D., J. Stanford, J. Kimball. (2002) Application of airborne multispectral digital imagery to quantify riverine habitats at different base flows. *River Research and Applications.* 18: 583-594.

Schimel, D., T. Kittel, S. Running, R. Monson, A. Turnipseed, D. Anderson. (2002) Carbon Sequestration Studied in Western U.S. Mountains. *EOS, Transactions, American Geophysical Union.* 83:40, 445-449.

Running, S.W. (2002) New Satellite Technologies Enhance Study of Terrestrial Biosphere. *EOS, Transactions, American Geophysical Union* 83: 41, 458-460.

Running, S.W.(2002) MODIS Vegetation Workshop Report. *The Earth Observer.* 14: 5, 14-15.

Myneni, R.B., S. Hoffman, J. Glassy, Y. Zhang, P. Votava, R. Nemani, S. Running. (2002) Global products of vegetation leaf area and fraction absorbed PAR from year one of MODIS data. *Remote Sensing of Environment.* 83: 214-231.

Nemani, R.M., White, P. Thornton, K. Nishida, S. Reddy, J. Jenkins, S. Running. (2002) Recent trends in hydrologic balance have enhanced the terrestrial carbon sink in the United States. *Geophysical Research Letters.* 29 (10): 106-1 – 106-4.

White, J., S. Running, K. Ryan, C. Key. (2002) Fuzzy Logic Merger of Spectral and Ecological Information for Improved Montane Forest Mapping. *Geocarto International.* 17(1): 59-66.

Baldocchi, D., E. Falge, L. Gu, R. Olson, D. Hollinger, S. Running, P. Anthoni, C. Bernhofer, K. Davis, R. Evans, J. Fuentes, A. Goldstein, G. Katul, B. Law, X. Lee, Y. Malhi, T. Meyers, W. Munger, W. Oechel, K. T. Paw U, K. Pilegaard, H. P. Schmid, R. Va (2001). FLUXNET: A new tool to study the temporal and spatial variability of ecosystem-scale varbon dioxide, water vapor, and energy flux densities. *Bulletin of the American Meteorological Society*. 82, 2415-2434.

Chase, T.N., R. A. Pielke St., T. G. F. Kittel, R. R. Nemani, S. W. Running (2001). Simulated impacts of historical land cover changes on global climate in northern winter. *Climate Dynamics*. 16, 93-105.

Chase, T.N., R. A. Rielke Sr., T.G.F. Kittel, M. Zhao, A.J. Pitman, S. W. Running, R.R. Nemani (2001). Relative climatic effects of landcover change and elevated carbon dioxide combined with aerosols: A comparison of model results and observations. *Journal of Geophysical Research*. 106, 31,685-31,69.

Coops, N.C., R. H. Waring, S. R. Brown, S. W. Running (2001). Comparisons of predictions of net primary production and seasonal patterns in water use derived with two forest growth models in Southwestern Oregon. *Ecological Modelling*. 142, 61-81.

Nemani, R.R., M.A. White, D.R. Cayan, G. V. Jones, S.W. Running, J.C. Coughlan, D.L. Peterson (2001). Asymmetric warming over coastal California and its impact on premium wine industry. *Climate Research*. 19, 25-34.

Reeves, M.C., J.C. Winslow, S.W. Running (2001). Mapping Weekly Rangeland Vegetation Productivity Using MODIS Algorithms. *Journal of Range Management.* 54, A90-A105.

White, M. A., S. W. Running (2001). Identification of optimal satellite compositing length using GLOBE budburst measurements. *Proceedings of the Sixth Annual GLOBE Conference*. Blaine, Washington. July, 2001, 270-276.

Canadell, J.G., H.A. Mooney, D.D. Baldocchi, J.A. Berry, J. R. Ehleringer, C. B. Field, S. T. Gower, D. Y. Hollinger, J. E. Hunt, R. B. Jackson, S. W. Running, G. R. Shaver, W. Steffen, S. E. Trumbore, R. Valentini, B. Y. Bond (2000). Carbon metabolism of the terrestrial biosphere: A multitechnique approach for improved understanding. *Ecosystems*. 3 , 115-130.

Hasenauer, H., Nemani, R., Schadauer, K., and Running, S. (2000). Climate variations and tree growth between 1961 and 1995 in Austria.. *Proceedings of the European Forest Institute*. 75-86.

Justice, C.O., Townshend, J.R.G., Vermote, E.F., Sohlberg, R., Descloitres, J., Roy, D., Hall, D., Salomonson, V., Riggs, G., Huete, A., Didan, K., Miura, T., Wan, Z., Strahler, A., Schaaf, C., Myneni, R., Running, S., Glassy, J., Nemani, R., El Saleous, (2000). Preliminary land surface products from the NASA Moderate Resolution Imaging Spectroradiometer(MODIS) . *Proceedings of the International Geoscience and Remote Sensing Symposium (IGARSS 00)*, Honolulu, Hawaii.

Keyser, A., Kimball, J., Nemani, R. and Running, S. (2000). Simulating the effects of climate change on carbon balance of north American high latitude forests.. *Global Change Biology*. 6, 1-11.

Kimball, J.S., A.R. Keyser, S.W. Running, S.S. Saatchi (2000). Regional assessment of boreal forest productivity using an ecological process model and remote sensing parameter maps. *Tree Physiology*. 20, 761-775.

Nemani, R., White, M., Cayan, D., Jones, G., Running, S. and Coughlan, J. (2000). Climate and California vintages. *Proceedings of " International Conference on Climate forecasts in Agriculture".*

Running, S., Thornton, P., Nemani, R., Glassy, J. (2000). Global Terrestrial Gross and Net Primary Productivity from the Earth Observing System.. *Methods in Ecosystem Science*, 44-57.

Running, S.W. (2000). Why the earth observing system matters to all of us.. *The Earth Observer*, 12(1).

Running, S.W., J.B. Way, K.C. McDonald, J.S. Kimball, S. Frolking, A.R. Keyser (2000). Radar remote sensing proposed for monitoring freeze-thaw transitions in boreal regions. *Earth in Space*, 12, 1-9.

Running, S.W., L.P. Queen, M. Thornton (2000). The earth observing system and forest management. *Journal of Forestry*, 98(6), 29-31.

Chase, T.N., R. A. Pielke St., T. G. F. Kittel, R. R. Nemani, S. W. Running. (2000) Simulated impacts of historical land cover changes on global climate in northern winter. *Climate Dynamics* 16, 93-105.

Tian, Y., Zhang, Y., Knyazikhin, Y., Myneni, R. B. & Running, S. W. (2000). Prototyping of MODIS LAI/FPAR algorithm with LASUR and Landsat data. *IEEE Transaction on Geoscience and Remote Sensing*, 38(5), 2387-2401.

White, M. A., M. D. Schwartz, S. W. Running (2000). Young students, satellites aid understanding of climate-biosphere link. . *EOS, Transactions, American Geophysical Union*, 81, 1-5.

White, M., Asner, G., Nemani, R., Privette, J., & Running, S. (2000). Monitoring fractional cover and leaf area index in arid ecosystems: digital camera, radiation transmittance, and laser altimetry results. *Remote Sensing of Environment*, 74, 45-57.

White, M.A., P. E. Thornton, S. W. Running, R. R. Nemani (2000). Parameterization and sensitivity analysis of the BIOME-BGC terrestirial ecosystem model: net primary production controls. *Earth Interactions*. Paper No. 3

Churkina, G., S.W. Running. (2000) Investigating the balance between timber harvest and productivity of global coniferous forests under global change. *Climatic Change*. 47: 167-191.

Keyser, A.R., J.S. Kimball, R.R. Nemani, S.W. Running. (2000) Simulating the effects of climate change on the carbon balance of North American high latitude forests. *Global Change Biology.* 6: 1-11.

Churkina, G., Running, S. W., & Schloss, A. L. (1999). Comparing global models of terrestrial net primary productivity (NPP): The importance of water availability. *Global Change Biology.* 5, 46-55.

Kimball, J. S., S. W. Running, S. S. Saatchi (1999). Sensitivity of boreal forest regional water flux and net primary production simulations to sub-grid scale landcover complexity. *Journal of Geophysical Research.* 104(D22), 27789-27801.

Nemani, R. R., Running, S. W., Thornton, P. E., & Glassy, J. G. (1999). Monitoring terrestrial net primary production during NASA/EOS era. In: *Proceedings of the International Conference on Global Environmental Monitoring*. Tsukuba, Japan, March 9-11, 1999, 65-68.

Running, S. W., Baldocchi, D. D., Cohen, W. B., Gower, S. T., Turner, D. P., Bawkin, P. S., Hibbard, K. A. (1999). A global terrestrial monitoring network integrating tower fluxes with ecosystem modeling and EOS satellite data.. *Remote Sensing of Environment*. 70, 108-127.

Running, S. W., Collatz, G. J., Washburne, J., & Sorooshian, S. (1999). Chapter 5: Land ecosystems and hydrology. *EOS Science Plan*. 197-260.

Running, S. W., J. B. Way, K. C. McDonald (1999). Radar remote sensing proposed for monitoring freeze-thaw transitions in boreal regions. *EOS, Transactions, American Geophysical Union.* 80(213), 220-221.

Running, S.W. (1999). A blueprint for improved global change monitoring of the terrestrial biosphere. *Proceedings of International Workshop on Land-Surface Water Budget*. Tsukuba, Japan, 271-297.

Thornton, P. E., & Running, S. W. (1999). An improved algorithm for estimating incident daily solar radiation from measurements of temperature, humidity, and precipitation. *Agriculture and Forest Meteorology*. 93, 211-228.

Waring, R. H., & Running, S. W. (1999). Chapter 2: Remote sensing requirements to drive ecosystem models at the landscape and regional scale. *Integrating Hydrology, Ecosystem Dynamics and Biogeochemistry in Complex Landscapes*. 23-37.

White, M. A., Running, S. W., & Thornton, P. E. (1999). The impact of growing season length variability on carbon assimilation and evapotranspiration over 88 years in the eastern U.S. deciduous forests. *International Journal of Biometeorology.* 42, 139-145.

Churkina, G., & Running, S. W. (1998). Contrasting climatic controls on the estimated productivity of different biomes. *Ecosystems.* 1(2), 206-215.

Cienciala, E., Running, S. W., Lindroth, A., Grelle, A., & Ryan, M. G. (1998). Analysis of carbon and water fluxes from the NOPEX boreal forest: comparison of measurements with FOREST-BGC simulations. *Journal of Hydrology.* 212-213, 62-78.

Justice, C., Vermote, E., Townshend, J. R. G., Defries, R., Roy, D. P., Hall, D. K., Salomonson, V. V., Privette, J., Riggs, G., Strahler, A., Lucht, W., Myneni, R., Knjazihhin, Y., Running, S., Nemani, R., Wan, Z., Huete, A., van Leeuwen, W., Wolfe, R., (1998). The Moderate Resolution Imaging Spectroradiometer (MODIS): Land remote sensing for global change research. I*EEE Transactions on Geoscience and Remote Sensing.* 36(4), 1228-1249.

Knyazikhin, Y., Martonchik, J. V., Myneni, R. B., Diner, D. J., & Running, S. (1998). Synergistic algorithm for estimating vegetation canopy leaf area index and fraction of absorbed photosynthetically active radiation from MODIS and MISR data. *Journal of Geophysical Research.* 103(D24), 32257-32276.

Running, S. W. (1998). A Blueprint for Improved Global Change Monitoring of the Terrestrial Biosphere. *The Earth Observer*. 10.

Waring, R. H., & Running, S. W. (1998). . *Forest Ecosystems: Analysis at Multiple Scales*. (Book)

White, J. D., Running, S. W., Nemani, R., Keane, R. E., & Ryan, K. C. (1998). Measurement and remote sensing of LAI in Rocky Mountain Montana ecosystems. *Canadian Journal of Forest Research.* 27(11), 1714-1727.

White, J. D., Running, S. W., Thornton, P. E., Keane, R. E., Ryan, K. C., Fagre, D. B., & Key, C. H. (1998). Assessing simulated ecosystem processes for climate variability research at Glacier National Park, USA. *Ecological Applications.* 8(3), 805-823.

Coughlan, J. C., & Running, S. W. (1997). Regional ecosystem simulation: A general model for simulating snow accumulation and melt in mountainous terrain. *Landscape Ecology.* 12(3), 119-136.

Kimball, J., Running, S. W., & Nemani, R. (1997). An improved method for estimating surface humidity from daily minimum temperature. *Agricultural and Forest Meteorology.* 85(1-2), 87-98.

Kimball, J.S., M. A. White, S. W. Running. (1997). BIOME-BGC simulations of stand hydrologic processes for BOREAS. *Journal of Geophysical Research.* 102(D24), 20043-20051.

Myneni, R. B., Ramakrishna, R., Nemani, R., & Running, S. (1997). Estimation of global leaf area index and absorbed par using radiative transfer models. *IEEE Transactions on Geoscience and Remote Sensing*. 35(6), 1380-1393.

Nemani, R. R., & Running, S. W. (1997). Landcover characterization using multi-temporal red, near-IR and thermal-IR data from NOAA/AVHRR. *Ecological Applications.* 7(1), 79-90.

Schimel, D. S., S. W. Running (VEMAP Participant), B. H. Braswell (1997). Continental scale variability in ecosystem processes: models, data, and the role of disturbance. *Ecological Monographs.* 67, 251-271.

Thornton P. E., Running, S. W., & White, M. A. (1997). Generating surfaces of daily meteorological variables over large regions of complex terrain. *Journal of Hydrology.* 190(3-4), 214-251.

White, J. D., S. W. Running, R. R. Nemani, R. E. Keane, K. C. Ryan (1997). Measurement and remote sensing of LAI in Rocky Mountain montane ecosystems. *Canadian Journal of Forest Research.* 27, 1714-1727.

White, M. A., Thornton, P. E., & Running, S. W. (1997). A continental phenology model for monitoring vegetation responses to interannual climatic variability. *Global Biogeochemical Cycles*. 11(2), 217-234.

Baldocchi, D., Valentini, R., Running, S., Oechel, W., & Dahlman, R. (1996). Strategies for measuring and modeling carbon dioxide and water vapour fluxes over terrestrial ecosystems. *Global Change Biology*. 2, 159-168.

Chase, T. N., Pielke, R. A., Kittel, T. G. F., Running, S. W., & Nemani, R. (1996). Sensitivity of a general circulation model to global changes in leaf area index. J*ournal of Geophysical Research*. 101(D3), 7393-7408.

Coughlan, J. C., & Running, S. W. (1996). Biophysical aggregations of a forested landscape using an ecological diagnostic system. *Transactions on GIS.* 1(1), 25-39.

Hunt, E. R., Piper, S. C., Nemani, R., Keeling, C. D., Otto, R. D., & Running, S. W. (1996). Global net carbon exchange and intra-annual atmospheric CO2 concentrations predicted by an ecosystem process model and three-dimensional atmospheric transport model. *Global Biogeochemical Cycles*. 10(3), 431-456.

Keane, R. E., Ryan, K., & Running, S. W. (1996). Simulating effects of fire on northern Rocky Mountain landscapes using the ecological process model FIRE-BGC. *Tree Physiology.* 16(3), 319-331.

Korol, R. L., Milner, K. S., & Running, S. W. (1996). Testing a mechanistic model for predicting stand and tree growth. *Forest Science.* 42(2), 139-153.

Kremer, R. G., & Running, S. W. (1996). Simulating seasonal soil water balance in contrasting semi-arid vegetation communities. *Ecological Modeling.* 84(1-3), 151- 162.

Kremer, R. G., Hunt, Jr, E. R., Running, S. W., & Coughlan, J. C. (1996). Simulating vegetational and hydrologic responses to natural climatic variation and GCM-predicted climate change in a semi-arid ecosystem in Washington, USA. *Journal of Arid Environments.* 33(1), 23-38.

Milner, K. S., Running, S. W., & Coble, D. W. (1996). A biophysical soil/site model for estimating potential productivity of forested landscapes. *Canadian Journal of Forest Research*. 26(7), 1174-1186.

Nemani, R., & Running, S. W. (1996). Implementation of a hierarchical global vegetation classification in ecosystem function models. *Journal of Vegetation Science.* 7(3), 337-346.

Nemani, R., Running, S. W., & Pielke, R. A. (1996). Global vegetation cover changes from coarse resolution satellite data. *Journal of Geophysical Research-Atmospheres.* 101(D3), 7157-7162.

Thornton, P. E., & Running, S. W. (1996). Generating daily surfaces of temperature and precipitation over complex topography. *GIS and Environmental Modeling: Progress and Research Issues.* 93-98.

Valentini, R., D. Baldocchi, S.W. Running (1996). The IGBP-BAHC global flux network initiative (FLUXNET): current status and perspectives. *Global Change Newsletter*. (28), 14-16.

White, J. D., Ryan, D. C., Key, C. C., & Running, S. W. (1996). Remote sensing of forest fire severity and vegetation recovery. *International Journal of Wildland Fire.* 6(3), 125-136.

Zheng, D., Hunt, Jr., E. R., & Running, S. W. (1996). Comparison of available soil water capacity estimated from topography and soil series information. *Landscape Ecology*. 11(1), 3-14.

Korol, R.L., S.W. Running, K.S. Milner (1995). Incorporating inter-tree competition into an ecosystem model. *Canadian Journal Forest Research.* 25, 413-424.

Nemani, R. R., & Running, S. W. (1995). Satellite monitoring of global landcover changes and their impact on climate. *Climatic Change.* 31(2-4), 395-413.

Pierce, L.L., S.W. Running. (1995). The effects of aggregating sub-grid land surface variation on large-scale estimates of net primary production. *Landscape Ecology.* 10(4), 239-253.

Running, S. W. et al. (1995). Vegetation/ecosystem modeling and analysis project: Comparing biogeography and biogeochemistry models in a continental-scale study of terrestrial ecosystem responses to climate change and CO2 doubling. *Global Biogeochemical Cycles.* 9(4), 407-437.

Running, S. W., Justice, C. O., Salomonson, V., Hall, D., Barker, J., Kaufman, Y. J., Strahler, A. H., Huete, A. R., Muller, J.-P., Vanderbilt, V., Wan, Z.-M., Teillet, P., & Carneggie, D. (1995). Terrestrial remote sensing science and algorithms planned for EOS/MODIS. *International Journal of Remote Sensing.* 15(17), 3587-3620.

Running, S. W., Loveland, T. R., Pierce, L. L., Nemani, R. R., & Hunt, E. R. (1995). A remote sensing based vegetation classification logic for global landcover analysis. *Remote Sensing of Environment.* 51(1), 39-48.

Ford, R., S.W. Running, R.R. Nemani (1994). A modular system for scalable ecological modeling. *IEEE Computational Science and Engineering*. 1, 32-44.

Glassy, J., S.W. Running (1994). Validating diurnal climatology logic of the MT-CLIM logic across a climatic gradient of Oregon. *Ecological Applications.* 4, 248-257.

Pierce, L.L., S.W.Running, J.Walker (1994). Regional-scale relationships of leaf area index to specific leaf area and leaf nitrogen content. *Ecological Applications*. 4, 313-321.

Running, S. W., Loveland, T. R., Pierce, L. L. (1994). A vegetation classification logic based on remote sensing for use in global biogeochemical models. *Ambio*. 23, 77-81.

Running, S.W. (1994). Testing FOREST-BGC ecosystem process simulations across a climatic gradient in Oregon. *Ecological Applications.* 4, 238-247.

Running, S.W., C.O.Justice, V.Salomonson, D.Hall, J.Barker, Y.J.Kaufmann, A.H.Strahler, A.R.Huete, J-P.Muller, V.Vanderbilt, Z.M.Wan, P.Teillet, D.Carneggie (1994). Terrestrial remote sensing science and algorithms planned for EOS/MODIS. *International Journal of Remote Sensing*. 15(17), 3587-3620.

White, J.D., S.W. Running (1994). Testing scale dependent assumptions in regional ecosystem simulations. *Journal of Vegetation Science.* 5, 687-702.

Band, L.E. P.Patterson, R.R. Nemani, S.W. Running (1993). Forest ecosystem processes at the watershed scale: incorporating hillslope hydrology. *Agriculture Forest Meteorology.* 63, 93-126.

Kremer, R.G., S.W. Running (1993). Community type differentiation using NOAA/AVHRR data within a sagebrush-steppe ecosystem. *Remote Sensing of Environment.* 47, 1-25.

Nemani, R. R., Pierce, L. L., Running, S. W., & Band, L. (1993). Forest ecosystem processes at the watershed scale: Sensitivity to remotely sensed leaf area index estimates. *International Journal of Remote Sensing.* 14(13), 2519-2534.

Nemani, R., Pierce, L., Running, S., & Goward, S. (1993). Developing satellite-derived estimates of surface moisture status. *Journal of Applied Meteorology.* 32(3), 548-557.

Nemani, R.R., L.Pierce, L.E.Band, S.W. Running (1993). Forest ecosystem processes at the watershed scale: sensitivity to remotely sensed leaf area index observations. *International Journal of Remote Sensing.* 14, 2519-2534.

Nemani, R.R., S.W.Running, L.E.Band, D.L.Peterson (1993). Regional hydro-ecological simulation system: an illustration of the integration of ecosystem modeling with a GIS. *Environmental Modeling with GIS.* 296-304.

Pierce, L.L., K.Walker, T.Dowling, T.McVicar, T.Hatton, S.Running, J.Coughlan (1993). Ecohydrological changes in the Murray-Darling Basin. III. A simulation of regional hydrological changes. *Journal of Applied Ecology.* 30, 283-294.

Running, S.W. (1993). Modeling terrestrial carbon cycles at varying temporal and spatial resolutions. *The Global Carbon Cycle.* 201-218.

Running, S.W., K.S.Milner (1993). Extrapolating forest ecosystem processes from tree to landscape scales. *Modeling Sustainable Forest Ecosystems.* 1-15.

Running,S.W., E.R. Hunt Jr. (1993). Generalization of a forest ecosystem process model for other biomes, BIOME-BGC, and an application for global-scale models. In: *Scaling Processes Between Leaf and Landscape Levels.* 141-158.

Zheng, D., E.R.Hunt Jr., S.W. Running. (1993). A daily soil temperature model based on air temperature and precipitation for continental applications. *Climatic Research.* 2, 183-191.

Hunt, E. R., & Running, S. W. (1992). Effects of climate and lifeform on dry matter yield from simulations using BIOME-BGC. *Proceedings of IGARSS '92 - International Geoscience and Remote Sensing Seminar.* 2, 1631-1633.

Hunt, E.R.Jr., S.W. Running (1992). Simulated dry matter yields for aspen and spruce stands in the North American Boreal forest. *Canadian Journal of Remote Sensing.* 18, 126-133.

Band, L.E., D.L. Peterson, S.W. Running, J.Coughlan, R.Lammers, J.Dungan, R. Nemani (1991). Forest ecosystem processes at the watershed scale: basis for distributed simulation. *Ecological Modeling.* 56, 171-196.

Hunt, E.R. Jr., F.C.Martin, S.W.Running (1991). Simulating the effects of climatic variation on stem carbon accumulation of a ponderosa pine stand: comparison with annual growth increment data. *Tree Physiology*. 9, 161-172.

Hunt, E.R. Jr., S.W. Running, T.A. Federer. (1991). Extrapolating plant water flow resistances and capacitances to regional scales. *Agriculture and Forest Meteorology*. 54, 169-195.

Riggs, G.A., S.W. Running (1991). Detection of canopy water stress in conifers using the airborne imaging spectrometer. *Remote Sensing of Environment*. 35, 51-68.

Roughgarden, J., S.W.Running, P.A.Matson (1991). What does remote sensing do for Ecology?. *Ecology*. 72, 1918-1922.

Running, S.W. (1991). Computer simulation of regional evaportranspiration by integrating landscape biophysical attributes with satellite data. In: *Land Surface Evaporation: Measurement and Parameterization*. 359-369.

Hunt, E.R.Jr., S.W. Running. (1990) Problems with scaling leaf water relations to regional scales. IN: *1990 Proceedings International Geosciences and Remote Sensing Symposium*. pp. 1259-1262.

Pierce, L.L., S.W.Running, G.A.Riggs. (1990) Remote detection of canopy water stress in coniferous forests using the NS001 thematic mapper simulator and the thermal infrared multispectral scanner. *Photogrammetric Engineering and Remote Sensing*. 56: 579-586.

Riggs, G.A., S.W.Running. (1990) Estimating forest water stress with high resolution imaging spectrometer. IN: *1990 Proceedings International Geosciences and Remote Sensing Symposium*. pp. 893-896.

Running, S.W. (1990) Estimating terrestrial primary productivity by combining remote sensing ecosystem simulation. In: *Ecological Studies, Vol. "Remote Sensing of Biosphere Functioning."* H. Mooney and R. Hobbs. Eds., Springer-Verlag, pp. 65-86.

Running, S.W. (1990) A modified integrated NDVI for improving estimates of terrestrial net primary production. In: *Proceedings Society of Optical Engineering*, Orlando, FL, 17-21, April 1990.

Running, S.W., J.C. Coughlan, D.L.Peterson, L.E. Band. (1990) Mapping regional forest evapotranspiration and photosynthesis by coupling satellite data with ecosystem simulation. In: *1990 Proceedings International Geosciences and Remote Sensing*. pp. 265-268.

Spanner, M.A., L.L. Pierce, S.W. Running, D.L. Peterson. (1990) Remote sensing of temperate coniferous forest leaf area index: The influence of canopy closure, understory vegetation and background reflectance. *International Journal of Remote Sensing.* 11: 95-111.

Spanner, M.A., L.L. Pierce, D.L. Peterson, S.W. Running. (1990) The Seasonality of AVHRR Data of Temperate coniferous forests: Relationship with Leaf Area Index. *Remote Sensing Environ.* 33: 99-112.

Coughlan, J.C., S.W. Running. (1989) An expert system to aggregate forested landscapes within a geographic information system. *Artificial Intelligence Applications in Natural Resource Management* 3: 35-43.

Hungerford, R.D., S.W. Running, R.R. Nemani, J.C. Coughlan. (1989) MTCLIM: A mountain microclimate extrapolation model. *USDA Forest Service. INT Res. Paper INT 414* 52pp.

Nemani, R.R., S.W. Running. (1989) Estimation of regional surface resistance to evapotranspiration from NDVI and thermal infrared AVHRR data. *Journal of Applied Meteorology*. 28: 276-284.

Nemani, R.R., S.W. Running. (1989) Testing a theoretical climate-soil-leaf area hydrologic equilibrium of forests using satellite data and ecosystem simulation. *Agriculture and Forest Meteorology*. 44: 245-260.

Peterson, D.L., S.W. Running, J.D. Aber. (1989) Analysis of airborne multi-spectral imagery for forest ecosystem parameters. In: *3rd Interagency Airborne Science Workshop*. La Jolla, Calif. Feb 21-24, 1989.

Running, S.W., R.R. Nemani, D.L. Peterson, L.E. Band, D.F. Potts, L.L. Pierce, M.A. Spanner. (1989) Mapping regional forest evapotranspiration and photosynthesis by coupling satellite data with ecosystem simulation. *Ecology*. 70: 1090-1101.

Meeting Report of the MODIS Vegetation Workshop II at Univ. Montana, Aug 17-19, 2004.

Submitted to AGU Eos, 16 Sept 2004.

GLOBAL LAND DATASETS for NEXT GENERATION BIOSPHERIC MONITORING

The Mauna Loa atmospheric CO_2 record initiated in 1957 was the first dataset to show that the entire Earth was being impacted by human activity. C.D. Keeling relived the history and current trends of that CO_2 dataset in a keynote address at a recent earth observation meeting where next generation capabilities in global biospheric monitoring were unveiled. The 2nd MODIS Vegetation Workshop Aug 17-19 at the University of Montana, was attended by 170 scientists from 27 states and 19 countries.

The MODIS (Moderate Resolution Imaging Spectroradiometer) is a visible/infrared optical sensor launched on both the Terra Dec 1999, and more recent (May 2002) Aqua platforms of the NASA Earth Observing System to provide daily global moderate resolution earth observation at 250-1000m spatial resolution. The MODIS Land Science Team since 1990 has developed algorithms to analyze the spectral data to produce biophysical variables globally over 110 million km^2 of land surface for global science http://modis-land.gsfc.nasa.gov/products/ .

Since the first MODIS Vegetation Workshop in July 2002, there have been significant improvements in the quality and quantity of processed and available global vegetation datasets. For example, the geolocation accuracy of the MODIS land data now averages around 50m, substantially better than the original sensor technical specification of 150m. The current forward processing is now accomplished within 1 day of acquisition by the Terra and Aqua platforms. Daily MODIS data production at the Goddard Space Flight Center is about 742GB/day, of which the Land data is 330GB/day. The entire Terra MODIS land dataset has now been reprocessed four times, beginning from March 2000, to improve the performance of algorithms for each variable, and to build absolute processing consistency for the entire period of record, a basic requirement for global change science. This Land dataset is archived and distributed from the Eros Data Center, where MODIS holdings now exceed 500Tb, and about 0.5TB/day of MODIS land datasets are distributed to interested users world wide from the website at http://edcdaac.usgs.gov/modis/dataproducts.asp .

Full technical details of each algorithm are available here, and the latest users guides. In addition, a variety of reprojection, reformatting, browse, search and ordering tools now are available.

The MODIS Land processing system is sequential and interdependent, providing substantial advantages to higher level data products. The raw MODIS sensor data is first calibrated to absolute radiances, and geolocated. Next, cloud masking and atmospheric aerosol corrections are done, dependent on the land/sea masking and landcover computed in previous processing iterations. These atmospheric corrections inhance the radiometric accuracy and sensitivity of all resulting spectral land data products. The land surface spectral reflectances are then the input data for Level 2 algorithms computing snow and sea ice cover, land vegetation cover type, albedo, bidirectional reflectance distribution function (BRDF), land surface temperature and emissivity, fire disturbances. Global snowcover, computed at 500m and updated every 8 days, has a large seasonal range from >50 million km^2 in winter to <5 million km^2 in summer in the northern hemisphere. The radiometric quality of MODIS is proving to be excellent. For example, the land surface temperatures range from 190 – 340degK, and validations have shown accuracy to 1degK. Weather forecasting models are now ingesting these land surface energy balance variables to provide current land surface conditions updated daily for the forecasts.

Quantifying landcover type, and detecting changes in landcover resulting from either climatic forcings or human or natural disturbances is fundamental to assessing global change of the biosphere. The MODIS Landcover uses a full year of seven spectral channels at 250m and 500m resolution, normalized to nadir reflectances, to generate a global 1km landcover that is updated annually and defines 17 landcover types, including 14 vegetated classes. Classification accuracy for the 2001 dataset was globally around 80%. One spinoff of this effort is substantial improvements in land/sea and urban masking used in many global climate and biospheric modeling activities. Another related activity involves computing a continuous field of bare ground and forest cover, rather than attempting to define discrete classes that separate forest from savannah from grasslands for example. The fractional forest cover estimate between 0 – 100% is made at 1km globally using 500m spectral data from MODIS and is updated annually.

Another important derivation of landcover data is following large-scale disturbances such as wildfire and agricultural burning. Fire influences an estimated 1 – 8 million km^2 per year, producing around 4Pg of carbon emissions and is a substantial land management activity in many agricultural areas. The MODIS fire dataset is computed using a channel with high saturation temperature of 500degC, and includes daily mapping of the area of active fires and a final evaluation of the area burned after the fire ends.

Global vegetation analysis was pioneered with the Normalized Difference Vegetation Index (NDVI), computed from 2 spectral channels of AVHRR data since 1981. Now with MODIS, both a standard NDVI and an Enhanced Vegetation Index are produced every 16 days at 250m, 500m and 1km using both the 1030 AM overpass Terra MODIS and the 1330 overpass Aqua MODIS. The EVI uses red, near-infrared and blue wavelength channels that reduces both atmospheric and soil background contamination of the vegetation signal desired. The effects of multi-year drought on declining vegetation density in the Southwestern US are clear in the 2000-2003 time series.

One of the major advances in the MODIS land dataset is regular global production of advanced biophysical variables that go beyond simple spectral indices such as NDVI. Leaf area index (LAI), and the fraction of absorbed photosynthetically active radiation (FPAR) are measures of vegetation canopy density used for advanced modeling of climate, carbon cycles and water balance of the land surface. The MODIS LAI/FPAR dataset now extends four years, is produced every 8 days at 1km, and since mid-2002, the Terra and Aqua MODIS data are combined to provide the most complete cloud-free image possible. Current validation activities show good success for all except high LAI evergreen forest biomes. The LAI/FPAR datastream is then used as input for a daily gross primary production and annual net primary production algorithm (GPP/NPP). The daily GPP, reported every 8 days at 1km and annual NPP are components of the land carbon cycle, and provide a first step in CO2 source sink analysis for land surfaces. This MODIS GPP/NPP algorithm was used on the historical NDVI record from 1981-1999 to discern that a 6% increase in global terrestrial NPP has occurred over that 18yr period. A monthly and annual anomaly map is now being generated to follow current trends in global NPP.

Two new experimental products were reported on, a canopy water content metric based on a spectral reflectance index, and an evaporative index based on surface energy partitioning principles. Both are currently under development so have not been produced regularly, but both will have high value for regional drought analysis, wildfire ignition potential, and water management.

Validation of global datasets requires coordinated global test sites and field measurements. The FLUXNET system is a coordinated network of 190 eddy flux towers distributed across all biome types that measure CO_2, energy and water vapor fluxes continuously from micrometeorological towers. The Ameriflux regional network in North America, Euroflux in Europe, Asiaflux in Japan, and Ozflux in Australia all are actively testing the MODIS land datasets against their local measures of ecosystem metabolism. These networks are evaluating the MODIS Landcover, LAI, and GPP data to interpret the daily flux measurements. For example, both the MODIS FPAR and GPP registered roughly 20% reductions during the summer 2003 as vegetation responded to the drought and heat wave in central Europe. The Bigfoot project develops statistically valid multi-kilometer field sampling of these data for validation with the 1km MODIS datasets. Field vs MODIS data comparisons have been completed for arctic tundra, boreal forests, temperate grasslands, crops, and temperate deciduous and evergreen forests. These networks originated in international science planning from the International Geosphere-Biosphere Program, and the Global Terrestrial Observing System of the World Climate Research Program.

The MODIS sensor on Terra is now scheduled to operate until 2008, and the Aqua sensor may operate until 2010. Continuity of the global change measurements initiated by MODIS will be part of the National Polar Orbiting Environmental Satellite System (NPOESS). An optical/thermal sensor very similar to MODIS is planned, the Visible Infrared Imaging Radiometer Suite (VIIRS), that will have nested 375 and 750m nadir resolution, and 22 spectral channels. It will retain most of the heritage from MODIS of on-board radiometric calibration, orbital stability, prelaunch calibration, and the kind of global vegetation datasets from MODIS presented at this conference. Global change can only be detected by consistent continuous observation of the earth for many decades. The science community only now is beginning to have a global satellite record of this length, and papers were presented on merging the global AVHRR vegetation index record from 1981 to the present with MODIS from 2000 – 2010, and ultimately with VIIRS from 2006 – future. A NPOESS Preparatory mission is scheduled for launch in 2006 to provide crosscalibration while AVHRR, MODIS and the new VIIRS are all flying.

In the future, terabytes of raw satellite data have to be distilled into a few megabytes of easily interpreted graphics or images for policy and management uses. A prototype for future information development of these satellite datasets was presented where multiple satellite datastreams are integrated with surface meteorology and ground data in real-time to provide agriculture, water management and fire management information for immediate decision making. A future ecological forecasting capability is being assembled using the MODIS data, and driven with the midterm 1-3 month advance weather forecasts.

In addition to the 25 verbal presentations summarized here, 64 posters were presented by other workshop participants, illustrating substantial international utilization of the MODIS Land data. All of the presentation Powerpoint files and posters are available at http://www.ntsg.umt.edu/MODISCon/ .

I know figures are not normally allowed in meeting reports, but suggest this summary figure for the Eos Editors consideration.

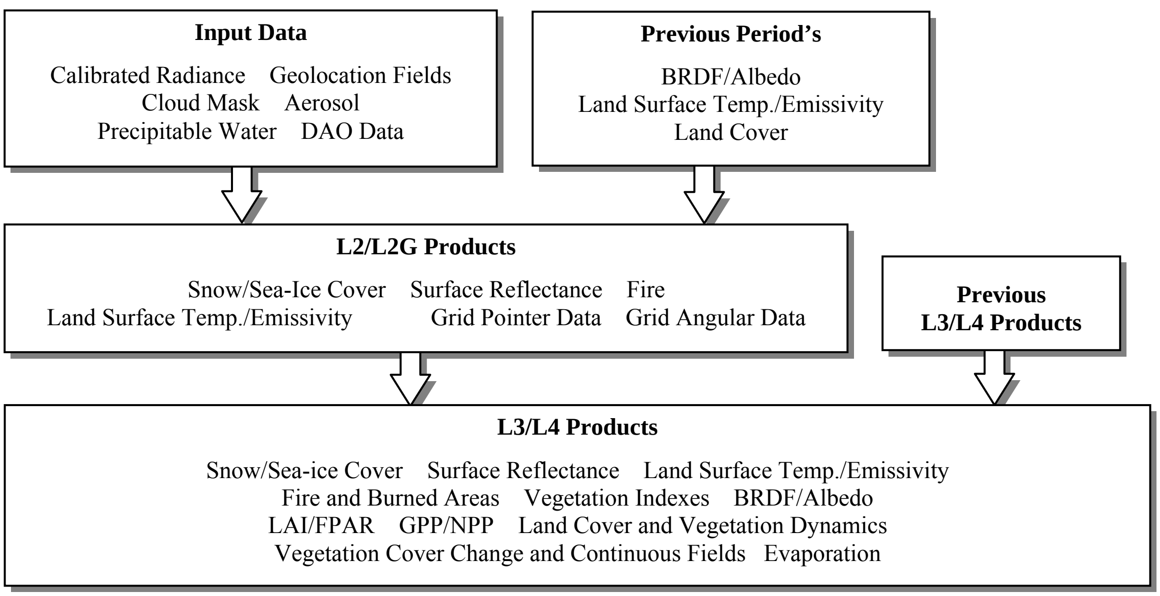

Figure 1. Schematic of the data flow pathway for MODIS Land processing and the dependencies amongst variables.

Professor Steven Running, AGU Fellow
Numerical Terradynamic Simulation Group
University of Montana
Missoula, MT 59812 USA

A Continuous Satellite-Derived Measure of Global Terrestrial Primary Production

STEVEN W. RUNNING, RAMAKRISHNA R. NEMANI, FAITH ANN HEINSCH, MAOSHENG ZHAO, MATT REEVES, AND HIROFUMI HASHIMOTO

Until recently, continuous monitoring of global vegetation productivity has not been possible because of technological limitations. This article introduces a new satellite-driven monitor of the global biosphere that regularly computes daily gross primary production (GPP) and annual net primary production (NPP) at 1-kilometer (km) resolution over 109,782,756 km² of vegetated land surface. We summarize the history of global NPP science, as well as the derivation of this calculation, and current data production activity. The first data on NPP from the EOS (Earth Observing System) MODIS (Moderate Resolution Imaging Spectroradiometer) sensor are presented with different types of validation. We offer examples of how this new type of data set can serve ecological science, land management, and environmental policy. To enhance the use of these data by nonspecialists, we are now producing monthly anomaly maps for GPP and annual NPP that compare the current value with an 18-year average value for each pixel, clearly identifying regions where vegetation growth is higher or lower than normal.

Keywords: net primary production, MODIS, carbon cycles, terrestrial remote sensing, biosphere

Earth systems science—the integrated analysis of the atmosphere, oceans, cryosphere, and biosphere as a functioning system—had its origins in the early 1980s. A few years earlier, the introduction of the now famous atmospheric "Keeling curve" for carbon dioxide (CO_2), measured at Mauna Loa, Hawaii, had shown definitively for the first time that humans were progressively changing Earth's total atmosphere (Keeling et al. 1976). Atmospheric scientists had recently completed the first primitive global models of atmospheric circulation. Ocean and cryospheric scientists were taking measurements of ocean temperature and ice sheet area, which, although not global, were certainly regional in scope. Unfortunately, however, ecologists (including the senior author) had no background in addressing ecology at global scales. Before the 1980s, biology focused on the organism level, and ecological studies, at best, embraced a 0.1-hectare (ha) field plot. No global ecological measurement was even considered, so analyzing seasonal trends in atmospheric CO_2 concentrations was the only option for assessing global biospheric activity. In early discussions, ecologists considered measuring vegetation density, canopy height, plant biomass, species classes, and other common ecological variables. Only slowly, by realizing that true global measurements could only be made using satellite remote sensing, did ecologists begin to develop a conceptual basis for computing a satellite-based estimate of net primary production (NPP).

From a theoretical standpoint, NPP marks the first visible step of carbon accumulation; it quantifies the conversion of atmospheric CO_2 into plant biomass. The earliest attempts to evaluate ecosystem processes such as NPP at a global scale were made by geographers, and the famous estimates by Lieth and Whittaker (1975) of global NPP are still quoted today. These estimates were based on regressions of temperature data from about a thousand weather stations, computed to a simple annual measure of actual evapotranspiration (AET) in millimeters (mm) per year and then regressed against a handful of NPP field plots. The resulting equation,

$$NPP = 3000\{1 - \exp[-0.0009695(AET - 20)]\},$$

was used to compute and map the first global estimate of NPP (118 billion metric tons per year of biomass) from essentially transformed and coarsely extrapolated meteorology data.

Three activities that first evolved in the early 1980s proved to be the foundations of global-scale terrestrial ecology. First,

Steven W. Running (e-mail: swr@ntsg.umt.edu) is a professor and director, Faith Ann Heinsch and Maosheng Zhao are research personnel, Matt Reeves is a graduate research assistant, and Hirofumi Hashimoto is a visiting graduate student in the Numerical Terradynamic Simulation Group, Department of Ecosystem and Conservation Sciences, University of Montana, Missoula, MT 59812. Ramakrishna R. Nemani is a research scientist in the Earth Science Division at the National Aeronautics and Space Administration, Ames Research Center, Moffett Field, CA 94035.

the expansion of atmospheric flask sampling to many additional sites made it possible to draw inferences on a biospheric scale about the photosynthetic uptake of CO_2 in summer, and the evolution of CO_2 in winter, in the Northern Hemisphere (Tans et al. 1990). Second, the global climate models began including simple submodels of land surface processes that incorporated some basic ecology (e.g., physiological controls by stomata on leaf gas exchange; structural vegetation measures such as leaf area index [LAI]). The biosphere-atmosphere transfer scheme, or BATS (Dickinson 1996), laid the foundation for all future representations of terrestrial vegetation in global climate models, such as the well-known SiB (simple biosphere) model of Sellers and colleagues (1986). Third, a few ecologists, most notably Compton J. Tucker of the National Aeronautics and Space Administration (NASA), began exploring data from meteorological satellites (i.e., AVHRR, or Advanced Very High Resolution Radiometer) to see whether some measure of vegetation was discernible. The cover of *Science* in August 1985 inaugurated global vegetation analysis, showing the first NDVI (normalized difference vegetation index) image of the African continent (Tucker et al. 1985).

In the early 1980s, the Reagan administration discouraged NASA from using the fledgling Earth remote sensing only for applications like crop yield analysis (the AgriStars and Lacie programs begun in the 1970s), urging that the technology be used to pursue more "big science" projects. These Reagan administration policies encouraged NASA to begin a new focus on global ecology. Early workshops were brainstorming sessions on "land-related global habitability science issues" (NASA 1983), exploring what kind of ecology could possibly be accomplished globally. It was not long before some initial exploration correlated the annual time series of NDVI to annual NPP, the first step in translating the radiometric index of NDVI to a real ecosystem variable (Goward et al. 1985). Analysis of growing-season dynamics, relating 7-day composites of NDVI to simulations of weekly photosynthesis and transpiration, showed the potential for satellite remote sensing to follow ecosystem canopy processes (Running and Nemani 1988). In the mid-1980s, there were still almost no continuous field measurements of evapotranspiration and photosynthesis; early models of ecosystem biogeochemistry were the only source of information on continuous trends in ecosystem carbon exchange. The late 1980s saw the first ecosystem models driven by remote sensing, operated over a few thousand square kilometers (Running et al. 1989, Burke et al. 1991).

From these beginnings, ecologists have struggled to define and produce a consistent monitor of the terrestrial biosphere, equivalent to the daily weather observations that help develop and test meteorological theory or to the river gauging that serves a similar function for the hydrologic community. Ecologists have sought a repeatable, consistent measurement of the global terrestrial ecosystem that would integrate ecosystem dynamics spatially across Earth's surface (Schimel 1995). This article presents the latest effort to assemble a terrestrial biospheric monitor, a satellite-derived measure of weekly gross primary production (GPP) from vegetation, which can be composited and expressed to provide an estimate of global annual NPP. Although other articles on global primary production have been published (Prince and Goward 1995, Field et al. 1998), they were based on individual research projects, not on products derived from a continuing and expanding standardized data set. The calculations presented here are executed across the entire vegetated land surface every day and distributed globally every 8 days within 2 to 3 days of acquisition. Although the NASA Earth Observing System (EOS) Terra satellite used for these calculations was launched in December 1999, this data set only began dependable production in mid-2002. The MODIS (Moderate Resolution Imaging Spectroradiometer) sensor is used for the spectral reflectances of terrestrial vegetation used for this research. We briefly summarize the algorithm and processing details, describe current validation efforts, and provide some examples of the scientific value and practical applications of the new products.

Theoretical basis of the algorithm for global NPP

The derivation of a satellite estimate of terrestrial NPP has three theoretical components: (1) the idea that plant NPP is directly related to absorbed solar energy, (2) the theory that a connection exists between absorbed solar energy and satellite-derived spectral indices of vegetation, and (3) the assumption that there are biophysical reasons why the actual conversion efficiency of absorbed solar energy may be reduced below the theoretical potential value. We will briefly consider each of these components.

Relating NDVI, APAR, GPP, and NPP. The original logic of John L. Monteith (1972) suggested that the NPP of well-watered and fertilized annual crop plants was linearly related to the amount of solar energy the plants absorbed over a growing season. This logic combined the meteorological constraint of available sunlight reaching a site with the ecological constraint of the amount of leaf area absorbing the solar energy, while avoiding many complexities of canopy micrometeorology and carbon balance theory. Measures of absorbed photosynthetically active radiation (APAR) integrate the geographic and seasonal variability of day length and potential incident radiation with daily cloud cover and aerosol attenuation of sunlight. In addition, APAR implicitly quantifies the amount of leafy canopy that is displayed to absorb radiation (i.e., LAI). A conversion efficiency, ε, translates APAR (in energy units) to final tissue growth, or NPP (in biomass). GPP is the initial daily total of photosynthesis, and daily net photosynthesis (PSN_{net}) subtracts leaf and fine-root respiration over a 24-hour day. NPP is the annual sum of daily net PSN minus the cost of growth and maintenance of living cells in permanent woody tissue.

Sellers (1987) showed that APAR could be estimated from remote sensing. Spectral vegetation indices derived from remotely sensed data have several forms (Huete et al. 2002); the most widely applied currently is NDVI, which is calculated from surface reflectance in red and near-infrared (NIR) wavelengths as

$$NDVI = (NIR - red)/(NIR + red)$$

and

$$APAR/PAR \approx NDVI,$$

where PAR is the incident radiation in photosynthetic wavelengths (in megajoules). Consequently, spectral vegetation indexes such as NDVI most directly quantify the fraction of photosynthetically active radiation (FPAR) that is absorbed (ranging from 0 to 1):

$$FPAR = APAR/PAR \approx NDVI.$$

FPAR and LAI are combined into a MODIS land surface variable that is computed daily and composited at 8-day intervals (Myneni et al. 2002). When FPAR, derived from a spectral vegetation index, is multiplied by daily incident radiation (PAR, in megajoules per square meter) and the conversion efficiency (ε, in grams [g] of carbon per megajoule),

$$GPP = \varepsilon \times FPAR \times PAR \approx \varepsilon \times NDVI \times PAR.$$

An intermediate variable of daily net photosynthesis, PSN_{net}, is computed as

$$PSN_{net} = GPP - R_{lr},$$

where R_{lr} is 24-hour maintenance respiration of leaves and fine roots.

The annual NPP is

$$NPP = \Sigma\,(PSN_{net}) - R_g - R_m,$$

where R_g is the annual growth respiration required to construct leaves, fine roots, and new woody tissues, and R_m is the maintenance respiration of live cells in woody tissues (Running et al. 2000). Combined, these simple relationships derived from a satellite radiometric index, vegetation canopy reflectance properties, and CO_2 fluxes provide the basis for scientists to use remote sensing to extrapolate carbon cycle processes globally.

Biophysical variability of ε. The PAR conversion efficiency, ε, varies widely with different vegetation types (Field et al. 1995, Prince and Goward 1995, Turner et al. 2003a). There are two principal sources of this variability. First, with any vegetation, some photosynthesis is immediately used for maintenance respiration. For the annual crop plants from the original theory of Monteith (1972), these respiration costs were minimal, so ε was typically around 2 g carbon per megajoule. Respiration costs, however, increase with the size of perennial plants. Hunt (1994) found that published ε values for woody vegetation were much lower, from about 0.2 to 1.5 g carbon per megajoule, and hypothesized that this was the result of respiration from the 6% to 27% of living cells in the sapwood of woody stems (Waring and Running 1998).

The second source of variability in ε is attributed to suboptimal climatic conditions. To extrapolate Monteith's original theory, designed for well-watered crops only during the growing season, to perennial plants living year-round, certain severe climatic constraints must be recognized. Evergreen plants such as conifers absorb PAR all during the nongrowing season, yet subfreezing temperatures stop photosynthesis, because leaf stomata are forced to close (Waring and Running 1998). As a global generalization, the algorithm truncates GPP on days when the minimum temperature is below –8 degrees Celsius (°C). High vapor pressure deficits, or VPDs (> 2000 pascals), have also been shown to induce stomatal closure in many species. This level of daily atmospheric water deficit is commonly reached in semiarid regions of the world for much of the growing season. Our algorithm mimics this physiological water stress control, progressively limiting daily GPP by reducing ε when high VPDs are computed from the surface meteorology. We also assume nutrient constraints on vegetation growth to be quantified by limiting leaf area, rather than attempt to compute a constraint through ε. This assumption is not entirely accurate, as ranges of leaf nitrogen and photosynthetic capacity occur in all vegetation types (Schulze et al. 1994). Spectral reflectances are somewhat sensitive to leaf chemistry, so the MODIS-derived FPAR and LAI may represent some differences in leaf nitrogen content, but in an undetermined way.

To quantify these biome- and climate-induced ranges of ε, we simulated global NPP in advance with a complex ecosystem model, Biome-BGC (biome biogeochemical cycles), and computed the ε, or conversion efficiency, from APAR to final NPP. The resulting biome parameter look-up table, or BPLUT, contains parameters for temperature and VPD limits as well as specific leaf area and respiration coefficients for representative vegetation in each biome type (Running et al. 2000, White et al. 2000). Only very general biome types are defined, such as evergreen needleleaf forest, deciduous broadleaf forest, shrubland, savanna, grassland, and cropland. The BPLUT also defines biome differences in carbon storage and turnover rates.

Global surface meteorology. The NASA Data Assimilation Office (DAO) collects data from all available surface weather observations globally every 3 hours. The DAO then interpolates and grids these point data, runs a global climate model on a short time sequence, and produces an estimate of climatic conditions for the world, at 10 meters above the land surface (approximating canopy height conditions) and at a resolution of 1° by 1.25°. From these data, the MODIS NPP algorithm retrieves four measurements: (1) average 24-hour daily temperature (°C), (2) daily 24-hour minimum temperature (°C), (3) actual vapor pressure (derived from DAO specific humidity, in pascals), and (4) incident shortwave solar

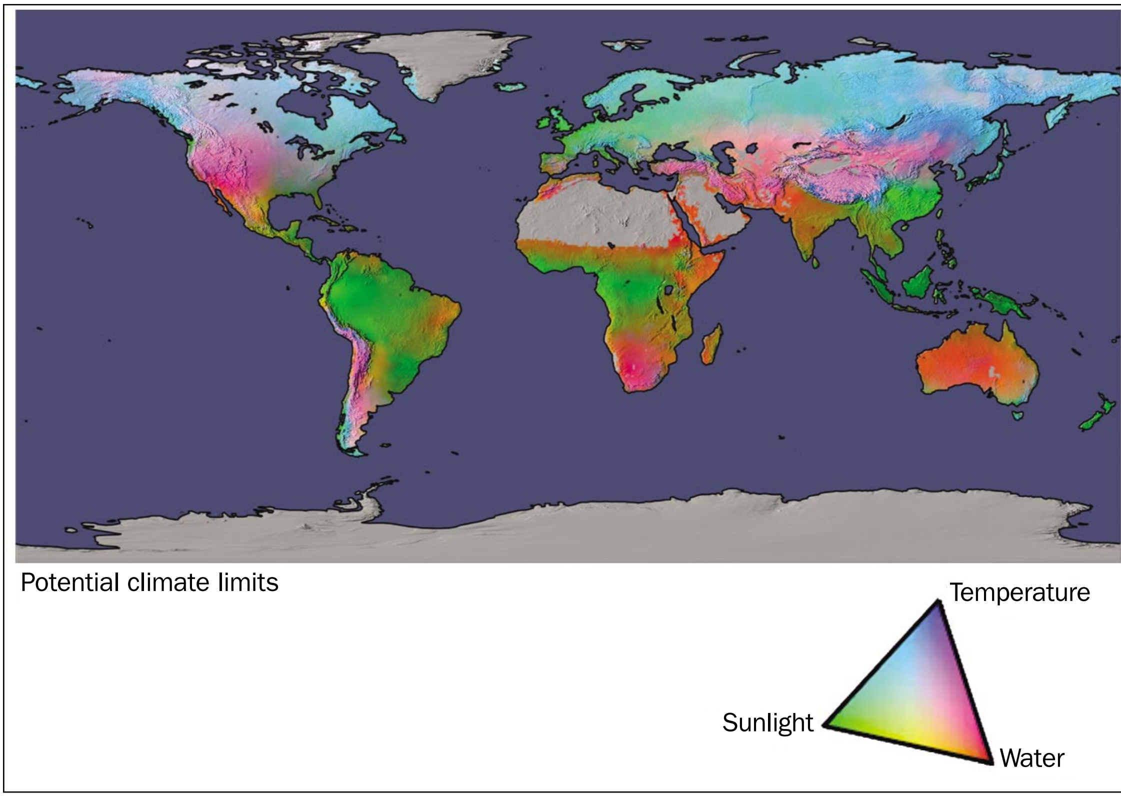

Figure 1. Analysis of the geographic variation in climatic controls of terrestrial net primary production from water, temperature, and radiation limitations. Data are from Nemani and colleagues (2003).

radiation (megajoules per square meter per 3-hour time step). GPP is then computed daily for each 1-square-kilometer (km) pixel with these meteorological data.

Availability and retrieval of global NPP data. Each day, a data system known as EOSDIS (Earth Observing System Data Information System) computes calibrated and atmospherically corrected reflectances from each spectral channel of the MODIS sensor for each cloud-free pixel. To make the daily GPP computation for each global terrestrial pixel, three other variables must first be retrieved: (1) the biome type, which is recomputed annually; (2) the FPAR, which can change weekly during rapid vegetation growth and senescence; and (3) the daily surface climate conditions, which change diurnally.

The final global GPP is computed daily and summed every 8 days for 109,782,756 km^2 of vegetated land area at 1-km spatial resolution. The file to produce this global data set is 2.1 gigabytes in the standard EOS data format, but it can be reduced substantially by translating it into different resolutions and projections. NASA's current policy is that global EOS data sets such as those for GPP and NPP will be available to the international scientific community at no more than the cost of reproduction. The NPP data set is archived and distributed from a NASA-authorized data center within 2 to 3 days of the end of each 8-day computational period (Justice et al. 2002). Full details of the EOS GPP and NPP data availability, and of the algorithms and processing associated with the data, can be found at *www.ntsg.umt.edu/*.

Controls and historic trends of global NPP

Figure 1 gives a sense of the climatic controls and range of global annual NPP, distributed from arctic tundra to tropical rain forests. Water is the factor that limits NPP most strongly on 40% of the land surface, including regions with negative water balances as low as –3000 mm per year (figure 2). Temperature is the strongest limiting factor on 33% of the land surface, with annual temperature ranges from –20°C in arctic tundra to 30°C in deserts. Incident solar radiation is the primary limiting factor in 27% of global vegetated areas, mostly in wet tropical regions where temperatures and water availability are usually adequate (Nemani et al. 2003). While it is easy to imagine boreal areas being temperature limited and deserts being water limited, partial constraints limit the NPP of temperate regions in a complex fashion at different times of the growing season. A temperate mid-latitude forest may be limited by radiation and temperature in winter, by temperature in spring, and by water in midsummer.

Applying the MODIS NPP algorithm to AVHRR satellite data, Nemani and colleagues (2003) evaluated recent trends in global NPP from 1982 through 1999. The somewhat surprising result is that overall global NPP increased by 6.2% during this period, with 25% of global vegetated area showing significant increases and only 7% showing decreasing trends. The complex geographic pattern of these trends (figure 3) illustrates that the Amazon basin accounted for 42% of the increase in global NPP. These trends in NPP are a biospheric response to recent changes in global climate, including higher temperatures, longer temperate growing seasons, more rainfall in some previously water-limited areas, and increased radiation (a result of reduced cloudiness) in regions such as the Amazon basin. Other analyses of the AVHRR NDVI satellite record from 1982 through 1999 for North America have also shown increases in NPP in certain regions (Hicke et al. 2002, Nemani et al. 2002). Alaska and northwestern Canada showed a trend of higher spring temperatures and longer growing seasons; the Midwest agricultural region and New England forests showed higher midsummer NPP correlated with increased precipitation; and the southeastern forests showed longer growing seasons in the fall, optimized by replacing deciduous hardwoods with evergreen pine trees.

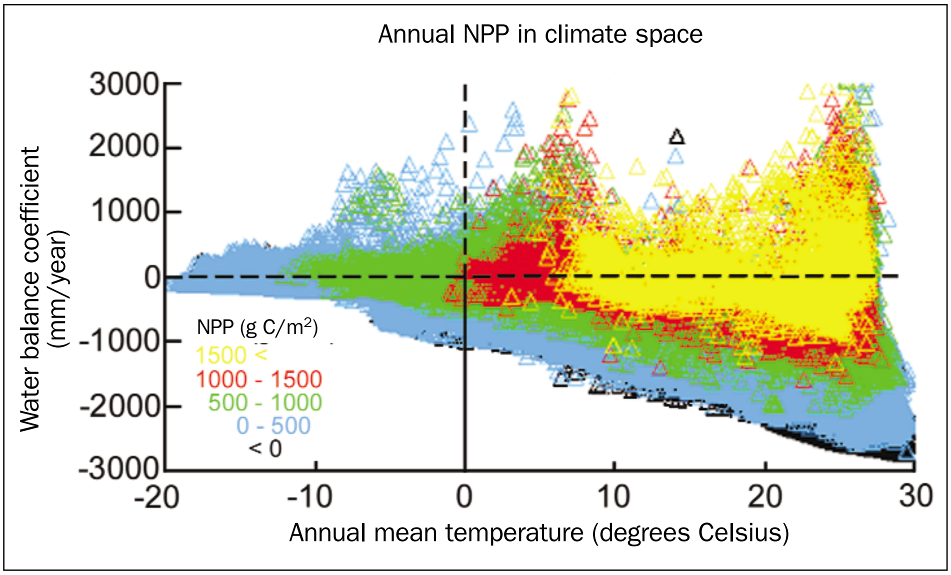

Figure 2. Model of simulated global annual net primary production (NPP) mapped in climate space to show the general range of water availability and temperatures where NPP exists. Modified from Churkina and Running (1998).

Nemani and colleagues (2003) compared the interannual variability of satellite-computed annual NPP with time series of atmospheric CO_2 anomalies. Although we would expect increases in NPP to decrease atmospheric CO_2 by increasing

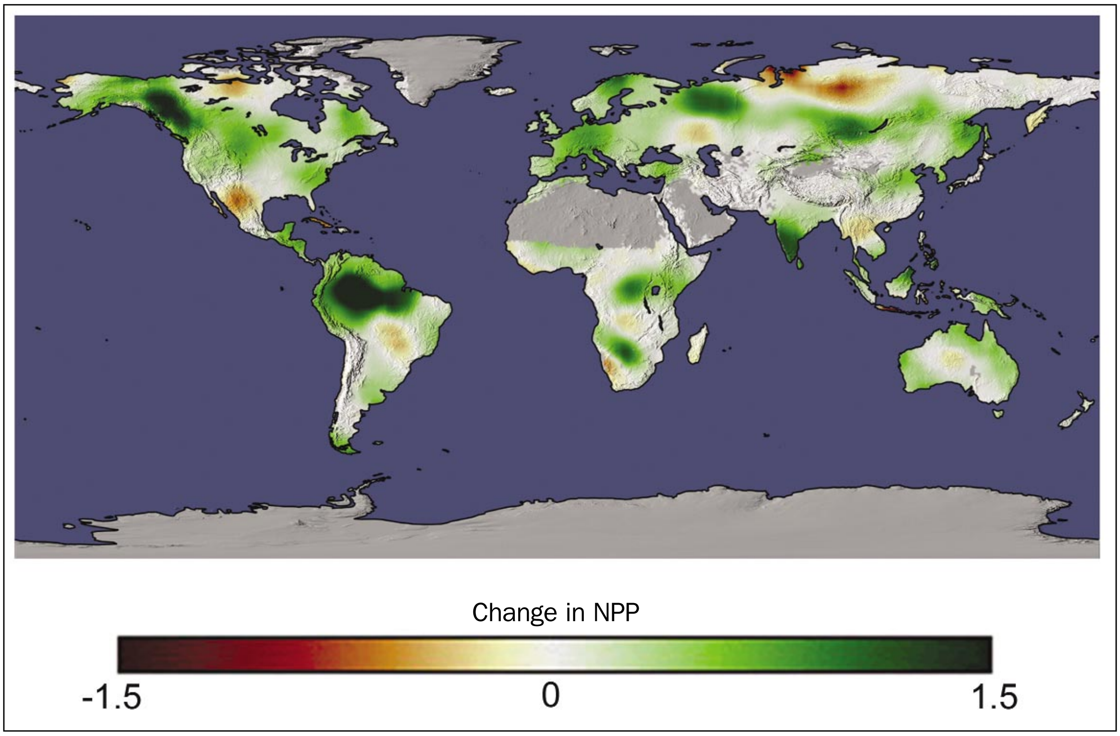

Figure 3. Trends in global net primary production (NPP) anomalies from 1981 through 1999, computed from the historical AVHRR-NDVI (Advanced Very High Resolution Radiometer–normalized difference vegetation index) data set. Data are from Nemani and colleagues (2003).

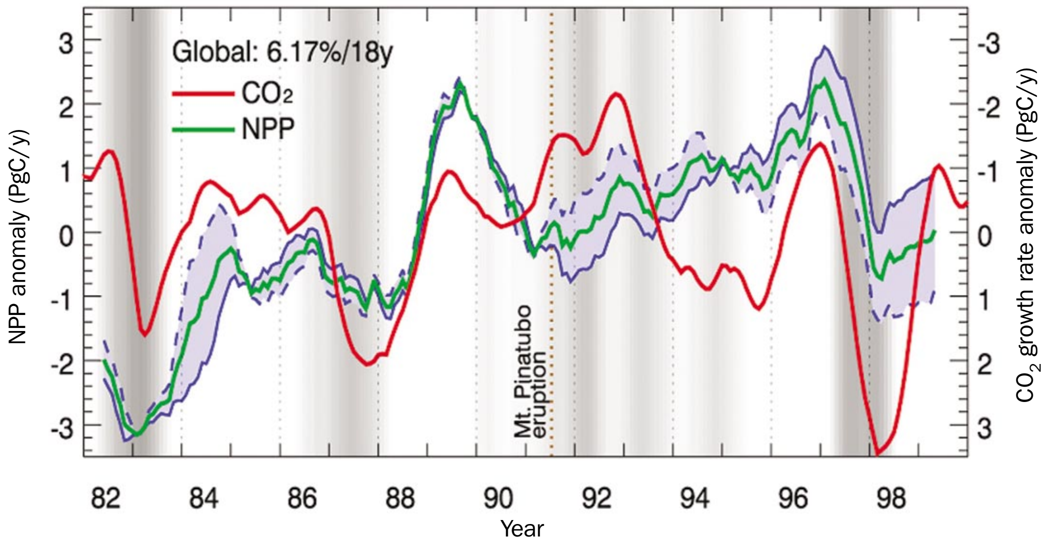

Figure 4. Relationship between the interannual anomaly of global net primary production (NPP) from the MODIS (Moderate Resolution Imaging Spectroradiometer) NPP algorithm and data on atmospheric carbon dioxide (CO_2) concentration, using AVHRR-NDVI (Advanced Very High Resolution Radiometer–normalized difference vegetation index) data from 1981 to 1999 (Nemani et al. 2003). Note that the CO_2 anomaly axis is inverted to align the NPP and CO_2 trends.

photosynthetic uptake, NPP does not include the CO_2 released by heterotrophic respiration. The NPP anomaly from 1982 through 1999 was inversely correlated to the atmospheric CO_2 anomaly, with an r of 0.70 (figure 4). The atmosphere mixes CO_2 sources and sinks with time dynamics somewhat shorter than the 8-day MODIS GPP, but it integrates a spatial area much larger than a 1-km pixel, making interpretations of these correlations difficult.

Validation of the MODIS daily GPP and annual NPP

Validation of a new global data set is daunting, as ideal testing would include measuring daily GPP and annual NPP across a full range of biome types and climates. An algorithm that is successful in a boreal needleleaf forest may be inadequate in a tropical rain-green savanna. Consequently, a global array of validation sites is needed (Morisette et al. 2002). More fundamentally, every measure available to validate GPP and NPP represents a different spatial scale and presents different limitations (Running et al. 1999). Three types of data seem useful for validating global GPP and NPP data: direct measurements of biomass, tower flux measurements, and measurements of atmospheric CO_2 concentration. However, each type of data is limited in its precision or scope. Direct biomass measures of NPP often are only annual, and the sample area is usually less than 1 ha. Tower flux measurements are continuous in time and sample a "footprint" near the MODIS 1-km pixel size, but the flux towers directly measure only net ecosystem exchange (NEE), so NPP and GPP must be derived from carbon balance principles. Measurements of atmospheric CO_2 concentration integrate a large, somewhat undefined land area and include anthropogenic CO_2 emissions, but they are gathered in an instantaneous sampling process that is repeated only monthly. In short, no single measure can match the detail that the MODIS GPP and NPP represent in terms of time, space, and ecosystem attributes. We must therefore employ a set of multiple estimations to define realistic values for daily GPP and annual NPP in time and space.

Ecologists have measured annual NPP through direct sampling of biomass growth increment for decades. Recently, intensive efforts have been made to compile all credible published estimates of terrestrial NPP (Clark et al. 2001, Scurlock and Olson 2002, Zheng et al. 2003). Scurlock and Olson (2002) found the known range of NPP for temporal and boreal biomes to be 20 to 1160 g carbon per square meter per year. Clark and colleagues (2001) estimated that the NPP for tropical forests ranged from 170 to 2170 g carbon per square meter per year. This range of two orders of magnitude in field-measured NPP reflects the large global climatic gradients in temperature and water availability constraining NPP (figure 2). Interannual variability in NPP also reflects these strong climatic constraints. Knapp and Smith (2001) found a range of aboveground NPP from 116 to 744 g carbon per square meter per year across 11 US LTER (Long Term Ecological Research) sites, ranging from arctic tundra to grasslands and deciduous forests. Moreover, in evaluating a decade or more of annual NPP from these sites, they discovered that interannual variability of 20% to 30% was common as the vegetation responded to normal year-to-year variation in precipitation and temperature. We estimate a global annual NPP for 2001 of 57.7 petagrams (Pg) carbon, an average of 509 g carbon per square meter, and an NPP for 2002 of 55.5 Pg carbon, or 489 g carbon per square meter of vegetated land (figure 5).

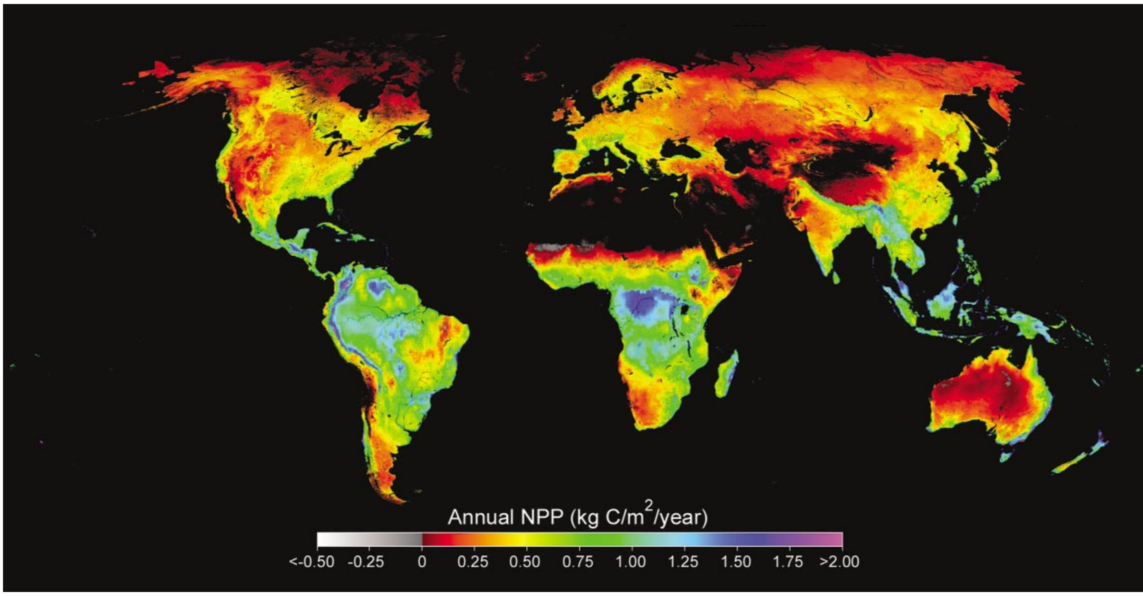

Figure 5. Global terrestrial net primary production (NPP) over 110 million square kilometers for 2002, computed from MODIS (Moderate Resolution Imaging Spectroradiometer) data.

For a more refined test, we checked the range and distribution of NPP produced for different biome types in 2002 (figure 6). The range of MODIS NPP for evergreen needleleaf forests was 150 to 900 g carbon, with a mean of 451 g carbon per square meter per year, close to the mean of 432 g compiled from field data by Zheng and colleagues (2003). Zheng and colleagues found a mean NPP for temperate broadleaf deciduous forests of 635 g carbon, in comparison with the mean of 492 g from our MODIS data set. MODIS estimates of tropical evergreen broadleaf NPP averaged 1218 g carbon per square meter, with a range from 400 to 1800 g. In field measurements of NPP for tropical forests, Clark and colleagues (2001) estimated an NPP ranging from 170 to 2170 g carbon, using extensive measurements from 39 sites. Grassland NPP ranged from 70 to 410 g carbon, with a mean of 203 g, in Zheng and colleagues' (2003) data set. The MODIS grassland NPP, by comparison, showed a mean of 254 g carbon and a maximum of 750 g. These initial comparisons indicate that the MODIS computations of NPP fall within the ranges of existing field data.

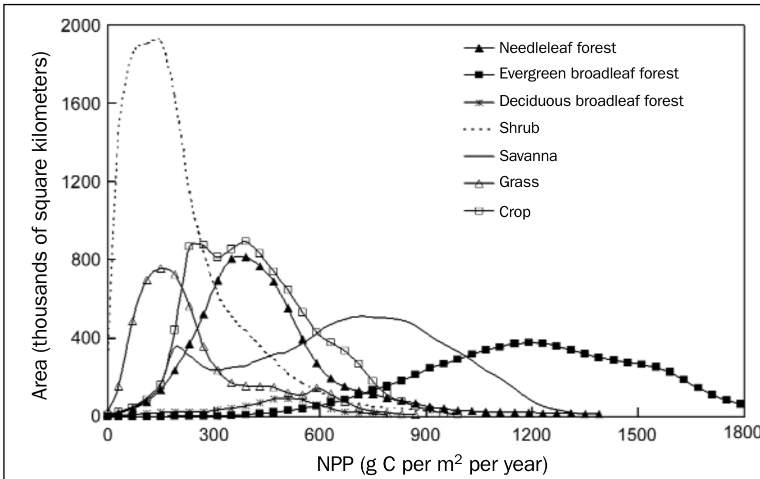

Figure 6. Global areal distribution of terrestrial net primary production (NPP) for 2002 by simple biome types (see figure 5).

Beginning in the early 1990s, scientists organized by the International Geosphere-Biosphere Programme planned an international network of eddy covariance flux stations that would continuously measure CO_2, water, and energy exchange from representative ecosystems (Baldocchi et al. 2001). This network, now called FLUXNET, includes more than 200 tower sites spanning all continents and biome types and providing accurate seasonal measures of vegetation carbon uptake and local land CO_2 balances (Falge et al. 2002). To test the MODIS 8-day GPP, we provide researchers from the AmeriFlux network (*http://public.ornl.gov/ameriflux/*) with estimates of GPP to compare with flux tower–based meteorological data and GPP estimates for 2001. Every 8 days, a window of the MODIS daily GPP (7 by 7 pixels) is retrieved at the exact location of these towers, and we make a direct comparison between the MODIS GPP and tower measurements of vegetation GPP (figure 7). This protocol is being expanded to all global FLUXNET sites in 2004 (see *http://daacl.esd.ornl.gov/FLUXNET/*).

Inputs to the algorithm included LAI and FPAR estimates from MODIS and the most recent version of the DAO global meteorology data set The results indicate that the MODIS algorithm captures the seasonality of site daily GPP quite well across a wide array of climates (figure 7). From the earliest

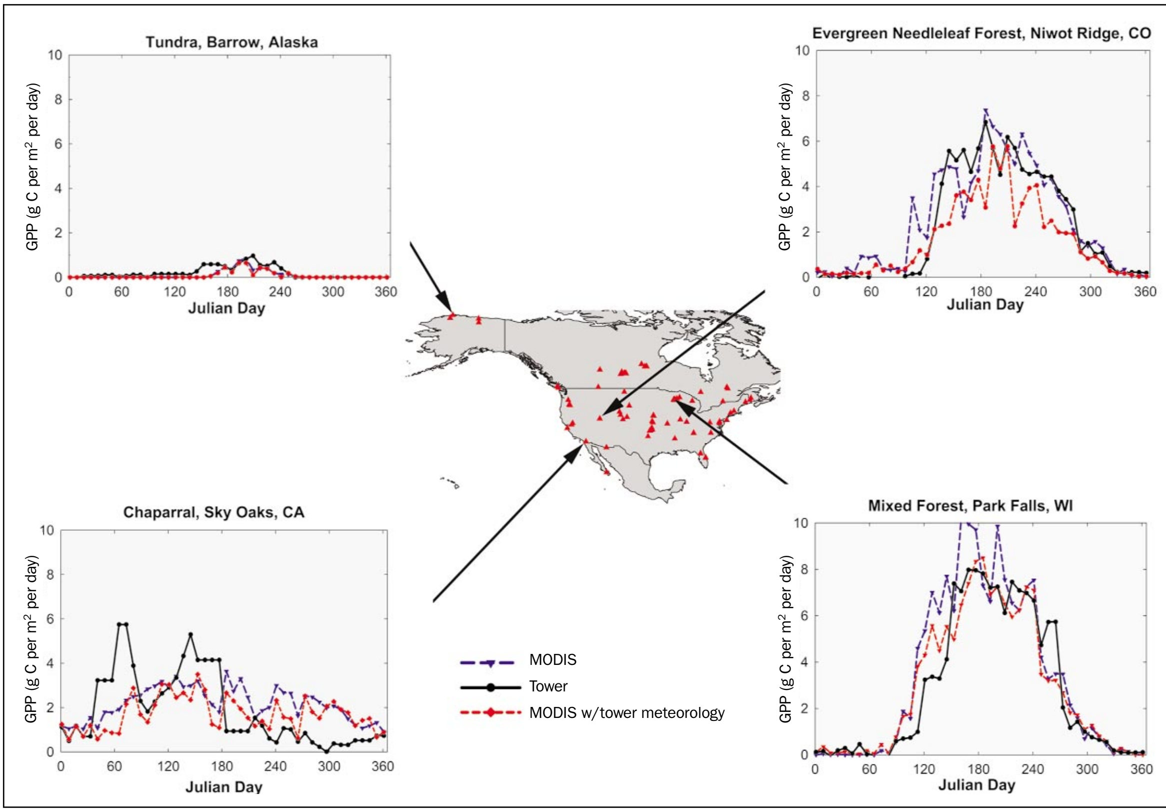

Figure 7. Intercomparison of gross primary production (GPP) computed from daily MODIS (Moderate Resolution Imaging Spectroradiometer) data summed at 8-day intervals with GPP measurements from flux towers at sites in the AmeriFlux network that represent different biomes and climatic regimes for 2001. Substituting higher-resolution (1 to 5 km) daily local tower meteorology data for the lower-resolution (1° by 1.25°) global meteorology data in a replicated calculation of GPP allows separation of error sources in the MODIS algorithms.

studies with NDVI, it has been evident that these satellite data do well at quantifying the length of the growing season, estimated as the number of days per year that green leaf area is displayed (Running and Nemani 1988, Myneni et al. 1997).

The MODIS algorithm appears to underestimate the initial burst of springtime GPP, yet it also consistently overestimates midsummer GPP, because of insufficient drought constraints for some of the biomes studied. To estimate the effects of the global meteorology data on algorithm results, tower data were then substituted for the DAO global meteorology data, and the MODIS GPP algorithm was recalculated. Our analysis indicates that much of this overestimation of daily GPP is a result of the discrepancy between global and tower meteorology data created by their spatial disparity. The global meteorology data are provided at a resolution of 1° by 1.25°, whereas the tower meteorology data represent a much smaller area (approximately 1 to 5 km^2). The primary difference between the two data sets is found in the VPD values. The VPD from global meteorology is consistently lower than tower VPD because of area averaging, resulting in increasingly erroneous estimates of GPP as a site dries (figure 7). The use of tower meteorology with the MODIS GPP algorithm usually improves GPP comparisons with tower results, indicating that the logic used in the MODIS algorithm is sound across biome types.

Additional errors propagate from the MODIS LAI/FPAR data set, in which cloud contamination is often an issue, leading to erroneously low estimates of LAI and producing data noise within the 8-day average GPP. This cloud contamination problem occurs most often in boreal and tropical regions but is also evident periodically throughout the United States. Biome-BGC estimates of GPP that incorporate a full mechanistic calculation of carbon balance are being used to explore other reasons for the differences between tower and MODIS estimates of daily GPP (Thornton et al. 2002, Turner et al. 2003b).

Sources and sinks of CO_2 are quantified by NEE, which is related to NPP on an annual basis as

$$NEE = NPP - R_h,$$

where R_h is the heterotrophic respiration or decomposition of biomass, primarily in the soil. This additional carbon cycle process is exceedingly difficult to quantify over large areas. NEE can range from 10% to 50% of NPP, depending on the soil carbon pools available for decomposition

(Baldocchi et al. 2001, Falge et al. 2002). NEE is measured directly by eddy covariance flux towers, and additional field measurements are taken to partition it into the components of NPP and soil respiration. Consequently, the MODIS NPP provides a critical first step for computing NEE globally, but additional modeling steps are required to compute the global NEE estimate (Schimel 1995, Potter 1999).

Satellite data are frequently combined with inversion of atmospheric CO_2 data to provide a constraint on global modeling of the CO_2 balance (Randerson et al. 1997). Using this technique, Schaefer and colleagues (2002) concluded that 44% of global interannual variability in NEE resulted from precipitation patterns, 23% from LAI, 16% from temperature, and 12% from soil carbon. Their study from 1983 to 1993 was limited by using monthly NDVI data at 1° by 1° resolution, whereas future studies will be able to use MODIS data on GPP distributed every 8 days at 1-km resolution.

Scientific applications of MODIS GPP and NPP

A continuously computed and openly disseminated measure of total daily GPP and annual NPP for Earth's land surface has never before existed. As summarized in the previous sections, development of the theory, algorithms, data streams, and validation of a regular measure of GPP and NPP has been an active research topic for the last two decades. Although refinement of this spatially continuous monitoring of the biosphere will continue for many years, we suggest that these GPP and NPP data sets are now sufficiently mature to be used in a wide variety of ways, wherever regular, spatially referenced measures of vegetation activity are desired. This section suggests a variety of applications for science, policy, and land management in which this regular measure of GPP and NPP should be valuable.

The original demand for global-scale land surface data was created by global climate and weather forecasting models, and this demand remains today (Sellers et al. 1986). Future global climate models will require dramatically more detailed definition of vegetation cover and physiology to reach the goal of comprehensive Earth systems models (Schimel 1999, Bonan et al. 2002). New models such as the community climate model at the National Center for Atmospheric Research now use MODIS GPP and NPP data to build algorithms computing seasonal changes in vegetation phenology, leaf area, roughness length, energy partitioning, and CO_2 source-sink relationships. Other greenhouse gases are also important as land surface feedbacks to the atmosphere for global climate modeling. Methane and nonmethane hydrocarbons (NMHCs) are thought to produce 20% to 30% of the current greenhouse gas forcing in the atmosphere (Houghton et al. 2001). Global methane and NMHC emissions can be calculated as a fraction of global NPP on the basis of biome type and temperature, providing reasonable spatial distribution and seasonal activity (Potter et al. 2001).

Because NPP is an essential component of the carbon cycle, virtually any science question involving the biospheric support of humankind begins by assessing NPP. The most fundamental questions of environmental degradation—desertification, deforestation, and the impacts of pollution and climate change—are often addressed by evaluating changes in NPP. Understanding differences in NPP among different biomes in different bioclimatic regimes is critical in defining a baseline of healthy biospheric function by which to measure future degradation. The Kyoto protocol on greenhouse gases focuses on the sources and sinks of CO_2 that begin with the NPP of terrestrial systems. Because NPP has natural interannual variability of 20% to 30%, regular monitoring may provide the most defensible estimations of CO_2 balance.

Natural disturbances such as wildfire also change the NPP over a total area of 1 million to 8 million km^2 per year, an estimate made with very little confidence. Human conversions of vegetation also change the NPP over millions of square kilometers each year. Deforestation rates are best quantified by methods of detecting land-cover change that automatically record abrupt changes in vegetation reflectance, signifying a severe disturbance such as deforestation (Zhan et al. 2002). The recovery of a site from a disturbance, however, is rarely followed so carefully, and measurement of such recovery may best be accomplished with the MODIS NPP data.

Biodiversity is commonly described as a measure of ecosystem health, yet at a global scale it is unquantifiable. Sala and colleagues (2000) defined five major drivers for change in global biodiversity in the next century: land use, climate, nitrogen deposition, biotic exchange, and atmospheric CO_2 increase. Although global NPP cannot count species, it integrates the biospheric response of all five of these primary drivers. Consequently, biodiversity has long been related in various ways to NPP. However, different biomes, bioclimatic regimes, disturbance histories, and other factors prevent a straightforward assessment of the relationship between NPP and biodiversity. Waring and colleagues (2002) recently suggested that biodiversity may be highest at sites with intermediate levels of NPP. Sites with high NPP often are dominated by relatively few fast-growing species, while sites with low NPP have insufficient resources to support a variety of species. Waring and colleagues found that a ratio of spring to summer photosynthesis best quantified the intermediate productivity. This ratio was easily calculated for the entire state of Oregon from AVHRR NDVI data and can now be computed directly from the MODIS 8-day GPP data stream (figure 8).

Estimates of NPP are often used as the beginning point of socioeconomic analyses of biomass utilization. For example, Haberl and Geissler (2000) used satellite data to produce a georeferenced map of NPP for Austria. They found that 50% of Austria's NPP was being appropriated by humans for food and fiber products (including forest and crop residues). Further, Haberl and Geissler estimated from a cascade utilization logic that unused biomass residues could fulfill 6% of Austria's commercial energy demand if they were fully utilized.

Terrestrial NPP is regularly identified as a key variable for various ecological monitoring activities (Niemeijer 2002). The Environmental Sustainability Index (*www.ciesin.*

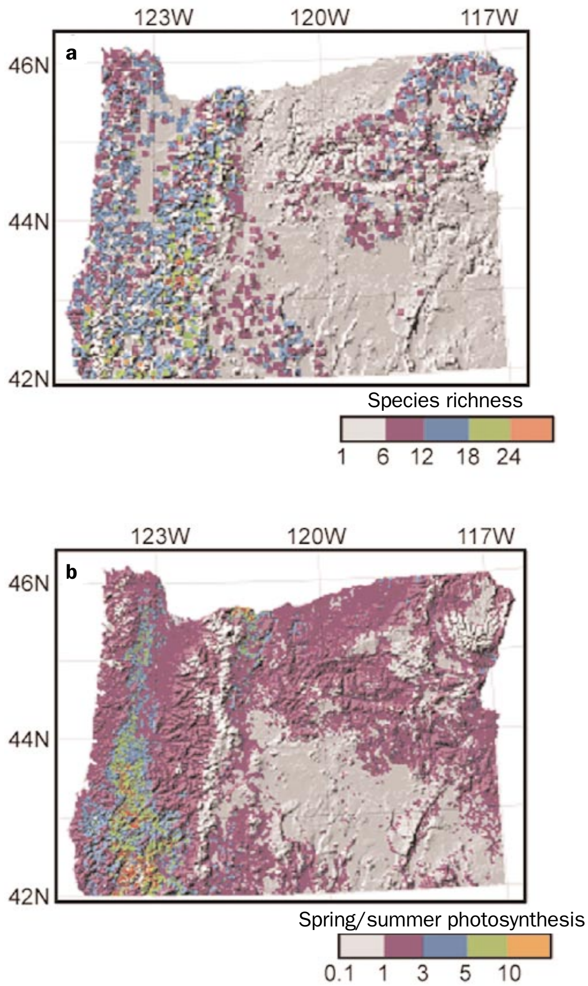

Figure 8. Testing an index of woody species biodiversity for Oregon. (a) Richness of woody species measured at field plots. (b) Ratio of spring (March–May) to summer (June–August) photosynthesis, computed by Waring and colleagues (2002) from a satellite-driven gross primary production (GPP) model. Biodiversity appears to be higher in areas with high ratios of spring to summer photosynthesis, a calculation easily performed for large areas with the GPP data gathered by MODIS (Moderate Resolution Imaging Spectroradiometer).

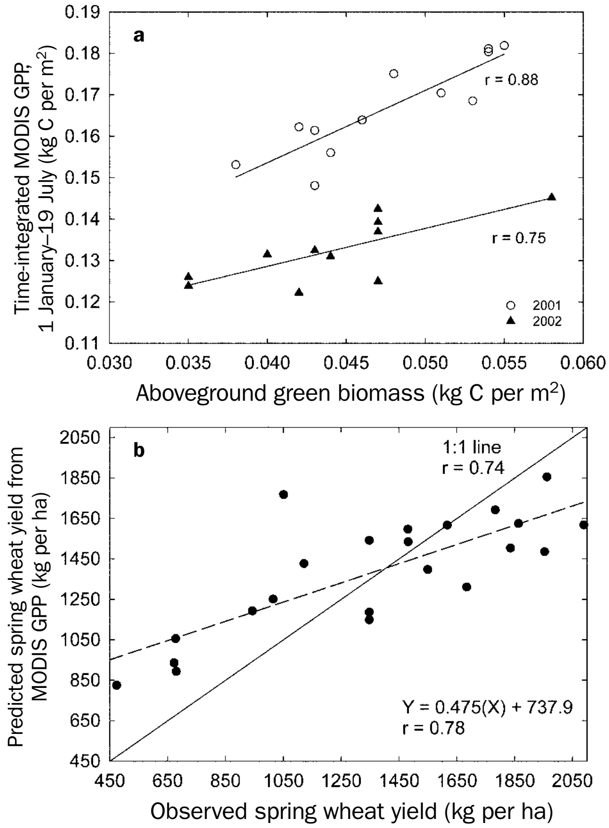

Figure 9. (a) The relationship between scaled aboveground green biomass (kilograms of carbon per square meter) and estimates of gross primary production (GPP), derived from MODIS (Moderate Resolution Imaging Spectroradiometer) data for 2001 and 2002. (b) Observed spring wheat yield for selected counties in Montana. Each point represents a county in Montana with more than 12,000 hectares (ha) of reported dryland-farmed spring wheat in 2001.

columbia.edu/indicators/ESI/) of the World Economic Forum, the Heinz Center's *State of the Nation's Ecosystems* report (*www.heinzctr.org/ecosystems/*), and the National Research Council report *Ecological Indicators for the Nation* (*www.nap.edu/books/0309068452/html/*) all identify NPP as a primary monitoring variable. The greatest interest of these indexes and reports is in quantifying trends of ecological indicators such as NPP and sounding an early alarm if an ongoing degradation is detected in any part of the nation or world. Reaching the overall objective of global sustainable development will require specific measurements of the stability of key biosphere attributes (Kates et al. 2001), and documentation of clear degradation in an ecosystem should trigger policy shifts in land management.

Regional landscape planning and management applications

Possible uses of the MODIS data on GPP and NPP range from regional strategic planning, such as quantifying decadal harvest targets for large tracts of forests, to more immediate decisions, such as when to move grazing animals among large pasture areas (Hunt et al. 2003). Immediate data access is not as important for strategic planning as it is for tactical decisionmaking. Strategic planning may use decadal trends in annual NPP as a measure of regional patterns and possible degradation of productive capability. Desertification of sub-Saharan Africa, for example, was long thought to be caused primarily by overgrazing, and substantial international aid was directed toward improving land management practices. Only after precipitation records were correlated

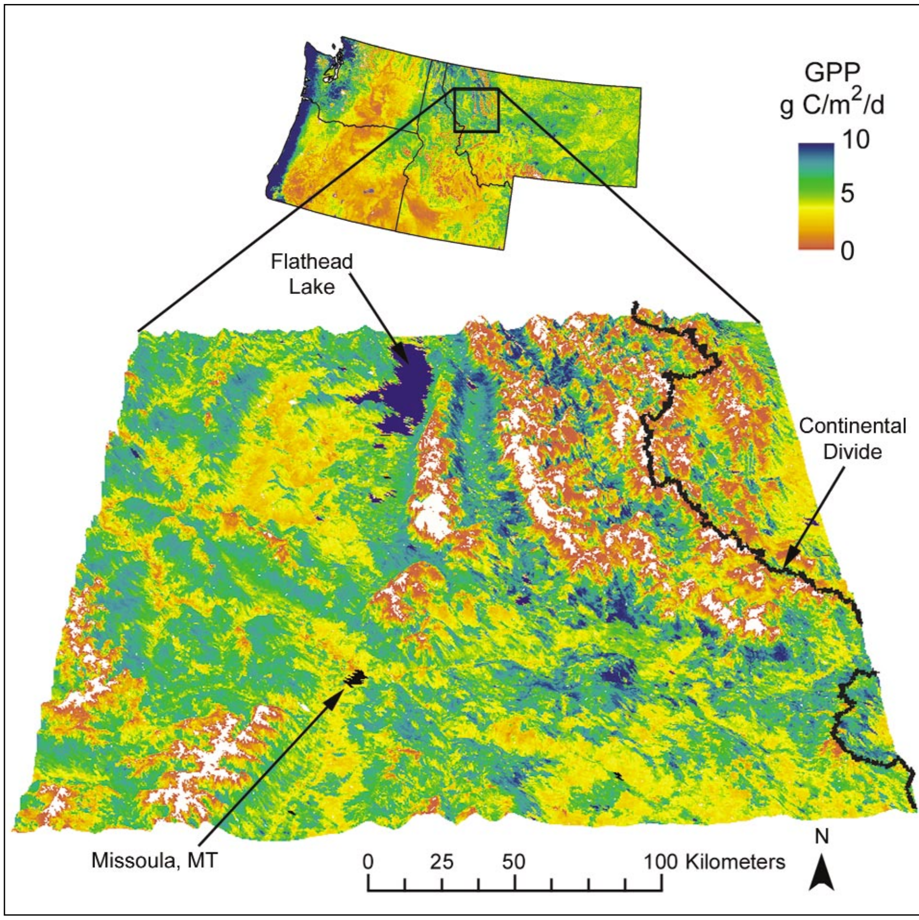

Figure 10. Improvement in landscape resolution that the new 250-meter MODIS (Moderate Resolution Imaging Spectroradiometer) measurement of gross primary production (GPP) attains over the standard global MODIS GPP/NPP (net primary production) data set. The map shows GPP from western Montana for 2–10 June 2003, draped over digital elevation data.

with satellite-based analysis of interannual variability in NDVI on a regional scale was it concluded that most of the apparent degradation was a result of decadal climate trends (Nicholson and Tucker 1998).

Decadal watershed degradation, including erosion and sedimentation, is also a serious land management problem. Local riverbank erosion and sedimentation is easily visible and documented on the ground, but the degradation of vegetation on a regional scale, such as the entire Colorado River basin or the basin of the Rio Grande, can only be quantified by repeated large-scale measurements such as those provided by remote sensing. Available fresh water is becoming possibly the scarcest natural resource; hence, monitoring and forecasting hydrologic runoff will have increasing socioeconomic value (Jackson et al. 2001). Evapotranspiration by vegetation consumes on average 70% of the precipitation that falls, and so computing dynamic runoff requires accurate analysis of vegetation growth.

Tactical decisionmaking on land management can benefit from immediate access to the latest MODIS data. Public land managers must reevaluate grazing schedules as seasonal weather changes the foraging conditions. Setting fixed calendar dates in grazing schedules is inappropriate because interannual weather variability can cause vegetation development to vary widely, and droughts reduce grazing capacities. Reeves (2004) established the relationship between MODIS GPP estimates and regional vegetation conditions during the 2001 and 2002 growing seasons. In his study, herbaceous vegetation was clipped at 2200 plots in the Little Missouri National Grasslands in western North Dakota. These field observations were spatially scaled to the zone of local meteorological influence established by creating Thiesson polygons around weather stations within the study area. Field observations compared favorably with MODIS GPP estimates, especially during the peak of greenness and of grass LAI (figure 9a).

The data on NPP gathered by MODIS have strategic and tactical uses for agriculture and agricultural economics. Commodity traders have clear interest in following how crops are growing in competing areas worldwide. The global price

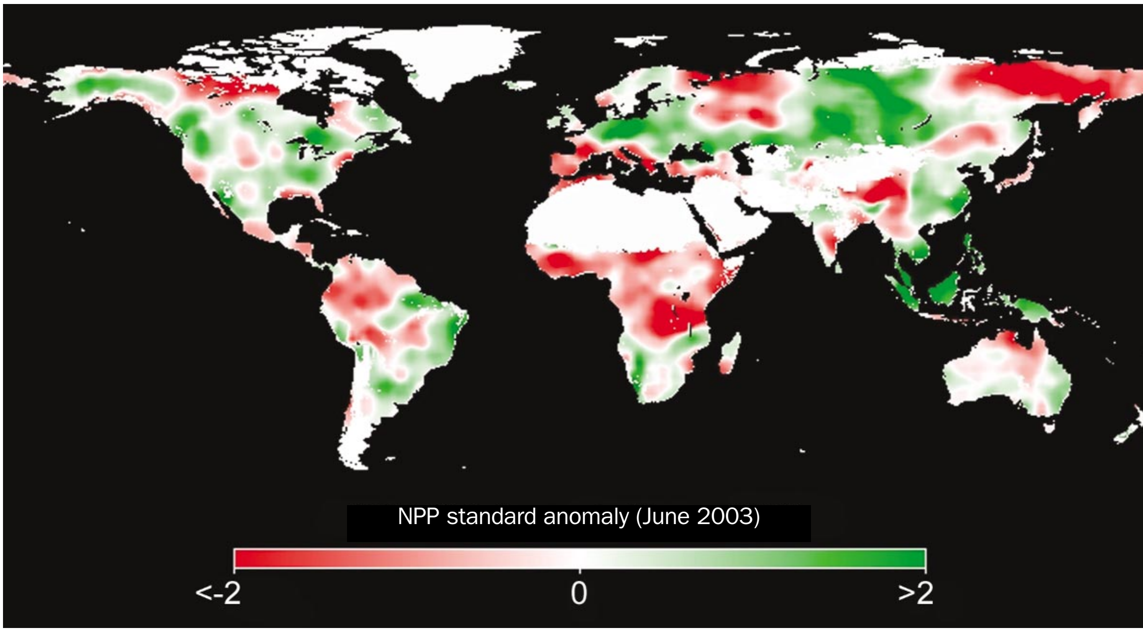

Figure 11. A trend of monthly net primary production (NPP) anomalies for the terrestrial biosphere, derived from the MODIS GPP data and expressed as the departure in standard deviations from the long-term (1982–2003) mean. The anomaly map suggests regional trends in ecosystem health without requiring understanding of carbon cycle details.

of wheat fluctuates in response to information on current crop conditions and expected yields in key exporting countries such as Canada, Argentina, and Australia. Even advance logistical decisions, such as requirements for leasing rail cars to transport crops to markets, can benefit from improved real-time assessments of crop development. Reeves (2004) demonstrated that combining 8-day MODIS GPP estimates with a simplified algorithm for wheat yield was an effective, timely tool for estimating county- and state-level spring wheat yield in Montana, the third largest wheat-producing state in the United States. In that study, GPP estimates were integrated over a defined growing season from 15 April through 4 August 2001 and converted to wheat yield using a simple harvest index (figure 9b).

Crop insurance is a $3-billion-per-year industry in the United States. Insurers need an objective means of evaluating whether an area meets some threshold of crop damage from hail or of retarded development from drought. The MODIS 8-day GPP may provide one means of arriving at decisions as to which farms qualify for insurance payments or for disaster relief from the federal government. At this stage, however, the MODIS NPP data should be considered only a general index of crop development. Until more detailed models are ready that begin with MODIS GPP and add computations of species, and even of cultivar-specific developmental sequences, we will lack the accuracy desired for specific crops and areas.

Wildfire has become the most costly wildland hazard in the United States, with the annual costs of fire suppression exceeding $1 billion in recent years. Sophisticated physical models of fire intensity and behavior now exist to aid in management, but these models require georeferenced databases of wildland fuels, the dead and live biomass that propagates fire spread (Keane et al. 2001). Seasonal development and senescence of the grasses and herbaceous plants that provide initial ignition for fire and promote its spread are being derived from the MODIS 8-day GPP. Postfire recovery of vegetation in burned areas can also be measured with MODIS NPP data.

For satellite data to have value for land management, the resolution must be sufficient to resolve major ownership and ecotonal boundaries. A 0.25-km version of the MODIS GPP and NPP data stream, using 1-km daily surface meteorology, is now being developed for the continental United States to provide a high-resolution GPP and NPP for land management. These products are designed for tactical decisionmaking and thus will be available only 2 to 3 days after the end of each 8-day MODIS compositing period (figure 10). The 0.25-km data set resolves details of vegetation productivity resulting from mountain topography, ownership boundaries, and microclimate gradients. In all these examples, the MODIS data alone are insufficient for decisionmaking, but the combination of spatial coverage and consistent continuous temporal monitoring provides valuable new insights into vegetation dynamics across landscapes.

Future availability of MODIS GPP and NPP

In the future, weekly mapping of terrestrial GPP and annual NPP should be as routine as the weather data that are presented today. Like weather maps, maps of GPP and NPP might even be shown occasionally on the evening news when abnormal conditions are discovered. To make these data easier for nonscientists to interpret, we present the daily GPP and annual NPP as anomalies (departures from normal) from the historical data in our 1982–2003 GPP/NPP database. We compute the 21-year average GPP for each pixel for each month and compare the most recent computed GPP to this long-term average (figure 11). This depiction of GPP, showing areas of recent above- or below-normal activity, is easily interpreted and mimics the way the public views weather information on the evening news report.

One goal of current MODIS research is to use the 8-day GPP to set the initializing conditions for an ecological forecast of future GPP. We now have prototypes of this type of biospheric prediction in a terrestrial observation and prediction system (*www.ntsg.umt.edu/tops/*). Among other possible uses, this forecasting could provide a tool for disease control. Hantavirus pulmonary syndrome is propagated by infected mice whose population cycles are highly correlated with the productivity of desert vegetation. Satellite monitoring of the changing length of vegetation growing seasons, and prediction of the seasonal timing of primary productivity, may provide health officers with an early warning system for disease outbreaks and colonization into new areas (Glass et al. 2000).

The National Polar Orbiting Environmental Satellite System (NPOESS) provides a long-range plan for the future heritage of AVHRR and MODIS sensors (Townshend and Justice 2002). NPOESS is planned for first deployment in 2009, after the planned retirement of current AVHRR sensors and the two MODIS sensors currently in orbit. NPOESS will continue to produce the data stream initiated by MODIS for GPP and NPP. At that point, we expect these weekly GPP and annual NPP data to be a routine part of land management, environmental policy analysis, agricultural economics, and monitoring of biospheric change. While we are optimistic about the general quality and reliability of these data, they do not meet all the needs and expectations of scientists, managers, policymakers, and the public. These satellite-derived data products however, are unique in that they provide global coverage and weekly continuity of a key measure of terrestrial ecosystem activity.

Acknowledgments

The National Aeronautics and Space Administration (NASA) Earth Science Enterprise has funded our MODIS (Moderate Resolution Imaging Spectroradiometer) research since 1984 with multiple awards, particularly the NAS5-31368 MODIS contract. S. W. R. acknowledges a McMaster fellowship for support at the CSIRO (Commonwealth Scientific and Industrial Research Organisation) Division of Land and Water in Australia during the writing of this article. We also acknowledge the MODIS processing team, at NASA's Goddard Space Flight Center, who operate the data system for EOS (Earth Observing System). Andrew Neuschwander, at the University of Montana's Numerical Terradynamic Simulation Group, provided color images.

References cited

Baldocchi D, et al. 2001. FLUXNET: A new tool to study the temporal and spatial variability of ecosystem-scale carbon dioxide, water vapor, and energy flux densities. Bulletin of the American Meteorological Society 82: 2415–2434.

Bonan GB, Levis S, Kergoat L, Oleson KW. 2002. Landscapes as patches of plant functional types: An integrating concept for climate and ecosystem models. Global Biogeochemical Cycles 16 (2): 1021 (doi: 10.1029/2000GB001360).

Burke IC, Kittel TGF, Lauenroth WK, Snook P, Yonker CM, Parton WJ. 1991. Regional analysis of the central Great Plains. BioScience 41: 685–692.

Churkina G, Running SW. 1998. Contrasting climatic controls on the estimated productivity of different biomes. Ecosystems 1: 206–215.

Clark DA, Brown S, Kicklighter DW, Chambers JQ, Thomlinson JR, Ni J, Holland EA. 2001. Net primary production in tropical forests: An evaluation and synthesis of existing field data. Ecological Applications 11: 371–384.

Dickinson RE. 1996. Land surface processes and climate modeling. Bulletin of the American Meteorological Society 76: 1445–1448.

Falge E, et al. 2002. Phase and amplitude of ecosystem carbon release and uptake potentials as derived from FLUXNET measurements. Agriculture and Forest Meteorology 113: 75–95.

Field CB, Randerson, JT, Malmstrom CM. 1995. Global net primary production: Combining ecology and remote sensing. Remote Sensing of Environment 51: 74–88.

Field CB, Behrenfeld MJ, Randerson JT, Falkowski P. 1998. Primary production of the biosphere: Integrating terrestrial and oceanic components. Science 281: 237–240.

Glass GE, et al. 2000. Using remotely sensed data to identify areas at risk for hantavirus pulmonary syndrome. Emerging Infectious Diseases 6: 238–247.

Goward SN, Tucker CJ, Dye DG. 1985. North American vegetation patterns observed with the NOAA-7 AVHRR. Vegetatio 64: 3–14.

Haberl H, Geissler S. 2000. Cascade utilization of biomass: Strategies for a more efficient use of a scarce resource. Ecological Engineering 16: S111–S121.

Hicke JA, Asner GP, Randerson JT, Tucker CJ, Los S, Birdsey R, Jenkins JC, Field C. 2002. Trends in North American net primary productivity derived from satellite observations, 1982–1998. Global Biogeochemical Cycles 16 (2): 1018 (doi: 10.1029/2001GB001550).

Houghton JT, Ding Y, Griggs DJ, Noguer M, van der Linden PJ, Xiaosu D, eds. 2001. Climate Change 2001: The Scientific Basis. Contribution of Working Group I to the Third Assessment Report of the Intergovernmental Panel on Climate Change. New York: Cambridge University Press.

Huete A, Didan K, Miura T, Rodriguez EP, Gao X, Ferreira LG. 2002. Overview of the radiometric and biophysical performance of the MODIS vegetation indices. Remote Sensing of Environment 83: 195–213.

Hunt ER Jr. 1994. Relationship between woody biomass and PAR conversion efficiency for estimating net primary production from NDVI. International Journal of Remote Sensing 15: 1725–1730.

Hunt ER, Everitt JR, Ritchie JH, Moran JC, Booth MS, Anderson DT, Clark GL, Seyfried MS. 2003. Applications and research using remote sensing for rangeland management. Photogrammetric Engineering and Remote Sensing 69: 675–693.

Jackson RB, Carpenter SR, Dahm CN, McKnight DM, Naiman RJ, Postel SL, Running SW. 2001. Water in a changing world. Issues in Ecology 9: 1–16.

Justice CO, Townshend JRG, Vermote EF, Masuoka E, Wolfe RE, Saleous N, Roy DP, Morisette JT. 2002. An overview of MODIS Land data processing and product status. Remote Sensing of Environment 83: 3–15.

Kates RW, et al. 2001. Sustainability science. Science 292: 641–642.

Keane RE, Burgan R, Wagtendonk JV. 2001. Mapping wildland fuels for fire management across multiple scales: Integrating remote sensing, GIS and biophysical modeling. International Journal of Wildland Fire 10: 301–319.

Keeling CD, Bacastow RB, Bainbridge AE, Ekdahl CA Jr, Guenther PB, Waterman LS. 1976. Atmospheric carbon dioxide variations at Mauna Loa Observatory, Hawaii. Tellus 28: 538–551.

Knapp AK, Smith MD. 2001. Variation among biomes in temporal dynamics of aboveground primary production. Science 291: 481– 484.

Lieth H, Whittaker RH, eds. 1975. Primary Productivity of the Biosphere. New York: Springer-Verlag.

Monteith JL. 1972. Solar radiation and productivity in tropical ecosystems. Journal of Applied Ecology 9: 747–766.

Morisette JT, Privette JL, Justice CO. 2002. A framework for the validation of MODIS land products. Remote Sensing of Environment 83: 77–96.

Myneni RB, Keeling CD, Tucker CJ, Asrar G, Nemani RR. 1997. Increased plant growth in the northern high latitudes from 1981 to 1991. Nature 386: 698–702.

Myneni RB, et al. 2002. Global products of vegetation leaf area and fraction absorbed PAR from year one of MODIS data. Remote Sensing of Environment 83: 214–231.

[NASA] National Aeronautics and Space Administration. 1983. Land-Related Global Habitability Science Issues. Washington (DC): NASA. Technical Memorandum no. 85841.

Nemani R, White M, Thornton P, Nishida K, Reddy S, Jenkins J, Running S. 2002. Recent trends in hydrologic balance have enhanced the terrestrial carbon sink in the United States. Geophysical Research Letters 29 (10): 1468 (doi: 10.1029/2002GL014867).

Nemani RR, Keeling CD, Hashimoto H, Jolly WM, Piper SC, Tucker CJ, Myneni RB, Running SW. 2003. Climate-driven increases in global terrestrial net primary production from 1982 to 1999. Science 300: 1560–1563.

Nicholson SE, Tucker CJ. 1998. Desertification, drought, and surface vegetation: An example from the West African Sahel. Bulletin of the American Meteorological Society 79: 815–829.

Niemeijer D. 2002. Developing indicators for environmental policy: Data-driven and theory-driven approaches examined by example. Environmental Science and Policy 5: 91–103.

Potter CS. 1999. Terrestrial biomass and the effects of deforestation on the global carbon cycle. BioScience 49: 769–778.

Potter CS, Davidson E, Nepstad D, Carvalho CR. 2001. Ecosystem modeling and the dynamic effects of deforestation on trace gas fluxes in Amazon tropical forests. Forest Ecology and Management 152: 97–117.

Prince SD, Goward SN. 1995. Global primary production: A remote sensing approach. Journal of Biogeography 22: 815–835.

Randerson JT, Thompson MV, Conway TJ, Fung IY, Field CB. 1997. The contribution of terrestrial sources and sinks to trends in the seasonal cycle of atmospheric carbon dioxide. Global Biogeochemical Cycles 11: 535–560.

Reeves MR. 2004. Agricultural and rangeland productivity patterns in the northern Great Plains estimated with MODIS vegetation data. PhD dissertation, University of Montana, Missoula.

Running SW, Nemani RR. 1988. Relating seasonal patterns of the AVHRR vegetation index to simulated photosynthesis and transpiration of forests in different climates. Remote Sensing of Environment 24: 347–367.

Running SW, Nemani RR, Peterson DL, Band LE, Potts DF, Pierce LL, Spanner MA. 1989. Mapping regional forest evapotranspiration and photosynthesis by coupling satellite data with ecosystem simulation. Ecology 70: 1090–1101.

Running SW, Baldocchi DD, Turner DP, Gower ST, Bakwin PS, Hibbard KA. 1999. A global terrestrial monitoring network integrating tower fluxes, flask sampling, ecosystem modeling and EOS satellite data. Remote Sensing of Environment 70: 108–127.

Running SW, Thornton PE, Nemani RR, Glassy JM. 2000. Global terrestrial gross and net primary productivity from the earth observing system. Pages 44–57 in Sala O, Jackson R, Mooney H, eds. Methods in Ecosystem Science. New York: Springer-Verlag.

Sala OE, et al. 2000. Global biodiversity scenarios for the year 2100. Science 287: 1770–1774.

Schaefer K, Denning AS, Suits N, Kaduk J, Baker I, Los S, Prihodko L. 2002. Effect of climate on interannual variability of terrestrial CO_2 fluxes. Global Biogeochemical Cycles 16 (4): 1102 (doi: 10.1029/2002GB001928).

Schimel DS. 1995. Terrestrial biogeochemical cycles: Global estimates with remote sensing. Remote Sensing of Environment 51: 49–56.

———. 1999. The terrestrial biosphere and global change: Implications for natural and managed ecosystems. Nature 400: 522–523.

Schulze E-D, Kelliher FM, Körner C, Lloyd JN, Leuning R. 1994. Relationships among stomatal conductance, ecosystem surface conductance, carbon assimilation rates, and plant nitrogen nutrition: A global ecology scaling exercise. Annual Review of Ecology and Systematics 25: 629–660.

Scurlock JMO, Olson RJ. 2002. Terrestrial net primary productivity—a brief history and a new worldwide database. Environmental Reviews 10: 91–109.

Sellers PJ. 1987. Canopy reflectance, photosynthesis, and transpiration, pt. II: The role of biophysics in the linearity of their interdependence. Remote Sensing of Environment 21: 143–183.

Sellers PJ, Mintz Y, Sud YC, Dalcher A. 1986. A simple biosphere model for use with general circulation models. Journal of Atmospheric Science 43: 505–531.

Tans PP, Fung IY, Takahashi T. 1990. Observational constraints on the global atmospheric CO_2 budget. Science 247: 1431–1438.

Thornton PE, et al. 2002. Modeling and measuring the effects of disturbance history and climate on carbon and water budgets in evergreen needleleaf forests. Agricultural and Forest Meteorology 113: 185–222.

Townshend JRG, Justice CO. 2002. Towards operational monitoring of terrestrial systems by moderate resolution remote sensing. Remote Sensing of Environment 83: 351–359.

Tucker CJ, Townshend JRG, Goff TE. 1985. African landcover classification using satellite data. Science 227: 369–374.

Turner DP, Urbanski S, Bremer D, Wofsy SC, Meyers T, Gower ST, Gregory M. 2003a. A cross-biome comparison of daily light-use efficiency for gross primary production. Global Change Biology 9: 383–395.

Turner DP, Ritts WD, Cohen WB, Gower ST, Zhao M, Running SW, Wofsy SC, Urbanski S, Dunn A, Munger JW. 2003b. Scaling gross primary production (GPP) over boreal and deciduous forest landscapes in support of MODIS GPP product validation. Remote Sensing of Environment 88: 256–270.

Waring R, Running SW. 1998. Forest Ecosystems: Analysis at Multiple Scales. San Diego: Academic Press.

Waring RH, Coops NC, Ohmann JL, Sarr DA. 2002. Interpreting woody plant richness from seasonal ratios of photosynthesis. Ecology 83: 2964–2970.

White MA, Thornton PE, Running SW, Nemani RR. 2000. Parameterization and sensitivity analysis of the BIOME-BGC terrestrial ecosystem model: Net primary production controls. Earth Interactions 4 (3): 1–85.

Zhan X, Sohlberg RA, Townshend JRG, DiMiceli C, Carroll ML, Eastman JC, Hansen MC, DeFries RS. 2002. Detection of land cover changes using MODIS 250 m data. Remote Sensing of Environment 83: 336–350.

Zheng D, Prince S, Wright R. 2003. Terrestrial net primary production estimates for 0.5° grid cells from field observations—a contribution to global biogeochemical modeling. Global Change Biology 9: 46–64.

Climate-Driven Increases in Global Terrestrial Net Primary Production from 1982 to 1999

Ramakrishna R. Nemani,[1*†] Charles D. Keeling,[2] Hirofumi Hashimoto,[1,3] William M. Jolly,[1] Stephen C. Piper,[2] Compton J. Tucker,[4] Ranga B. Myneni,[5] Steven W. Running[1]

Recent climatic changes have enhanced plant growth in northern mid-latitudes and high latitudes. However, a comprehensive analysis of the impact of global climatic changes on vegetation productivity has not before been expressed in the context of variable limiting factors to plant growth. We present a global investigation of vegetation responses to climatic changes by analyzing 18 years (1982 to 1999) of both climatic data and satellite observations of vegetation activity. Our results indicate that global changes in climate have eased several critical climatic constraints to plant growth, such that net primary production increased 6% (3.4 petagrams of carbon over 18 years) globally. The largest increase was in tropical ecosystems. Amazon rain forests accounted for 42% of the global increase in net primary production, owing mainly to decreased cloud cover and the resulting increase in solar radiation.

Between 1980 and 2000, Earth experienced dramatic environmental changes (*1*). It had two of the warmest decades in the instrumental record (1980s and 1990s), had three intense and persistent El Niño events (1982 to 1983, 1987 to 1988, and 1997 to 1998), and saw noteworthy changes in tropical cloudiness (*2*) and monsoon dynamics (*3*). Meanwhile, atmospheric CO_2 levels increased by 9% [337 to 369 parts per million (ppm)] and human population increased by 37% (4.45×10^9 to 6.08×10^9). Changes in terrestrial net primary production (NPP) integrate these and other climatic, ecological, geochemical, and human influences on the biosphere. Several regional studies have reported increases in NPP (*4–10*), but a globally comprehensive analysis of the impacts of climatic changes on NPP is lacking. For the northern mid-latitudes and high latitudes, these studies suggest that multiple mechanisms (e.g., nitrogen deposition, CO_2 fertilization, forest regrowth, and climatic changes) have promoted increases in NPP, whereas increases in the tropics have been primarily attributed to CO_2 fertilization. Here we analyze nearly two decades of recent global climatic data and satellite observations of vegetative activity and show that climatic changes have eased multiple climatic constraints to plant growth, increasing NPP over large regions of Earth.

Temperature, radiation, and water interact to impose complex and varying limitations on vegetation activity in different parts of the world (*11*). To provide a comprehensive interpretation of climate change impacts on plant growth, we first constructed a map of the relative contributions of climatic controls on global vegetation. We used long-term monthly climate statistics to build simple

[1]School of Forestry, University of Montana, Missoula, MT 59801, USA. [2]Scripps Institution of Oceanography, University of California, San Diego, CA 92037, USA. [3]Graduate School of Agricultural and Life Sciences, The University of Tokyo, 1-1-1 Yayoi, Bunkyo-ku, Tokyo 113, Japan. [4]NASA/Goddard Space Flight Center, Greenbelt, MD 20771, USA. [5]Department of Geography, Boston University, Boston, MA 02215, USA.

*Address after September 2003: NASA/Ames Research Center, Moffett Field, CA 94035, USA.
†To whom correspondence should be addressed. E-mail: nemani@ntsg.umt.edu

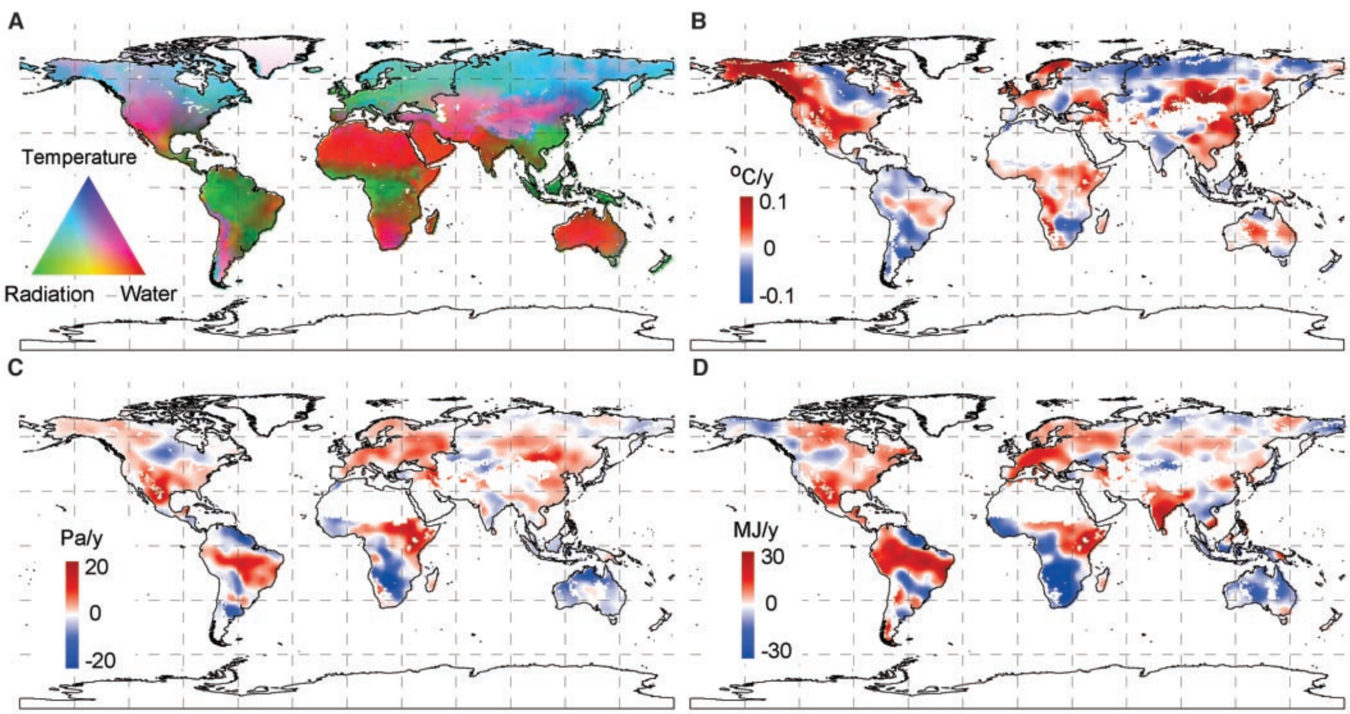

Fig. 1. (**A**) Geographic distribution of potential climatic constraints to plant growth derived from long-term climate statistics. (**B** to **D**) Recent climatic changes, estimated from reanalysis data from 1982 to 1999, in the growing season average temperature (B), vapor pressure deficit (VPD) (C), and solar radiation (D). Reductions in VPD are indicative of increased water availability (C). The growing season is defined as those months with 1982 to 1999 average air temperatures above 0°C.

bioclimatic indices (*12*). From these indices, we estimated that water availability most strongly limits vegetation growth over 40% of Earth's vegetated surface, whereas temperature limits growth over 33% and radiation over 27% of Earth's vegetated surface (Fig. 1A). These factors tend to be colimiting. For example, cold winter temperatures and cloudy summers limit high-latitude Eurasian vegetation, whereas cold winters and dry summers limit vegetation in western North America. Tropical areas are never limited by low temperatures but may have either a sustained dry season or nearly perpetual cloud cover that limits solar radiation (*13*).

We have estimated the trends in these growth-limiting climate factors from 1982 to 1999 using daily reanalysis data from the National Center for Environmental Prediction (NCEP) (*14*). The observed trends were confirmed with independent data sets of ground- and satellite-based observations (figs. S1 to S3) (*12*). Air temperatures that regulate the growing-season dynamics have increased over temperature-limited regions of North America and northwest Europe (Fig. 1B), promoting earlier plant growth (*7*) and additional carbon sequestration (*15*). Changing monsoon dynamics produced wetter rainfall regimes and associated reductions in vapor pressure deficit (VPD) in water-limited ecosystems of Australia, Africa, and the Indian subcontinent (Fig. 1C) (*3*). Importantly, increasing incident solar radiation was evident over radiation-limited regions of Western Europe and the equatorial tropics (*2*, *16*) (Fig. 1D).

Most of the observed climatic changes have been in the direction of reducing climatic constraints to plant growth. To quantify this effect, we used a biome-specific production efficiency model (PEM) (*12*, *17*) that combines monthly estimates of satellite-derived vegetation properties with daily NCEP climate data to estimate monthly and annual NPP at 0.5° × 0.5° resolution. The satellite-derived vegetation properties used were the fraction of absorbed photosynthetically active radiation (FPAR) and leaf area index (LAI) derived from remotely sensed normalized difference vegetation index (NDVI) and a biome map (*18*, *19*). The PEM that we used is similar in logic to other PEMs (*8*, *13*, *20*) but has parameters derived from field studies and a global ecosystem process model (*17*, *21*). To account for differences in satellite data processing, we used two independent data sets of LAI and FPAR derived from Global Inventory Monitoring and Modeling Studies (GIMMS) (*22*) and Pathfinder Advanced Very High Resolution Radiometer Land (PAL) (*23*) NDVI data sets (*12*).

From 1982 to 1999, modeled NPP increased the most (6.5%) in water- and radiation-limited regions, followed by temperature- and radiation-limited regions (5.7%) and temperature- and water-limited regions (5.4%). NPP increased significantly ($P < 0.01$) over 25% of the global vegetated area, with a mean rate of 6.3 g C m^{-2} $year^{-1}$, and decreased significantly over only 7% of the area, with a mean rate of 4.2 g C m^{-2} $year^{-1}$ (Fig. 2).

To isolate the role of climate from other mechanisms that could enhance carbon sequestration—such as CO_2 fertilization, nitrogen deposition, and forest regrowth—and to remove spurious trends in satellite data due to residual sensor-calibration effects, we alternately estimated NPP by assuming constant vegetation (1982 to 1999 monthly average FPAR and LAI) with changing climate or by assuming constant climate (average daily climate from 1982 to 1999) with changing vegetation. Changes in climate (with constant vegetation) directly contributed nearly 40% of the total increase in NPP from 1982 to 1996 (table S2). Changes in vegetation (with constant climate) over the same period contributed ~60% of total NPP increase, possibly as a result of climate-vegetation feedbacks, changes in land use, and growth stimulation from other mechanisms. Over parts of North America, Western Europe, the Amazon, south and central Africa, Australia, and the Indian subcontinent, changing climate alone produced persistent NPP increases (fig. S8).

Globally, NPP increased (Fig. 3) by 6.17%, 3.42 PgC over 18 years ($P < 0.001$), between 1982 and 1999. Ecosystems in all tropical regions and those in the high latitudes of the Northern Hemisphere accounted for 80% of the increase. Although terrestrial NPP accounts for only part of the biosphere-atmosphere carbon exchange, interannual variations of NPP are negatively correlated with global increases in atmospheric CO_2 growth rate ($r = 0.70$, $P < 0.001$). NPP anomalies attributable to climate alone (calculated with constant vegetation) explained nearly the same amount of variation in the NPP-CO_2 relation ($r = 0.71$, $P < 0.001$), indicating that climatic variability over land exerts a strong control over the variation in atmospheric CO_2 (fig. S9).

NPP responded differentially with respect to latitude to major climatic events such as El Niño and volcanic eruptions (Fig. 4). Globally, NPP declined during all three major El Niño events with corresponding increases in global CO_2 growth rate (*24*). El Niño events dominate tropical NPP variability, which has the highest association with global CO_2 growth rate ($r = 0.75$, $P < 0.001$). This response is likely because NPP and soil respiration are more tightly coupled in tropical climates compared with ecosystems in other latitudes. Soil carbon residence times range from less than 4 years in hot, wet tropical areas to greater than 1000 years in cold boreal or dry desert conditions (*25*). A strong decline in NPP after the Mount Pina-

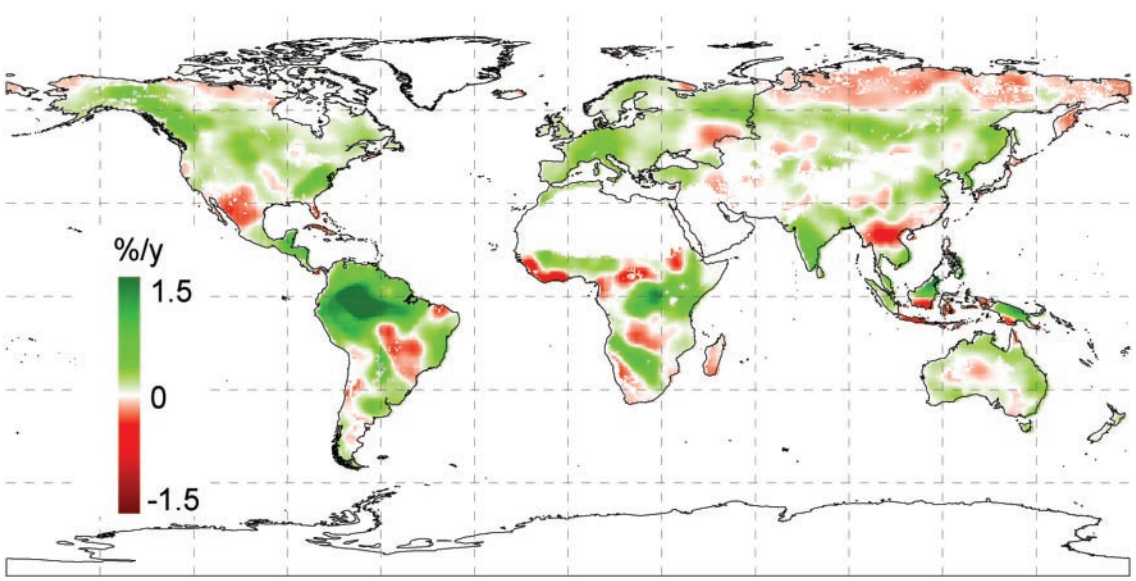

Fig. 2. Spatial distribution of linear trends in estimated NPP from 1982 to 1999. NPP was calculated with mean FPAR and LAI derived from GIMMS and PAL data sets.

tubo eruption (1991) was evident only at the high latitudes of the Northern Hemisphere. Cooler temperatures resulting from this eruption decreased the growing-season length there (*15*), but cooling, in association with favorable radiation regimes for photosynthesis (*26*), promoted plant growth in low-latitude ecosystems by reducing evaporative demand and respiration losses.

An increase in NPP of only 0.2% per 1-ppm increase in CO_2 could explain all of the estimated global NPP increase of 6.17% over 18 years and is within the range of experimental evidence (*27*). However, NPP increased by more than 1% per year in Amazonia alone, which accounts for 42% of the global NPP increase between 1982 and 1999. This result cannot be explained solely by CO_2 fertilization. We suggest that increases in solar radiation, owing to declining cloud cover in these predominantly radiation-limited forests, is the most likely explanation for the increased tropical NPP (*28*, *29*). Because there is no evidence of trends in rainfall or streamflows (*30*) concurrent with these declines in cloud cover in this region, it is likely that rainfall patterns have changed.

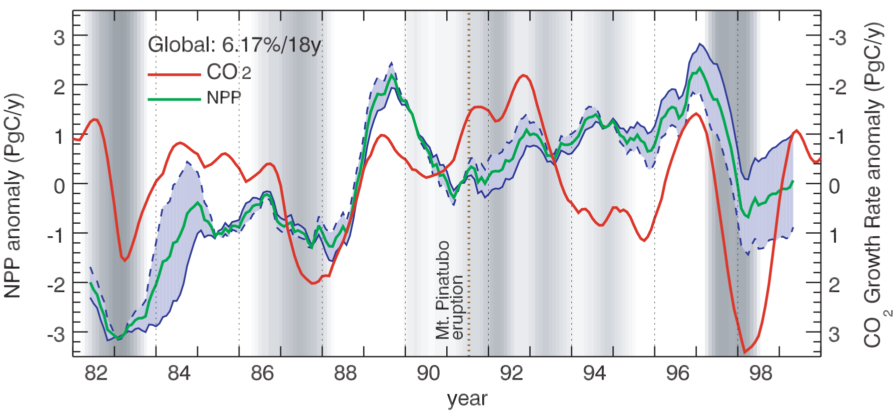

Fig. 3. Interannual variations from 1982 to 1999 in global NPP in relation to atmospheric CO_2 growth rate. Trends in global NPP anomalies are shown for GIMMS (solid blue line), PAL (dashed blue line), and their average (green line). CO_2 growth rate (inverted) is shown in red. Growth rates in ppm were converted to Pg of carbon with a conversion factor of 2.12 Pg per ppm (*24*). Mean NPP was 54.5 PgC year^{-1}. Mean CO_2 growth rate was 3.2 PgC year^{-1}. A multivariate ENSO (El Niño–Southern Oscillation) index (MEI) (*31*) is shown in gray scale, where darker shades represent higher MEI values.

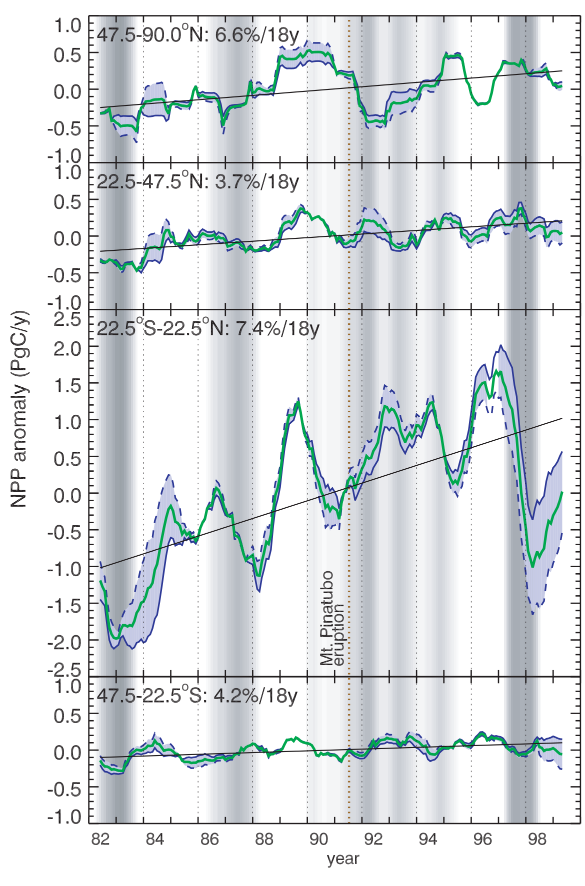

Fig. 4. Interannual variations in NPP distributed by latitudinal zones. Zonal NPP anomalies in each zone are shown for GIMMS (solid blue line), PAL (dashed blue line), and their average (green line).

Quantifying trends in NPP, as we have sought to do here, is necessary but not sufficient for understanding land surface net ecosystem exchange of CO_2. The same climatic changes that have caused decadal-scale increases in NPP can also change aboveground and belowground carbon allocation, decomposition rates, disturbance regimes, and other processes that cycle carbon between terrestrial ecosystems and the atmosphere. Atmospheric CO_2 inversion models show that northern mid-latitude ecosystems have recently been consistently large carbon sinks, and the tropics are either neutral or small sources, albeit with high uncertainty (*1*). Our satellite-based estimates of NPP, by contrast, show significant growth stimulation in both the tropics and the northern high-latitude ecosystems. Assuming that carbon emissions, including those from biomass burning and land-use changes, are properly accounted for in the atmospheric inversions, this spatial discrepancy means that respiration as well as NPP is a major driver of terrestrial carbon-sink dynamics. Global climate models project, in response to increasing greenhouse gases, an intensified hydrologic cycle altering the patterns of temperature, humidity, cloud cover, and rainfall (*1*). Our ability to predict the future of terrestrial ecosystems is contingent upon how well we can interpret such changes in the context of multiple limiting factors to biogeochemical cycling.

References and Notes

1. J. T. Houghton *et al.*, Eds., *Climate Change 2001: The Scientific Basis* (Cambridge University Press, Cambridge, 2001).
2. B. A. Wielicki *et al.*, *Science* **295**, 841 (2002).
3. K. K. Kumar, B. Rajagopalan, M. A. Cane, *Science* **284**, 2156 (1999).
4. A. R. Townsend, B. H. Braswell, E. A. Holland, J. E. Penner, *Ecol. Appl.* **6**, 806 (1996).
5. P. Friedlingstein *et al.*, *Global Biogeochem. Cycles* **9**, 541 (1995).
6. R. A. Houghton, J. L. Hackler, K. T. Lawrence, *Science* **285**, 574 (1999).
7. R. B. Myneni, C. D. Keeling, C. J. Tucker, G. Asrar, R. R. Nemani, *Nature* **386**, 698 (1997).
8. J. A. Hicke *et al.*, *Geophys. Res. Lett.* **29**, 10.1029/2001GL13578 (2002).
9. R. R. Nemani *et al.*, *Geophys. Res. Lett.* **29**, 10.1029/2002GL14867 (2002).
10. O. L. Phillips *et al.*, *Science* **282**, 439 (1998).
11. G. Churkina, S. W. Running, *Ecosystems* **1**, 206 (1998).
12. Materials and methods are available as supporting material on *Science* Online.
13. C. Potter *et al.*, *J. Geophys. Res.* **106**, 10423 (2001).
14. R. Kistler *et al.*, *Bull. Am. Meteorol. Soc.* **82**, 247 (2001).
15. W. Lucht *et al.*, *Science* **296**, 1687 (2002).
16. R. M. Trigo, T. J. Osborne, J. M. Corte-Real, *Clim. Res.* **20**, 9 (2002).
17. S. W. Running, P. E. Thornton, R. R. Nemani, J. M. Glassy, in *Methods in Ecosystem Science*, O. Sala, R. Jackson, H. Mooney, Eds. (Springer-Verlag, New York, 2000), pp. 44–57.
18. R. B. Myneni, R. R. Nemani, S. W. Running, *IEEE Trans. Geosci. Remote Sens.* **35**, 1380 (1997).

19. R. S. Defries, M. C. Hanson, J. R. G. Townshend, R. Sholberg, *Int. J. Remote Sens.* **19**, 3141 (1998).
20. S. D. Prince, S. N. Goward, *J. Biogeogr.* **22**, 815 (1995).
21. M. A. White, P. E. Thornton, S. W. Running, R. R. Nemani, *Earth Interactions* **4**, 1 (2000).
22. L. Zhou *et al.*, *J. Geophys. Res. Atmos.* **106**, 20069 (2001).
23. M. E. James, S. N. V. Kalluri, *Int. J. Remote Sens.* **15**, 3347 (1994).
24. C. D. Keeling *et al.*, *S.I.O. Reference Series No. 00-21* (Scripps Institution of Oceanography, University of California, San Diego, 2001).
25. D. J. Barrett, *Global Biogeochem. Cycles* **16**, 10.1029/2002GB0011860 (2002).
26. L. Gu *et al.*, *Science* **299**, 2035 (2003).
27. P. S. Curtis, X. Wang, *Oecologia* **113**, 299 (1998).
28. S. M. Fan, S. C. Wofsy, P. S. Bakwin, D. J. Jacob, D. R. Fitziarrald, *J. Geophys. Res.* **95**, 16851 (1990).
29. E. A. Graham, S. S. Mulkey, K. Kitajima, N. G. Phillips, S. J. Wright, *Proc. Natl. Acad. Sci. U.S.A.* **100**, 572 (2003).
30. M. H. Costa, J. A. Foley, *J. Geophys. Res.* **104**, 14189 (1999).
31. K. Wolter, M. S. Timlin, *Weather* **53**, 315 (1998).
32. We thank the reviewers and A. Keyser for helpful comments. This work was supported by grants from the NASA Earth Science Enterprise and Intelligent Data Understanding program to R.R.N., S.W.R., R.B.M., and C.J.T. C.D.K. and S.C.P. received financial support from NSF (ATM-01-20527), the U.S. Department of Energy (DE-FG03-95ER62075), and NASA (NAG5-11217).

Supporting Online Material
www.sciencemag.org/cgi/content/full/300/5625/1560/DC1
Materials and Methods
Figs. S1 to S9
Tables S1 and S2
References

24 January 2003; accepted 29 April 2003

Glacial Refugia: Hotspots But Not Melting Pots of Genetic Diversity

Rémy J. Petit,[1]* Itziar Aguinagalde,[2] Jacques-Louis de Beaulieu,[3] Christiane Bittkau,[4]† Simon Brewer,[3]‡ Rachid Cheddadi,[3] Richard Ennos,[5] Silvia Fineschi,[6] Delphine Grivet,[1]§ Martin Lascoux,[7] Aparajita Mohanty,[2]‖ Gerhard Müller-Starck,[4] Brigitte Demesure-Musch,[8] Anna Palmé,[7] Juan Pedro Martín,[2] Sarah Rendell,[5]¶ Giovanni G. Vendramin[9]

Glacial refuge areas are expected to harbor a large fraction of the intraspecific biodiversity of the temperate biota. To test this hypothesis, we studied chloroplast DNA variation in 22 widespread European trees and shrubs sampled in the same forests. Most species had genetically divergent populations in Mediterranean regions, especially those with low seed dispersal abilities. However, the genetically most diverse populations were not located in the south but at intermediate latitudes, a likely consequence of the admixture of divergent lineages colonizing the continent from separate refugia.

During the long glacial episodes of the Quaternary, European forests were considerably more restricted than in the present interglacial, because the Mediterranean Sea in the south and unsuitable environment in the north restricted temperate tree and shrub taxa to the Iberian, Italian, and Balkan peninsulas. For instance, at the time of the last glacial maximum, 25,000 to 17,000 years ago, networks of fossil pollen data and macrofossil remains such as charcoals indicate that several tree species were localized in small favorable spots within the Mediterranean region but also at the southern edge of the cold and dry steppe-tundra area in eastern, central, and southwestern Europe (*1–5*). After climate warming, some of these surviving populations expanded, whereas others remained trapped and either became extinct or persisted by shifting altitude (*2*, *6*). As a consequence of prolonged isolation, extant tree populations situated close to refugia should be highly divergent, especially if they were not the source of the expansion. Another related prediction is that intraspecific diversity should decline away from refugia, as a consequence of successive founder events during postglacial colonization (*7*, *8*). However, species attributes such as colonizing ability may alter these predictions (*9*). Furthermore, the individualistic migration behavior of tree species during interglacial periods (*6*, *9*) and the presence of more northern refugia (*4*, *5*) may have blurred this pattern. In Europe, range-wide genetic surveys of a few well-investigated tree species have been performed (*10–12*), but it is difficult to generalize from these studies. To get a broader picture and to test the previous predictions, we gathered data from several woody angiosperm taxa across Europe using standardized sampling and molecular screening techniques. Such knowledge on the genetic consequences of the recent history of woody plant species may be critical for the conservation and sustainable management of their genetic resources.

Plastids are generally maternally inherited in angiosperms and, therefore, moved by seeds only. Because colonization of new habitats occurs through seeds, chloroplast DNA (cpDNA) markers provide information on past changes in species distribution that is unaffected by subsequent pollen movements (*13*). We have investigated patterns of cpDNA diversity in 22 woody species. These were sampled in the same 25 European forests selected on the basis of their high species richness and limited human influence (table S1). About 10 individuals per species were sampled from each forest, following a standard procedure (*14*). Polymorphisms were detected by polymerase chain reaction (PCR) techniques (*14*) in all 22 species [4 to 50 haplotypes per species, mean 16.9 (Table 1)]. The degree of subdivision of cpDNA diversity (G_{ST}) was estimated for each species (*15*, *16*). This measure partly reflects the dispersal ability of the species considered, although long-term range fragmentation should also play a role. Low G_{ST} values (indicative of high levels of gene flow through seeds) were found in *Salix* and in *Populus* (0.09 to 0.11), characterized both by light, wind-dispersed cottony seeds. The species characterized by animal-ingested seeds also tended to have below-average values. In contrast, species with animal-cached seeds (i.e., nuts) exhibited higher than average values (Table 1).

To compare forests with each other, we calculated the mean number of haplotypes and within-population gene diversity by averaging across species in each forest (table S2). We also calculated a measure that expresses the average genetic divergence of the forest from all remaining populations (*17*) (table S2). The highest values were observed in Corsica, Italy, and the Balkans, including Croatia and Romania, whereas average or below-average values were

[1]Institut National de la Recherche Agronomique, UMR Biodiversité, Génes et Ecosystémes, F-33612 Cestas, France. [2]Departamento Biología Vegetal, Escuela Técnica Superior de Ingenieros Agrónomos, Universidad Politécnica de Madrid, E-28040 Madrid, Spain. [3]Institut Méditerranéen d'Ecologie et de Paléoécologie, Faculté de St Jérôme, F-13397 Marseille, France. [4]Technische Universität München, Fachgebiet Forstgenetik, D-85354 Freising, Germany. [5]Institute of Ecology and Resource Management University of Edinburgh, Edinburgh EH9 3JU, Scotland, UK. [6]CNR, Istituto di Biologia Agroambientale e Forestale, I-05010 Porano-TR, Italy. [7]Department of Conservation Biology and Genetics, Evolutionary Biology Centre, Uppsala University, 75236 Uppsala, Sweden. [8]Office National des Forêts, Département des Recherches Techniques, Conservatoire Génétique des Arbres Forestiers, F-45160 Ardon, France. [9]CNR, Istituto di Genetica Vegetale, Sezione di Firenze, I-50134 Firenze, Italy.

*To whom correspondence should be addressed. E-mail: petit@pierroton.inra.fr
†Present address: Institut für Spezielle Botanik und Botanischer Garten, Johannes Gutenberg-Universität Mainz, D-55099 Mainz, Germany.
‡Present address: CEREGE, Europôle Méditerranéen de l'Arbois, F-13545 Aix-en-Provence, France.
§Present address: University of California Los Angeles, Organismic Biology, Ecology and Evolution, Los Angeles, CA 90024, USA.
‖Present address: International Centre for Genetic Engineering and Biotechnology, Aruna Asaf Ali Marg, New Delhi-110067, India.
¶Present address: Department of Plant Sciences, University of Oxford, Oxford OX1 3RB, UK.

A Global Terrestrial Monitoring Network Integrating Tower Fluxes, Flask Sampling, Ecosystem Modeling and EOS Satellite Data

S. W. Running, D. D. Baldocchi,† D. P. Turner,‡ S. T. Gower,§ P. S. Bakwin,‖ and K. A. Hibbard¶*

Accurate monitoring of global scale changes in the terrestrial biosphere has become acutely important as the scope of human impacts on biological systems and atmospheric chemistry grows. For example, the Kyoto Protocol of 1997 signals some of the dramatic socioeconomic and political decisions that may lie ahead concerning CO_2 *emissions and global carbon cycle impacts. These decisions will rely heavily on accurate measures of global biospheric changes (Schimel, 1998; IGBP TCWG, 1998). An array of national and international programs have inaugurated global satellite observations, critical field measurements of carbon and water fluxes, and global model development for the purposes of beginning to monitor the biosphere. The detection by these programs of interannual variability of ecosystem fluxes and of longer term trends will permit early indication of fundamental biospheric changes which might otherwise go undetected until major biome conversion begins. This article describes a blueprint for more comprehensive coordination of the various flux measurement and modeling activities into a global terrestrial monitoring network that will have direct relevance to the political decision making of global change.*

* Numerical Terradynamic Simulation Group, School of Forestry, University of Montana, Missoula
† ATDD, Oak Ridge National Laboratory, Oak Ridge, Tennessee
‡ Forest Science Department, Oregon State University, Corvallis
§ Department of Forestry, University of Wisconsin, Madison
‖ NOAA/CMDL, Boulder, Colorado
¶ Climate Change Research Center, University of New Hampshire, Durham

Address correspondence to S. W. Running, Numerical Terradynamic Simulation Group, School of Forestry, University of Montana, Missoula, MT 59812. E-mail: swr@ntsg.umt.edu
Received 10 August 1998; revised 15 April 1999.

REMOTE SENS. ENVIRON. 70:108–127 (1999)

0034-4257/99/$–see front matter
PII S0034-4257(99)00061-9

OVERVIEW OF GLOBAL TERRESTRIAL MONITORING AND VALIDATION

The dynamics of the terrestrial biosphere are an integral part of global change. Society needs to know particularly if the "human habitability" of the biosphere is decreasing, especially because more humans are inhabiting the land each year. One direct way of quantifying human habitability is by evaluation of the vegetation cover and the primary productivity that provides food, fiber, and fuel for human endeavors. The distribution, health, and productivity of global vegetation is typically evaluated in the context of the global carbon budget. Much of what is known about the contemporary global carbon budget has been learned from careful observations of atmospheric CO_2 concentration trends and $^{13}C/^{12}C$ isotope ratios ($d^{13}C$), interpreted with global circulation models. From these studies we have learned the following important things about the global carbon cycle:

1. On average over the last 40 years roughly half of the annual anthropogenic input of CO_2 to the atmosphere is taken up by the oceans and the terrestrial biosphere (Keeling et al., 1989).
2. Interpretation of the latitudinal gradient of atmospheric CO_2, using transport models indicates that a significant portion of the net uptake of CO_2 occurs at midlatitudes of the Northern Hemisphere (Tans et al., 1990; Ciais et al., 1995; Denning et al., 1995).
3. There are large year-to-year changes in the net uptake of CO_2 by the terrestrial biosphere. These changes are associated with climate anomalies such as ENSO (Conway et al., 1994; Keeling et al., 1995; Keeling et al., 1996).
4. The seasonality of terrestrial biosphere carbon

flux appears to be changing as indicated by shifts in the timing and amplitude of the seasonal cycle of atmospheric CO_2 measured at many "background" sites. In particular, it appears that spring is beginning earlier and fall arriving later (Randerson et al., 1997; Field et al., 1998). This result is supported by satellite phenology observations (Myneni et al., 1997a).

These indications of biospheric changes point to the need to 1) better understand and monitor the processes that regulate uptake and release of CO_2 by terrestrial ecosystems, 2) provide verification from more direct ground-based measurements, and 3) employ satellite observations to clarify spatial patterns in ecosystem function. There is also new interest in computing sources and sinks of carbon for individual nations that will challenge current data availability. This article suggests how a number of current international research activities can be integrated into a biospheric monitoring program that efficiently collects and disseminates key data and analyses for evaluation of global change in terrestrial ecosystems (Running, 1998).

Necessary Components of a Biospheric Monitoring System

Accurate quantification of the trajectory of change and potential degradation of the terrestrial biosphere is essential because this understanding will influence many socioeconomic decisions concerning resource consumption and conservation. Global estimates of biospheric processes will require a permanent network of ground monitoring and model validation points, much like the surface weather station network, to quantify seasonal and interannual dynamics of ecosystem activity, that is, to cover the *Time* domain. Remote sensing must be used to quantify the heterogeneity of the biosphere, the *Space* domain. Finally, because these Time and Space measurement regimes cannot provide a complete view of biospheric biogeochemical activity, modeling is required to isolate unmeasured ecosystem processes, and to provide predictive capacity. In this article, we outline a nested terrestrial measurement network, a regular remote sensing product stream, and an integrating modeling framework to continuously monitor and validate large scale estimates of key variables in terrestrial carbon and water budgets.

Temporal Monitoring—Carbon, Water and Energy Fluxes

Eddy-covariance flux towers serve as the core infrastructure for three reasons. First, they measure carbon and water fluxes and the surface energy budget, processes directly related to ecosystem function, continuously and semiautomatically, representing an area of approximately 1–3 km^2. Second, a global representation of over 80 stations already exists. The current eddy flux network of sites is growing rapidly and becoming increasingly organized. Third, the flux towers provide a critical infrastructure of organized personnel and equipment for other comprehensive measurements, including ecophysiology, structure and biomass of the vegetation, fluxes of other greenhouse gases, and micrometeorology.

Monitoring of the spatial and temporal patterns in the concentration of CO_2, O_2, and their isotopic variants can provide the basis for estimates of carbon cycle fluxes at large scales (Tans et al., 1996). The remarkable achievements from the geochemistry approach, beginning with the observations at Mona Loa, which first detected the upward trend in the global atmospheric CO_2 concentration, establish its importance for biospheric monitoring. The limitations in the geochemistry approach for terrestrial monitoring are that it is not spatially explicit, and generally indicates the net effect of multiple, potentially opposing, processes.

Spatial Monitoring—Terrestrial Vegetation Products from EOS

After launch in mid-1999, the EOS (Earth Observing System) will inaugurate the first *regular, global* terrestrial vegetation products, including land cover, spectral vegetation indices (SVI), leaf area index LAI, fraction absorbed photosynthetic active radiation (FPAR), and net primary production (NPP) (Fig. 1; Running et al., 1994; Justice et al., 1998). Many labs now calculate global net primary production (NPP), evapotranspiration (ET), and/or precursor variables like leaf area index (LAI) or fraction absorbed PAR (FPAR) (Melillo et al., 1993; Ruimy et al., 1994; Field et al., 1995; Hunt et al., 1996; Prince and Goward, 1995; Randerson et al., 1997; Foley et al., 1996; Myneni et al., 1997b). Because these EOS variables provide the basis for spatial scaling of all relevant ground-based measurements, their validation is essential. The following web site has summaries and links to important EOS Land validation activities: http://www-eosdis.ornl.gov/eos_land_val/valid.html.

The field measurements required for this EOS land validation are primarily multitemporal sequences of vegetation structure and biomass accumulation and turnover, accurately georeferenced to provide spatial fractions of vegetation structure across the landscape. LAI and NPP, the most directly measured vegetation structural and functional variables, respectively, range by 2 orders of magnitude among the diverse terrestrial biomes and change seasonally with annual plant growth cycles. Spectral vegetation indices such as the well known NDVI and FPAR are radiometric products that can only be measured instantaneously but can be inferred by vegetation structural measurements, most commonly by LAI. The plans discussed below will measure LAI to provide inferred validation of VI and FPAR, and will measure fractional vegetation cover of regional study areas.

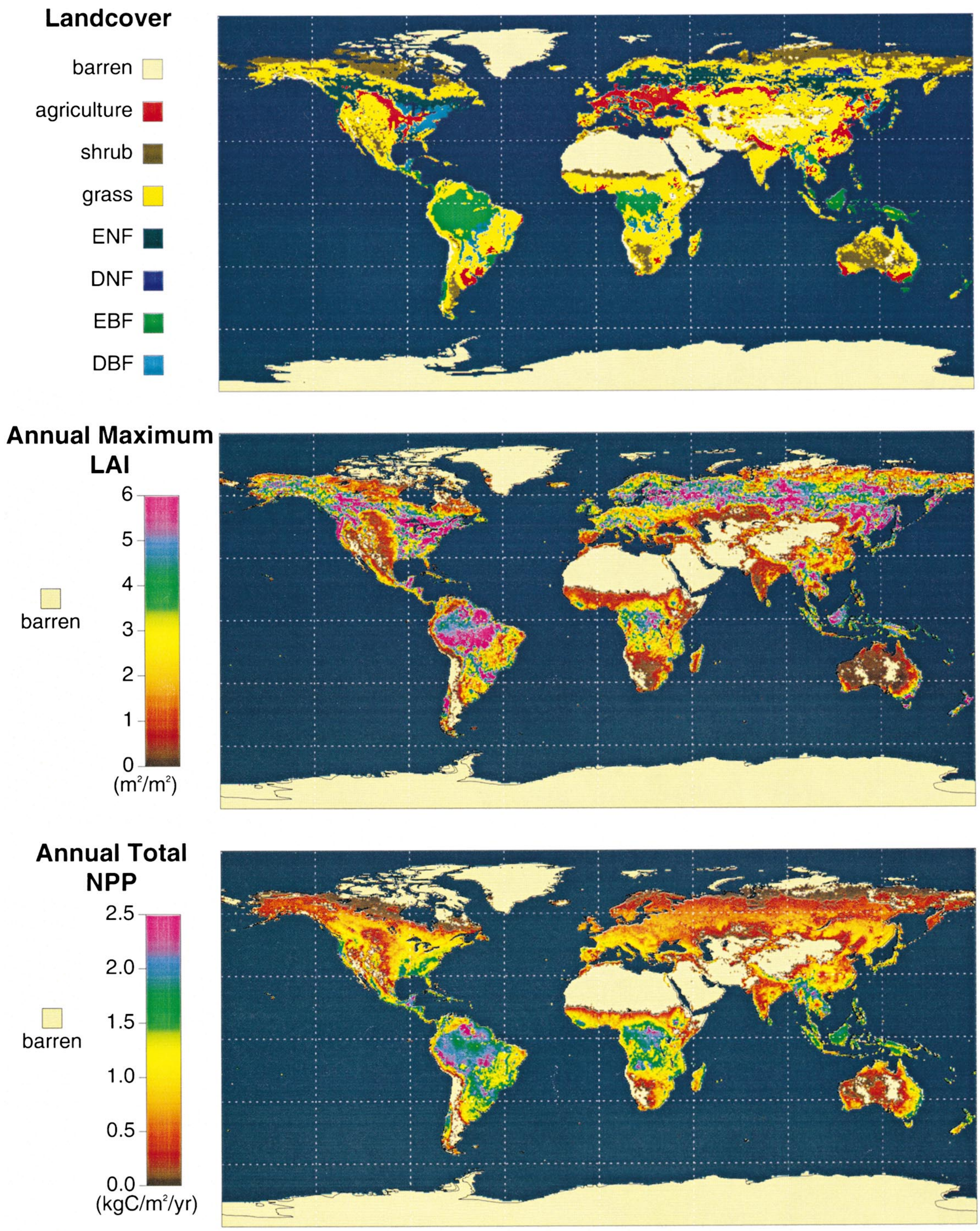

Figure 1. An example of global land cover (LC), leaf area index (LAI), and net primary production (NPP) terrestrial variables that will be produced from the Earth Observing System (EOS) every 8 days at 1 km. These data will be invaluable for scaling of ecological research and land management, but first need global field validation [see Running et al. (1994) and Justice et al. (1998) for details].

System Processes and Integration—Ecological Modeling
The eddy fluxes and ecophysiological measurements provide process level understanding of ecosystem function that can be incorporated into ecosystem models. However, there will never be sufficient eddy flux towers or field measures to adequately characterize all terrestrial ecosystems under all conditions. Models must then be used to interpolate and extrapolate flux measurements in time and space. Hence, models are and will be a key tool for making regional and global assessments (Waring and Running, 1998). Mechanistic ecosystem models also have the potential for *predicting* how ecosystems will respond

to future changes in atmospheric CO_2, temperature, land use change, nitrogen loading, and precipitation.

Critical Variables in a Global Terrestrial Monitoring System

We initially focus on one key variable each of the carbon and water cycles: net primary production (NPP) and evapotranspiration (ET). The carbon budget consists of several major processes that describe the exchange of carbon dioxide between terrestrial ecosystems and the atmosphere. Gross primary production (GPP) is the total carbon assimilated by vegetation. A fraction of GPP is lost back to the atmosphere as the result of autotrophic respiration (R_A). Net primary production (NPP), the balance between GPP and autotrophic respiration, is allocated to wood, foliage, roots, reproductive tissues, storage, etc. NPP, the direct measure of vegetation productivity, has been measured from field biomass surveys for decades and has the largest historical database. NPP relates directly to forest, range, and crop productivity, and so also has high socioeconomic value. NEE, the net exchange of CO_2 between terrestrial ecosystems and the atmosphere, is measured by flux towers. NEE has high scientific relevance for terrestrial carbon budgets and greenhouse gas production, but less direct socioeconomic significance.

Under optimal conditions, NEE is measured continuously and calculated on a half-hourly or hourly basis, whereas the field-based NPP is measured periodically and calculated on an annual basis. The two fluxes are related in that if NEE is summed over a year, the sum should be the difference between NPP and heterotrophic respiration (R_H) summed over the year. Thus

$$\mathrm{NEE}_{\mathrm{annual}}=\mathrm{NPP}_{\mathrm{annual}}-R_{H\ \mathrm{annual}}\,. \tag{1}$$

Note that on a daily time step NEE is related to GPP and R_A in Eq. (2):

$$\mathrm{NEE}_{\mathrm{daily}}=\mathrm{GPP}_{\mathrm{daily}}-(R_H+R_A)_{\mathrm{daily}}\,. \tag{2}$$

NPP and NEE are related theoretically, but the two carbon fluxes are measured at very different temporal and spatial scales, necessitating an integrated approach to provide global coverage for rapid validation and monitoring opportunities. The ultimate goal is to validate global measures of NEE *and* NPP.

The other primary variable, evapotranspiration (ET), is a component of the surface hydrologic balance and an integral part of surface energy partitioning. ET is also measured continuously by a flux tower, providing a high temporal resolution measurement of the partitioning of precipitation (PPT) in the hydrological budget of an ecosystem. However, much like with NPP and NEP, the variable of the hydrologic cycle with the longest history and widest distributed data is watershed discharge Q. These variables are generally related as in Eq. (3):

$$Q=\mathrm{PPT}-\mathrm{ET} \tag{3}$$

when soil moisture changes and groundwater losses are ignored. Also, both of these historical ecosystem measures, NPP and Q, are typically measured on a weekly-to-monthly basis, so are temporally inconsistent with the continuous flux tower measures of NEE and ET. Additionally, there are spatial scale mismatches. The tower fluxes represent a footprint of roughly 1–3 km^2, while NPP is typically measured on $\simeq$0.1 ha plot, and watersheds can drain many hundreds of square kilometers. Process-based terrestrial ecosystem models, driven by spatially represented climate and satellite derived vegetation parameters, are essential for integrating the suite of field-based measurements of inconsistent temporal and spatial scale to provide a complete and consistent view of global biospheric function.

We now visit each of four components critical to a comprehensive monitoring scheme and identify associated on-going research activities. In the temporal dimension, it is a global flux tower network and a global flask sampling network that are essential. For the spatial dimension, we discuss the EOS products. SVAT modeling is then examined as a means of scaling carbon and water flux over space and time. Subsequently, we consider the nature of the required information flow among these components and identify international programs concerned with integration.

GLOBAL FLUX TOWER NETWORK (FLUXNET)

The cornerstone of this global terrestrial vegetation monitoring is the tower flux network, FLUXNET. This global array of tower sites is currently comprised of regional networks in Europe (EUROFLUX), North America (AmeriFlux), Asia (JapanNet, OzFlux), and Latin America (LBA). The towers provide a continuous and representative measure of terrestrial carbon cycle dynamics, and an important ancillary suite of measurements of energy and water fluxes for interpreting carbon fluxes (Fig. 2). The role of FLUXNET includes coordinating the regional networks so that information can be attained at a global scale, ensuring site to site intercomparability, coordinating enhancements to current network plans and operation of a global archive and distribution center at the Oak Ridge DAAC. The FLUXNET project web address is http://daacl.ESD.ORNL.Gov/FLUXNET/. The web sites contain measurement protocols for consistency, and data on site, vegetation, climate, and soil characteristics. It provides a route for users to gain access of hourly meteorological and flux measurements and proper documentation.

The FLUXNET concept originated at a workshop on "Strategies for Long Term Studies of CO_2 and Water Vapor Fluxes over Terrestrial Ecosystems" held in March 1995 in La Thuile, Italy (Baldocchi et al., 1996). The first organized flux tower network was EUROFLUX, which now involves long-term flux measurements of carbon di-

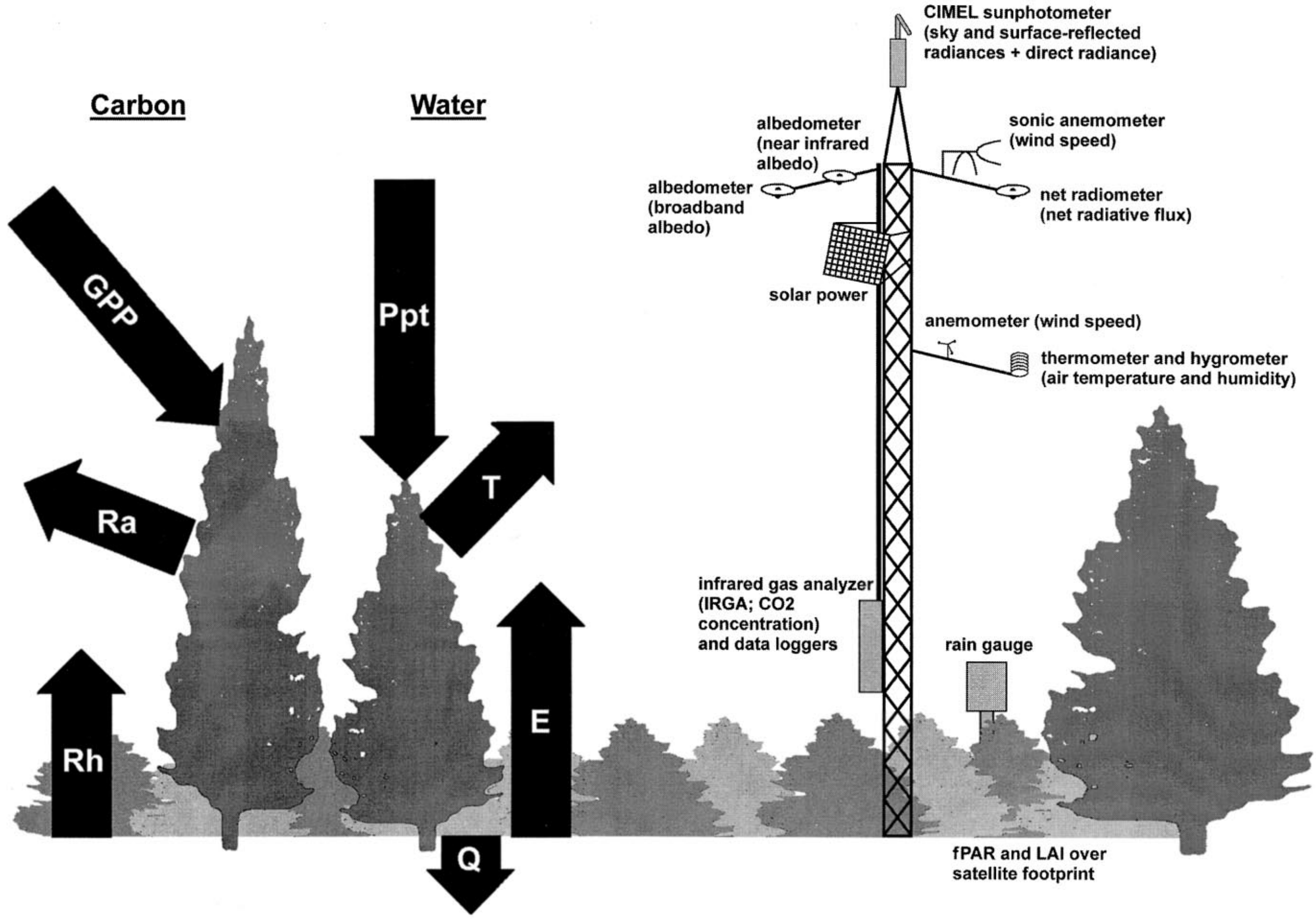

Figure 2. A generalized FLUXNET tower configuration diagram, showing instrument deployment and key carbon and water fluxes measured. Atmospheric optical measurements, automated surface spectral measurements, physiological process studies, flask sampling, and stable isotope sampling are all additions that can be accommodated into this framework to provide a more versatile monitoring system.

oxide and water vapor over 15 forest sites in the United Kingdom, France, Italy, Belgium, Germany, Sweden, Finland, Denmark, The Netherlands, and Iceland. A website is located at http://www.unitus.it/eflux/euro.html. In 1996, AmeriFlux was formed under the aegis of the DOE, NIGEC program, with additional support by NASA, and NOAA. The website is http://www.esd.ornl.gov/programs/NIGEC.

Eddy Covariance Principles

The eddy covariance method is a well-developed method for measuring trace gas flux densities between the biosphere and atmosphere (Baldocchi et al., 1988; Lenschow, 1995; Moncrieff et al., 1996). This method is derived from the conservation of mass and is most applicable for steady-state conditions over flat terrain with an extended tract of uniform vegetation. If these conditions are met, eddy covariance measurements made from a tower can be considered to be within the constant flux layer, and flux density measured several meters over the vegetation canopy is equal to the net amount of material entering and leaving the vegetation. Vertical flux densities of CO_2 and water vapor between the biosphere and the atmosphere are proportional to the mean covariance between vertical velocity and scalar fluctuations. This dependency requires the implementation of sensitive, accurate, and fast-responding anemometry, hygrometery, thermometry, and infrared spectrometry to measure the vertical and horizontal wind velocity, humidity, temperature, and CO_2 concentration.

Errors arise from atmospheric, surface, and instrumental origins, and they may be random, fully systematic and/or selective (Goulden et al., 1996). Most random errors are associated with violations of atmospheric stationarity and the consequences of intermittent turbulence. Instrument errors are systematic, caused by insufficient time response of a sensor, the spatial separation between a sensor and an anemometer, digital filtering of the time signal, aerodynamic flow distortion, calibration drift, loss of frequency via sampling over a finite space, and sensor noise (Moore, 1986; Moncrieff et al., 1996). The AmeriFlux, Euroflux, and FLUXNET programs are attempting to identify and minimize instrumental errors by circulating a set of reference instruments, to which all sites can be compared. Daily-averaged fluxes reduce the sampling errors associated with fluxes measured over 30–60 min intervals. Hence, daily integrals of net carbon flux can be accepted with a reasonable degree of confidence. Goulden et al. (1996) conclude that the long term precision of eddy covariance flux measurements is ±5–10% and the confidence interval about an annual estimate of net canopy CO_2 exchange is ±30 g C m^{-2} y^{-1}.

Implementation and Operation

A typical cost for purchasing instruments to make core measurements is on the order of $40–to $50k (US); this cost can double if spare sensors, data telemetry, and data archiving hardware are purchased. The cost of site infrastructure is extra and will vary according to the remoteness of the site (the need for a road and line-power), the height of the vegetation (whether or not a tall tower must be built), and the existence of other facilities. Recent advances in remote power generation and storage minimize the need and cost of bringing line power to a remote site. Advances in cellular telephone technology also allow access and query of a remote field station from home or the office. The requirement for on-site personnel is diminishing, as flux systems become more reliable and automated. At minimum, a team of two individuals are required to operate a flux system, and handle the day-to-day chores of calibration, instrument and computer maintenance, data archiving, and periodic site characterization (e.g., soil moisture and leaf area measurements).

Sites in an organized global flux network can also expect to attract additional activities. A synergism between flux and meteorological measurements and an array of other terrestrial science projects is likely. Terrestrial bioclimatology, remote sensing, atmospheric optical characterization, water resource, and nutritional biogeochemistry studies are examples of science that are being attracted to the flux network sites (Fig. 2).

Climate and Biome Distribution Requirements

Ideally, global terrestrial monitoring/validation sites should encompass the complete range of climate and biome type combinations. The current global array of flux towers is shown in Figure 3, mapped over the annual temperature/precipitation climate space of current global vegetation (Churkina and Running, 1998). It is clear that large regions, including several important biomes, remain underrepresented including hot desert and cold tundras, which is inevitable with an ad hoc volunteer global network (Table 1). Also, the correspondence between flux tower locations and permanent ecological field sites is low, illustrating the key role for modeling to spatially extrapolate results amongst sites. More sites are needed over intensive agricultural areas. Future planning should identify the climate/biome combinations of highest priority to improve global representativeness.

THE ATMOSPHERIC CO_2 FLASK NETWORK

Inverse Modeling of Carbon Sources and Sinks

The eddy flux tower studies are designed to aid understanding of processes that drive NEE at the ecosystem level, and for evaluation of ecosystem models used for regional and global integration. However, a top-down approach is also needed to test and validate the results of the model extrapolations to global and regional scales. Data from the global CO_2 mixing ratio and isotope ratio measurement network (NOAA/CMDL/Cooperative Air Sampling Network, website at http://www.cmdl.noaa.gov/ccg/), when interpreted within general circulation models, can provide constraints at least at this scale. The basic procedure in this approach is referred to as inverse modeling. It involves simulating the global 3-D atmospheric transport using a general circulation model and tracking the movement and interaction of air parcels having different CO_2 concentrations. Information on the spatial and temporal patterns in measured atmospheric CO_2 concentrations derived from flask samples is incorporated such that sources and sinks of carbon from the Earth's surface can be inferred.

Initially, flask sampling was primarily in well-mixed marine areas. Expansion of the monitoring networks over the last decade has improved the spatial resolution with which annual fluxes can be determined, so that currently fluxes are being estimated at continental scales (Fan et al., 1998). Sampling at continental sites reveals regional contrasts in seasonality of flux dynamics, and sampling at various heights on tall towers (500 m) identifies gradients of CO_2 in the boundary layer dynamics (Fig. 4; Bakwin et al., 1998). As sampling density is increased, it will be possible to use higher resolution transport models, such as mesoscale models, to deduce surface fluxes at finer spatial scales. Additional work is needed to develop and refine the transport models, and particular attention is required to develop parametrizations for simulation of the dynamics of the planetary boundary layer. It is important that the resulting estimates of NEE are entirely independent of the flux tower measurements, and nearly independent of the satellite data (satellite data define surface parameters used in the transport models).

Isotopic Sampling

The state of development of isotopic measurements (particularly in combination with CO_2 flux tower measurements), for better understanding the carbon cycle on local, regional, and global scales, was the topic of a workshop titled Biosphere–Atmosphere Stable Isotope Network (BASIN, Snowbird, Utah, 7–10 December 1997). A sum-

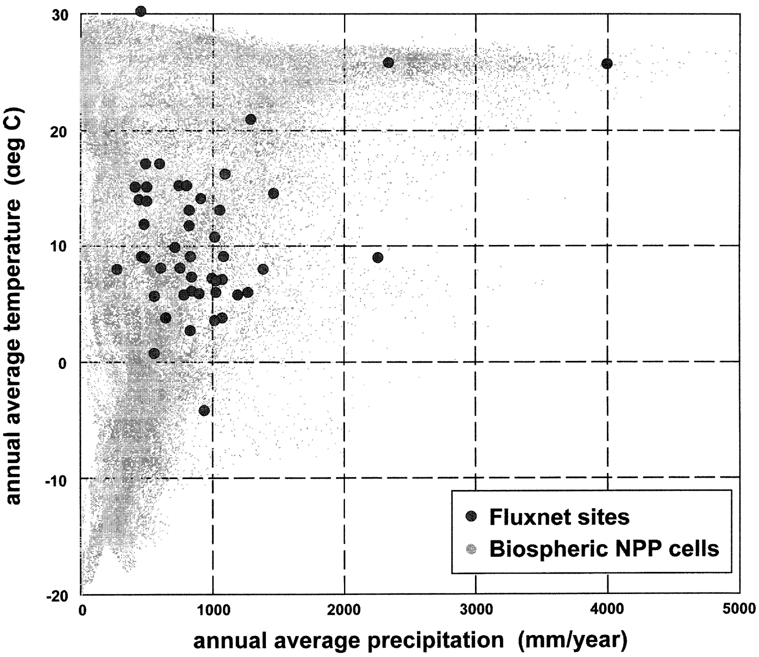

Figure 3. A two-dimensional climate diagram of the distribution of 1° global vegetation cells related to annual precipitation and temperature, suggesting the preferred climatic distribution of sites for complete biome sampling [regraphed from data in Churkina and Running (1998)]. The climates of the current FLUXNET sites as of early 1999 are superimposed.

mary can be found on the Web at http://gcte.org/basin.html. Isotopic data can be used to disaggregate component fluxes (e.g., photosynthesis and respiration, transpiration, and evaporation), and for regional and global scaling. Measurements of $d^{13}C$ in CO_2 can be used to partition net uptake between the oceans and the terrestrial biosphere, or, on a smaller spatial scale, between C_3 and C_4 vegetation. Recent advances in understanding the influence of vegetation (Farquhar et al., 1993) and soils (Tans, 1998) on the $^{18}O/^{16}O$ ratio of CO_2 have opened the possibility to use measurements of $d^{18}O$ to distinguish between photosynthetic and respiratory fluxes. Also, measurements of $^{18}O/^{16}O$ in H_2O could be used to distinguish between transpiration and evaporation from the soil. Recent work by Potosnak et al. (1998) indicates that it may be possible to use the flux tower measurements to assess the influence of local surface exchange, and hence compute regionally representative CO_2 mixing ratios from careful surface layer measurements. This is an exciting result because flux towers are located in continental areas currently underrepresented by the network for monitoring CO_2 mixing ratios, and could improve the accuracy of CO_2 mixing ratio measurements at the flux towers on the order of 0.2 ppm.

Table 1. Current Biome Distribution of the 80 Established FLUXNET Sites

Functional Type	*Percent*
Temperate conifer forest	22
Temperate broad-leaved forest	21
Semiarid woodland	16
Boreal conifer	7
Grassland	7
Crop	6
Alpine	6
Arctic	4
Tropical forest	3
Mixed forest	3
Boreal broad-leaved forest	1
Wetland	1

An alternative for regional flux scaling with good future potential is aircraft based mobile flux platforms (Crawford et al., 1996; Oechel et al., 1998). These light aircraft fly very close to the vegetated surface, often only 5–20 m above the ground, and ingest air samples that flow into a fast response infrared gas analyzer through a special nosecone sampler. Onboard aircraft velocity and micrometerological data are combined to compute fluxes of CO_2 and H_20 with about a 3 km^2 spatial resolution integrated across a multiple kilometer flight path.

VALIDATION OF EOS TERRESTRIAL VEGETATION PRODUCTS

Vegetation Measurements in the EOS/MODIS Grid

EOS will produce regular global vegetation products primarily from the MODIS sensor (Moderate Resolution Imaging Spectroradiometer) (Running et al., 1994; Justice et al., 1998). MODIS satellite products will be in a regular grid of square, 1 km^2 cells that do not exactly overlay a tower "footprint." The tower footprints vary in size (up to several km^2), shape, and orientation, depending on location, height above canopy, wind speed, and direction (Hollinger et al., 1994; Waring et al., 1995). In order to permit comparisons of tower-based NEE estimates and the satellite-based NPP estimates

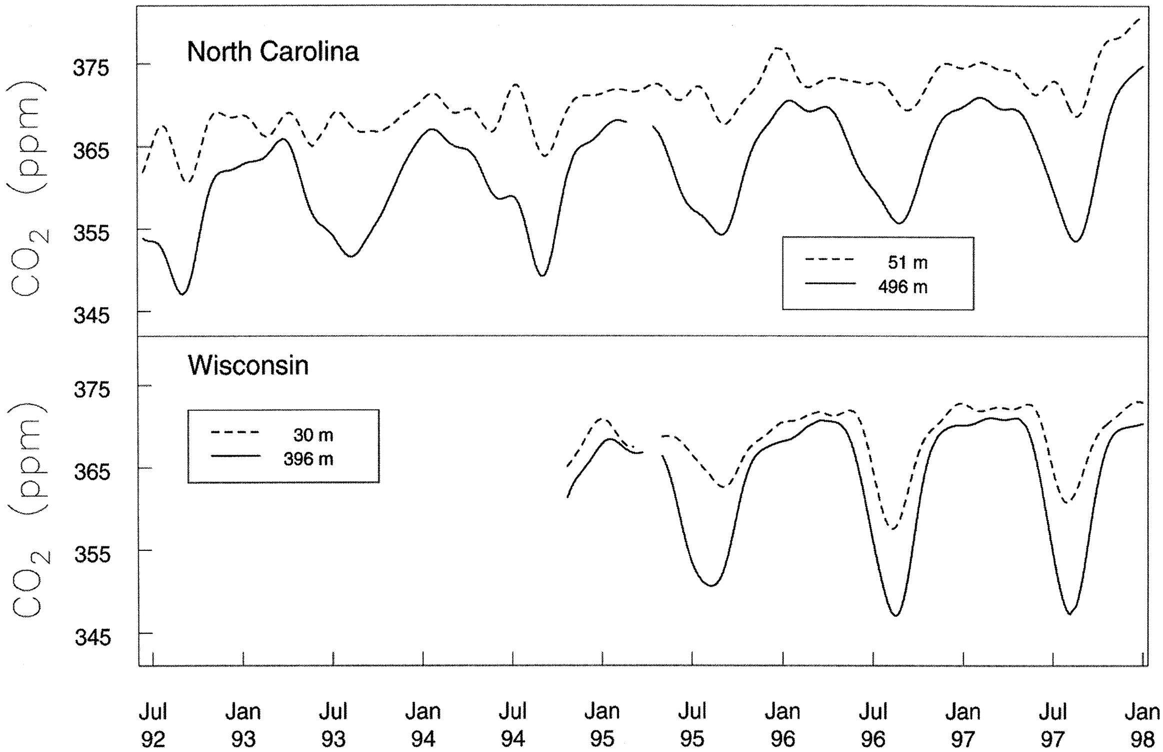

Figure 4. Multiyear trends in monthly atmospheric CO_2 measurements for two tall towers in contrasting climates of North Carolina and Wisconsin from the NOAA/CMDL flask monitoring network. Note the differential activity of CO_2 within the forest canopies at 30–50 m height dominated by biological dynamics compared to the midplanetary boundary layer at 400–500 m where atmospheric transport dominates. When coupled with atmospheric transport models, these data can be used to estimate CO_2 fluxes at regional scales as a "top-down" constraint on fluxtower data (Bakwin et al., 1998).

from the MODIS grid, certain transformations are needed (Fig. 5). A SVAT model that resolves component carbon balance processes of Eq. (1), and validated by local flux tower measurements over a grid of 10–100 km^2 around the tower, provides this scale transformation.

The most direct measurement of NPP for validation involves harvesting and weighing biomass production in a time sequence. The plot size here is considerably smaller than a tower footprint, for example, 1 m^2 for clipping in a grassland or 1 ha plots for tree coring and litterfall traps in forests. Multiple NPP measurements made in the 100 km^2 area surrounding a tower serves to extend the model validation over the local environmental gradients and variation in land use.

Quantifying Land Surface Heterogeneity for EOS Validation—BigFoot

Over a site consisting of homogenous vegetation cover and small environmental gradients, the scale inconsistencies between EOS/MODIS NPP estimates and ground-based validation measurements may be minimal. However, many important ecosystems are fairly complex in structure and topography, even over the relatively small area represented by a MODIS cell or a tower footprint. For example, much of the U.S. Pacific Northwest region is characterized by patches associated with forest clearcuts that are generally much smaller than 1 km on a side (Cohen et al., 1998). In the Lake States the choice of grain size up to 1 km greatly affects estimates of land surface occupied by aquatic versus terrestrial systems (Benson and MacKenzie, 1995). The tendency for the scale of human influence on ecosystem carbon flux to fall below the 1 km resolution was recognized during the design phase of the MODIS instrument (Townshend and Justice, 1988), and accounted in part for including channels at 250 m and 500 m in the visible and near-IR wavelengths.

The BigFoot project makes the link between purely satellite-based C flux estimates, tower fluxes and direct field measurements. The BigFoot website is at http://www.fsl.orst.edu/larse/bigfoot/. The goal is to develop three fine-grained surfaces (25 km^2) using a combination of Landsat Enhanced Thematic Mapper (ETM+), SVAT models, and field observations. These surfaces include the standard EOS products of land cover class, leaf area index (LAI), and NPP. BigFoot currently consists of a set of four sites (all are FLUXNET sites) spanning the climatic gradient from boreal to warm temperate, en-

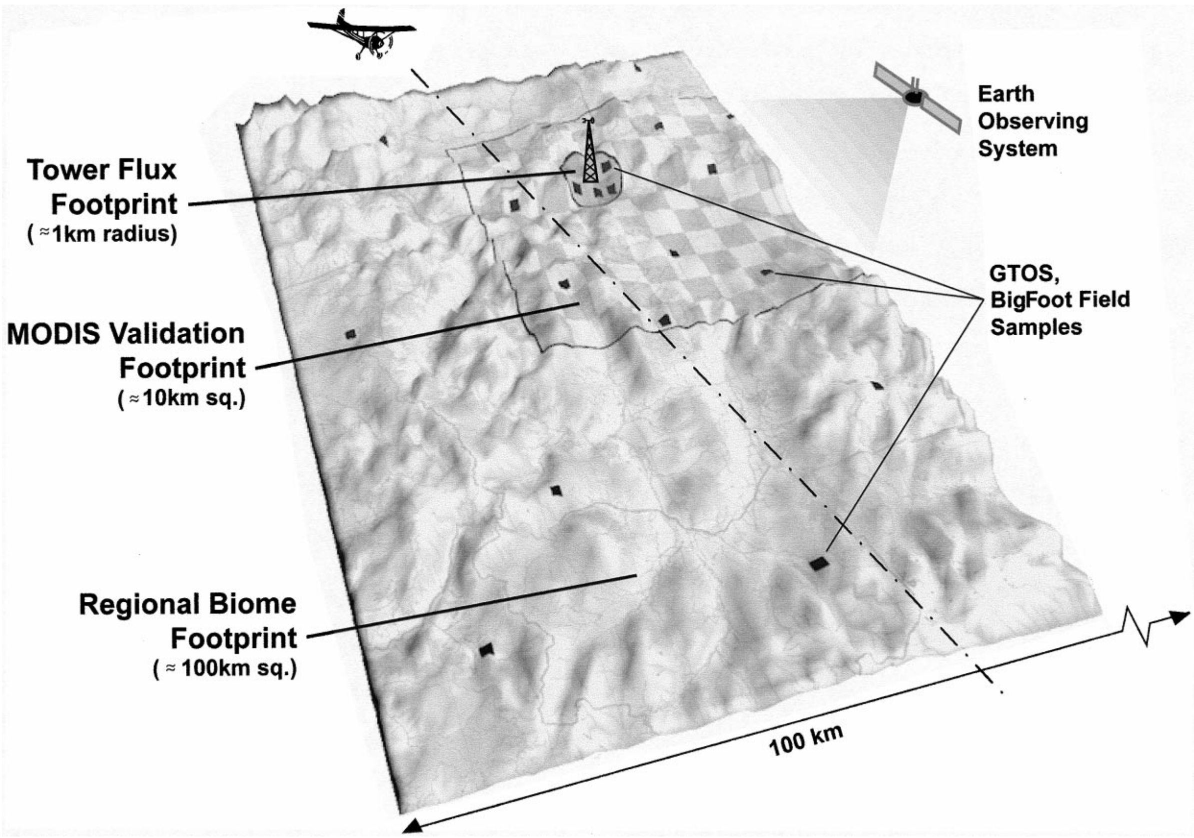

Figure 5. Illustration of the three spatial scales that must be considered for ecological scaling and validation. Measures of vegetation parameters (see Table 2) in the atmospheric footprint of the FLUXNET towers are required for SVAT models to simulate the NEE measured by the towers. Second, a larger area of minimum 3 km×3 km must be sampled to provide ground truth of MODIS LAI and NPP vegetation products. Third, the representativeness of the FLUXNET tower and MODIS sampling site to the larger biome/climate complex must be evaluated by cross biome sampling. Aircraft flux transects and atmospheric flask measurements can provide independent validation of regional flux calculations. Only after all of these scales of measurement are covalidated can comprehensive synthesis of ground data, ecosystem models, and satellite data be accomplished.

compassing several important biomes, and including a variety of land-use patterns. Additional sites will be added in the future, with highest priority being tropical forests, deserts, and arctic tundra, and this protocol is being adopted by the GTOS-NPP project (discussed in a later section) globally.

Land cover is an important variable for the purposes of the BigFoot scaling effort because physiological characteristics that influence carbon, nitrogen, and water vapor exchange between terrestrial ecosystems and the atmosphere differ among vegetation cover types (Landsberg and Gower, 1997). In addition, Thematic Mapper-based classifications are often able to resolve specific stages in local successional sequences (e.g., Cohen et al., 1995) and thus may indicate information about levels of coarse woody debris, an important input to SVAT models simulating heterotrophic respiration. Thus, SVAT models use land-cover type as a stratification factor (Reich et al., 1999, this issue). In BigFoot, land-cover classification will be accomplished using methods described by Thomlinson et al. (1999, this issue). Most importantly, these maps will consist of site-specific cover classes that are locally meaningful for ecological function and model parametrization.

LAI has also proved valuable in scaling efforts, and is an input to most existing SVAT models. LAI surfaces will be based on ETM+ imagery combined with field sampling (Gower et al., 1999, this issue) and will be developed using methods that minimize errors associated with the asymptotic relationship of commonly used spectral vegetation indices and LAI (Turner et al., 1999, this issue). Errors in the land cover and LAI data layers will be evaluated with independent field-collected data using the sampling protocols discussed by Thomlinson et al. (1999, this issue).

Following development of land cover and LAI surfaces, NPP grids will be developed for each BigFoot site using SVAT models (see the next section). These grids will be developed using the models in 2-dimensional mode in conjunction with the site-specific driver surfaces, land cover and LAI, and spatially distributed climatic drivers based on extrapolations from flux tower meteorological observations. Beside the daily time step validation of GPP and ET at BigFoot sites with flux towers, the BigFoot NPP surfaces will be carefully evaluated for error by reference to a gridded network of ground measurements of NPP, collected according to methods described by Gower et al. (1999, this issue). Assuming the errors in these NPP surfaces are acceptable, the fine-grained gridded surface over a 25 km^2 area can then be directly compared to NPP estimates derived from MODIS data over the same area. If the MODIS-based estimates do not satisfactorily agree with the BigFoot estimates, it will be critical to identify causal factors.

BigFoot will isolate and test three key factors—spatial resolution, land cover classification scheme, and light use efficiency factors—that may contribute to differences between EOS-based and BigFoot NPP estimates. To evaluate the role of spatial resolution, the BigFoot 25 m grids for input variables will be aggregated to resolutions of 250 m, 500 m, and 1000 m using a variety of standard and experimental algorithms. Model runs will then be made at each spatial resolution and comparisons of simulated NPP at the different resolutions (including 25 m) will be made with each other and with the EOS/MODIS 1 km NPP products. Results of these scaling exercises over the range of biomes and land use patterns included in BigFoot will test both SVAT models and satellite-based NPP algorithms.

SYSTEM INTEGRATION AND SCALING WITH MODELS

To transform basic tower flux and flask data and global remote sensing into an effective biospheric monitoring program, three steps are now required. *First*, SVAT models must be used at each tower site to compute the important system processes that cannot be directly measured, such as the component carbon fluxes of NEE. In order to operate the SVAT model, certain key site and vegetation characteristics must be measured to parametrize the model for the tower area (Table 2). *Second*, to provide a spatial frame of reference for the tower site, satellite-derived characterization of the surrounding vegetation is needed. The EOS/MODIS standard spatial resolution is 1 km, so as to provide adequate sample size, approximately a 10 m×10 km area needs to be efficiently sampled. *Third*, with validated MODIS vegetation products of landcover, LAI, and NPP, a larger region can now be evaluated to understand how the flux tower data represents the broader biome and region. This three-step scaling process, evaluating the tower footprint of (1 km^2, then the EOS/MODIS footprint of ≃100 km^2, and finally the regional biome footprint of thousands of square kilometers provide the scaling logic for global monitoring (Fig. 5).

SVAT Model Requirements for 1-D Flux Modeling

SVAT models have been designed with a wide array of system complexities (Fig. 6). For example, some models define each age class and branch whorl of leaves, while others use only simple LAI. Time resolutions of various models range from 1 h to monthly. The land surface models such as BATS and SiB in GCMs are effectively SVAT models despite being used at very coarse spatial grids (Dickinson, 1995). SVAT models of highest relevance to FLUXNET have time resolutions in the hourly–daily domain, treat canopy structure fairly explicitly, and resolve components of the carbon balance (photosynthesis, heterotrophic and autotrophic respiration, and allocation). Likewise, stand water balance components, (canopy interception, snowpack, soil water storage, evaporation, and transpiration) must be explicitly computed. All of the leading SVAT models incorporate some treatment of nutrient biogeochemistry interactions with carbon and water processes. However, given these requirements, there are still many available and appropriate SVAT models [see recent books by Landsberg and Gower (1997) and Waring and Running (1998)]. What is needed for a coordinated global program are some common protocols, of variables, units, timesteps, etc. that would allow cooperation and intercomparisons among groups using different SVAT models in their space/time scaling. The 1-D SVAT models require meteorological driving variables measured at the tower, the initializing biomass components of the vegetation, and certain soil physical and chemical properties. All SVAT models have somewhat different specific requirements, but the general list of inputs found in Table 2 covers most of them.

Relating NEE and NPP in the Flux Tower Footprint

Flux towers measure the net gain or loss of carbon over hourly to daily time scales (Fan et al., 1995; Baldocchi et al., 1996; Goulden et al., 1996; Frolking et al., 1996). Because SVAT models estimate photosynthesis, autotrophic, and heterotrophic respiration separately, they generate separate estimates of NEE and NPP. Besides comparisons of measured and modeled NEE and NPP, one specific output of these models is daily GPP (gross primary production or net photosynthesis). This modeled GPP can be compared directly to an estimate of GPP derived from tower data (daytime NEE minus estimated daytime ecosystem respiration) (Fig. 7). Diurnal evapotranspiration (ET) can also be directly compared to ET measured at the tower. Once a SVAT model is parametrized and validated over a daily time step at a tower site, it can be run to simulate NPP and ET for a full year. Using direct field measurements of NPP made at the tower sites, model estimates of annual NPP can also be validated. The SVAT models thus provide an essential link between NEE measurements by the tower, and

Table 2. The Suite of Measurements Collected at FLUXNET Sites and Needed for SVAT Modeling Activity

Variable	*Symbol*	*Unit*	*Frequency*	*Criticality*
Mass and energy flux densities				
CO_2	F_c	μmol m^{-2} s^{-1}	1–2 h^{-1}	Core
CO_2 storage		μmol m^{-2} s^{-1}	1–2 h^{-1}	Core
Latent heat (water vapor)	λE	W m^{-2}	1–2 h^{-1}	Core
Sensible heat	H	W m^{-2}	1–2 h^{-1}	Core
Soil heat conduction	G	W m^{-2}	1–2 h^{-1}	Core
Canopy heat storage	S	W m^{-2}	1–2 h^{-1}	Core
Momentum		kg m^{-1} s^{-2}	1–2 h^{-1}	Core
Dry deposition of N		kg ha^{-1} y^{-1}	Annual	Desired
Meteorology				
Global radiation	R_g	W m^{-2}	1–2 h^{-1}	Core
Net radiation	R_n	W m^{-2}	1–2 h^{-1}	Core
Photosynthetic photon flux density	Q_p	μmol m^{-2} s^{-1}	1–2 h^{-1}	Core
Diffuse radiation		μmol m^{-2} s^{-1} or W m^{-2}	1–2 h^{-1}	Desired
Air temperature	T_a	°C	1–2 h^{-1}	Core
Humidity			1–2 h^{-1}	Core
CO_2 concentration	$[CO_2]$	μmol mol^{-1}	1–2 h^{-1}	Core
Wind speed	U	m s^{-1}	1–2 h^{-1}	Core
Wind direction		deg	1–2 h^{-1}	Core
Precipitation			Daily	Core
Pressure	P	kPa	Hourly to daily	Desired
Canopy wetness			Hourly	Desired
Pollution (O_3, NO_2, NO, SO_2)		ppb	Hourly	Desired
Bole temperature	T_b	°C	1–2 h^{-1}	Core
Light transmission		μmol m^{-2} s^{-1}	1–2 h^{-1}	Desired
Soil characteristics				
Soil temperature profiles	T_s	°C	1–2 h^{-1}	Core
Soil moisture			Daily to weekly	Core
Bulk density			Once	Core
Soil texture			Once	Core
Root depth			Once	Core
CO_2 efflux		μmol m^{-2} s^{-1}	Hourly to seasonally	Core/desired
Litter decomposition			Annually	Core/desired
Litter chemistry (C, N, Lignin)			Annual	Desired
Soil (C, N)			Annual	Desired
Soil thermal conductivity			Once	Desired
Soil hydraulic conductivity			Once	Desired
Cation exchange capacity			Once	Desired
Vegetation characteristics				
Species composition			Once	Core
Above-ground biomass			Once	Core
Leaf area index			Seasonal to annual	Core
Canopy height	H	m	Seasonal to annual	Core
Albedo				
Aerodynamic roughness length	z_0	m	Once	Desired
Zero plane displacement	D	m	Once	Desired
Multispectral image			Annual	Desired
Above-ground growth increment			Annual	Core
Leaf N and C			Seasonal	Core
Specific leaf weight			Seasonal	Core
Ecophysiology				
Photosynthetic capacity	V_{cmax}, J_{max}	μmol m^{-2} s^{-1}	Weekly to seasonally	Desired
Tissue dark respiration		μmol m^{-2} s^{-1}	Weekly to seasonally	Desired
Predawn water potential	ψ	MPa	Weekly to seasonally	Desired
Stomatal conductance	g_s	mol m^{-2} s^{-1}	Weekly to seasonally	Desired
Tissue $^{13}C/^{12}C$				
Atmospheric $^{13}C/^{12}C$				
Sap flow		mol m^{-2} s^{-1}	Hourly	Desired

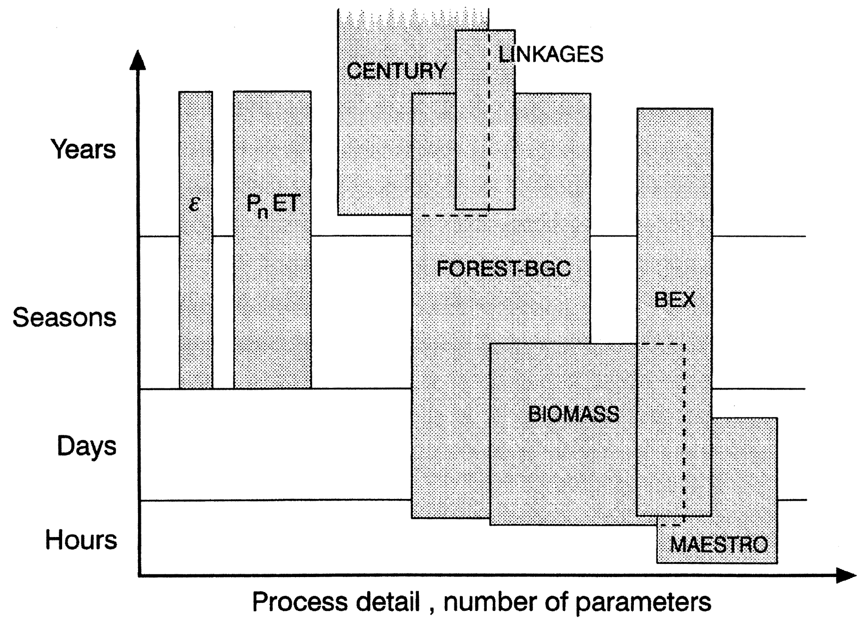

Figure 6. A general evaluation of the varying time scales and mechanistic complexity inherent in various current soil–vegetation–atmosphere–transfer (SVAT) models. The MODIS global NPP estimate is represented by the ε, a model of minimum process complexity. Models of higher process detail are required to validate and interpret the ε models, but cannot be run globally because of lack of data and computing limitations [redrawn from Landsberg and Gower (1997)].

NPP, the C-flux variable most relevant to the standard EOS NPP product.

Scaling to Regional Ecosystem Processes

In a large flat agricultural region with homogeneous topography, microclimate, soils, and crops, the tower footprint fluxes of NEE and ET may directly represent the entire regional flux activity. However, variable topography propagates variation in microclimate and soils, and human land use activity typically precludes homogeneity of land cover over hundreds of kilometers. Consequently, the ecosystem processes computed by a SVAT model with the local tower flux data must be put in the context of the region to be a meaningful biospheric monitor. Effectively this means extending the satellite-based analysis of the landscape planned by BigFoot methodology to an even broader region, and entails limited additional field sampling for validation of vegetation variables (Fig. 5). Mapping ecosystem process rates across thousands of square kilometers is then possible by executing the flux tower validated SVAT model across the landscape with satellite and ancillary data providing georeferenced representation of the landscape heterogeneity (Fig. 8).

Direct measurement of regional heterogeneity can now be accomplished with aircraft flux sampling. Oechel et al. (1998) measured a range of CO_2 flux of 0.1mg m^{-2} s^{-1}, and a range of latent energy flux of 100 W m^2 when flying a 100 km long transect of Alaskan tundra. Aircraft measured fluxes averaged 0.02 mg CO_2 m^{-2} s^{-1} less than tower-based fluxes; however, their measurement scales are different. Aircraft-based measurements will provide fluxes independent of SVAT model extrapolations, thus offering an important alternative for regional model validations.

Regional-scale validation may also be directly accomplished hydrologically. A SVAT model implemented regionally, and incorporating hydrologic flow routing, can reproduce stream discharge records. Accurate simulation of stream discharge tests the SVAT model calculations of snowmelt dynamics, soil water flow, and evapotranspiration (White et al., 1998).

Scaling Carbon and Water Fluxes to the Continental and Global Scales

Continental- to global-scale modeling of carbon and water fluxes has been limited to gridded surfaces of relatively coarse grain sizes. For example, Hunt et al. (1996) used grid cells of nearly 10^4 km^2 to simulate the influence of terrestrial sources and sinks of carbon on the seasonal oscillation in the atmospheric CO_2 concentration. Prince and Goward (1995) used a cell size of 64 km^2 in another global scale estimate of NPP. Field et al. (1998) used 1°×1° data for simulating terrestrial NPP using satellite data. Unfortunately, in areas with topographic and land-use heterogeneity, these resolutions can lead to significant errors associated with a loss of fine-scale vegetation patterns (Pierce and Running, 1995; VEMAP, 1995; Turner et al., 1996). Typically there has not been an effort to validate the global NPP estimates with a sample of site-level data, in part because of the mismatch in scales between model outputs and on-site measurements. The availability of MODIS satellite data will provide a strong impetus towards improved global NPP modeling.

Satellite remote sensing can be used to estimate NPP (see Fig. 1), but is not capable of validating model-generated surfaces for heterotrophic respiration (R_h) and hence NEE. In addition, process-based modeling of R_h

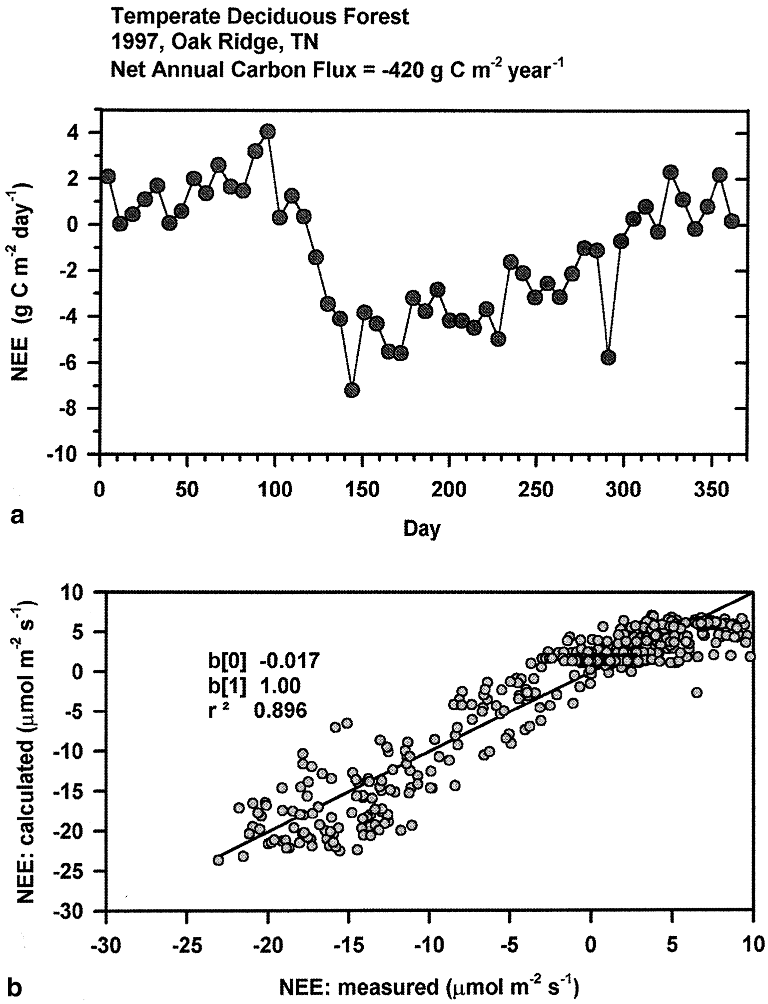

Figure 7. a) An example of FLUXNET carbon balance data, weekly net ecosystem exchange (NEE) for 1997 measured by an eddy covariance fluxtower for a temperate deciduous forest. b) The comparison of SVAT model simulation of NEE to observed NEE in 7a (Baldocchi, unpublished).

generally requires information on the size of the soil carbon pools. Global scale R_h algorithms often assume an equilibrium between R_h and NPP within a grid cell, and base estimated R_h on only the soil temperature and moisture status (e.g., Denning et al., 1996). However, sensitivity analyses have suggested that accounting for litter, soil organic matter, and coarse woody debris pool sizes will improve simulations of the seasonality of terrestrial C flux, and will be needed to capture the influence of interannual variability in climate on global R_h. Approaches to generating these important input surfaces for R_h models have included "spinning up" a carbon cycle model over a several thousand year period to establish pool sizes which are in rough equilibrium with the local climate and soil texture (VEMAP, see below), and recourse to maps of soil taxonomic units and related pedon databases (e.g., Kern et al., 1998). Flux tower sites, where SVAT model development includes the isolation of R_h from GPP and R_a, will provide an opportunity for validating the estimated pool sizes as well as the R_h flux. However, the next level of constraint on R_h flux estimates is apparently at the hemispheric or global scale, where inverse modeling based on spatial and temporal patterns in the atmospheric CO_2, O_2 and various isotopic variants indicate terrestrial sources and sinks of C (Tans et al., 1990; Keeling and Shertz, 1992).

GPPDI (web site at http://www-eosdis.ornl.gov/npp/npp_igbp.html) was launched following a meeting of ecosystem modelers organized under the IGBP-DIS (Data and Information System) at the Potsdam Institute for Climate Impact Research (PIK) in July 1994 (Prince et al., 1995). The Global Primary Production Data Initiative (GPPDI) is intended to provide quality data sets for validating global NPP models by identifying existing field data sets of primary production and associated environmental data. The program is using data sets for representative sites, and extrapolating or regionalizing the better data sets to grid cells sizes of up to 0.5°×0.5° with intelligent scaling logic similar to BigFoot. Emphasis is on variables needed to parameterize primary production models, including above and below ground NPP, standing crop, LAI, climate data, site data, and landscape variability. As of early 1999, over 900 published NPP data sets worldwide have been compiled, and 47 intensive sites

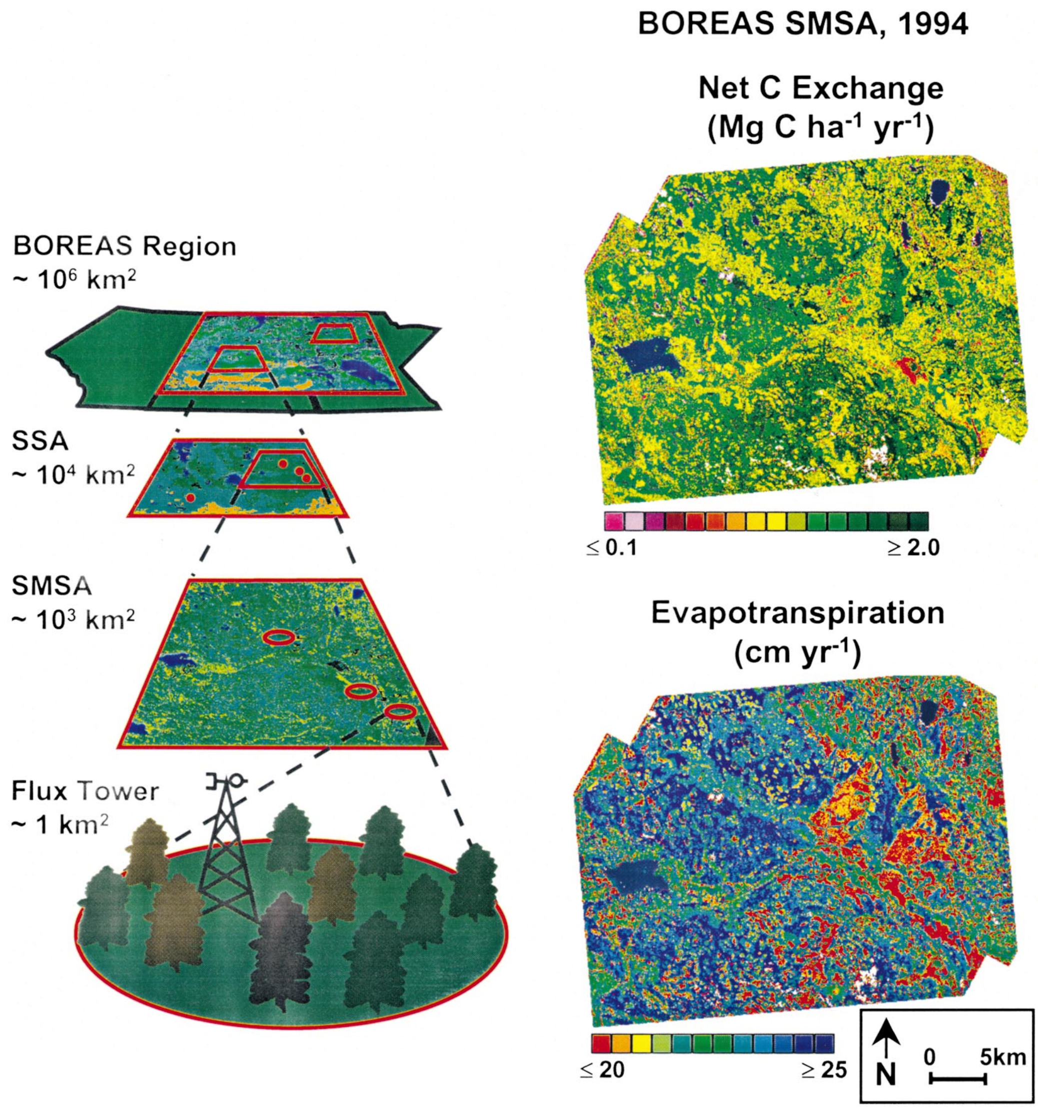

Figure 8. Ecosystem fluxes represented at regional scales by extrapolating FLUXNET data from three flux towers in the BOREAS project (Baldocchi et al., 1997; Black et al., 1996; Jarvis et al., 1997) with a SVAT model. These simulations for the BOREAS Southern Modeling Sub-area (SMSA) of 2000 km^2 used the BIOME-BGC SVAT model, spatially defined stand parameters with satellite data, integrated topography, soils, and microclimate data (Kimball et al., 1999). BIOME-BGC simulations were first validated with FLUXNET data from the three flux towers (Kimball et al., 1997a,b).

have been located to develop data sets with comprehensive ancillary data in this ongoing effort.

General circulation models also incorporate SVAT models such as BATS and SiB that represent the same canopy process dynamics as ecological SVAT models, but generalized to $\simeq$1–2° grid cells. Thus, the climate modeling community faces many of the same validation issues as the ecological SVAT modelers (Pielke et al., 1993; Dickinson, 1995), notably the gap between the ET estimate from a climate model grid cell ($\simeq 10^4$ km^2) and flux tower estimates of ET over the tower footprint. Methodologies such as the BigFoot project will be able to provide estimates of regional ET based on a SVAT model validated by flux tower ET measurements and extrapolated by EOS vegetation measurements.

Biospheric Model Intercomparisons

Another approach to assess accuracy of biospheric models when direct measurements are not possible is by global model intercomparisons. Major discrepancies in results among models draw attention to potential problem areas and data sets or weak process understanding. Two international biospheric model intercomparison activities are currently underway.

The ongoing IGBP sponsored 1995 Potsdam (PIK)-NPP model intercomparison can use FLUXNET derived

NPP estimates to test global NPP model estimates at locations sampled by the network. The website is at http://gaim.unh.edu/. The 1995 Potsdam NPP model intercomparison project was an international collaboration that produced single-year global NPP simulations (Cramer et al., 1999). There were large discrepancies amongst models of NPP in northern boreal forests and seasonally dry tropics. Over much of the global land surface, water availability most strongly influenced estimates of NPP; however, the interaction of water with other multiple limiting resources influenced simulated NPP in a non-predictable fashion (Churkina and Running, 1998).

VEMAP (http://www.cgd.ucar.edu:80/vemap/) is an ongoing multi-institutional, international effort addressing the response of terrestrial biogeography and biogeochemistry to environmental variability in climate and other drivers in both space and time domains. The objectives of VEMAP are the intercomparison of biogeochemistry models and vegetation distribution models (biogeography models) and determination of their sensitivity to changing climate, elevated atmospheric carbon dioxide concentrations, and other sources of altered forcing. The completed Phase 1 of the project was structured as a sensitivity analysis, with factorial combinations of climate (current and projected under doubled CO_2), atmospheric CO_2, and mapped and model-generated vegetation distributions. Maps of climate, climate change scenarios, soil properties, and potential natural vegetation were prepared as common boundary conditions and driving variables for the models (Kittel et al., 1995). As a consequence, differences in model results arose only from differences among model algorithms and their implementation rather than from differences in inputs (VEMAP, 1995). VEMAP is currently in the second phase of model intercomparison and analysis. The objectives of Phase 2 are to compare time-dependent ecological responses of biogeochemical and coupled biogeochemical–biogeographical models to historical and projected transient forcings across the conterminous United States. Because the VEMAP project has no validation component, interaction with FLUXNET and EOS can provide direct model validations. (Schimel et al., 1997)

INTERNATIONAL COORDINATION AND IMPLEMENTATION

Global validation and monitoring cannot be done without international cooperation that transcends any national

Figure 9. Potential synergism of international programs for validating terrestrial ecosystem variables at different space/time scales. Sites contributing to multiple programs have the highest synergism and efficiency. The programs depicted are: GPPDI=Global Primary Production Data Initiative, FLUXNET=the global network of eddy covariance flux towers, Atm FLASK=the global network of atmospheric flask sampling of NOAA/CMDL and C.D. Keeling and others, GTOS-NPP=a special project of the Global Terrestrial Observing System to measure net primary production of field sites worldwide, BigFoot=a study to establish scaling principles for sampling vegetation over large areas, EOS-MODIS=the Moderate Resolution Imaging Spectroradiometer on the Earth Observing System, the primary terrestrial observation sensor, VEMAP=the Vegetation/Ecosystem Modeling and Analysis Project, GAIM-NPP=the International Geosphere–Biosphere project in Global Analysis Integration and Modeling study of global NPP. See text for details of these projects.

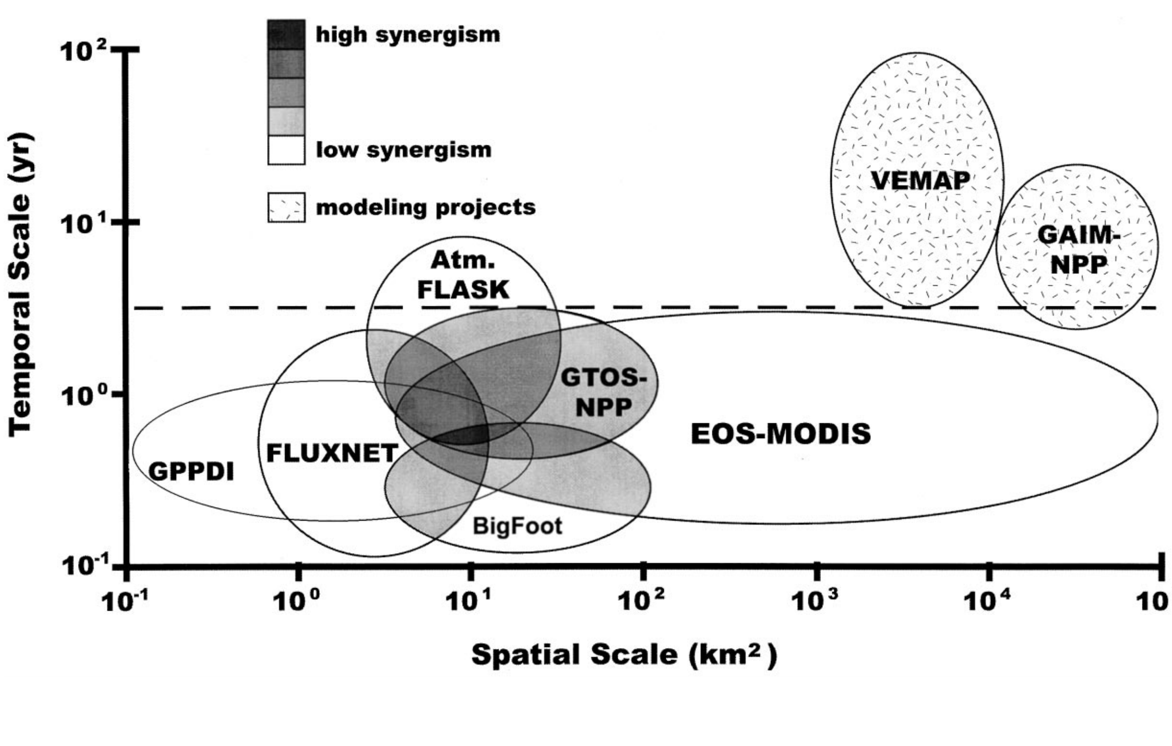

Table 3. The IGBP Terrestrial Transects Currently Identified

Region	*Contributing Transects in Initial Set*
Humid tropics	Tropical forest and its agricultural derivatives
	Amazon Basin/Mexico
	Central Africa/Miombo
	Southeast Asia/Thailand
Semiarid tropics	Forest–woodland–shrubland (the savannas)
	Savannas in the long term (West Africa)
	Kalahari (Southern Africa)
	Northern Australia Tropical Transect
Midlatitude semiarid	Forest–grassland–shrubland
	Great Plains (USA)
	Argentina
	North East China Transect
High latitudes	Boreal forest–tundra
	Alaska
	Boreal Forest Transect (Canada)
	Scandinavia
	Siberia

agency (Fig. 9). When planning global networks, it is essential to recognize that not all facilities have equal levels of scientific activity; however, all are needed to provide adequate global sampling. The Global Terrestrial Observing System (GTOS) and terrestrial components of the Global Climate Observing System GCOS have led in designing consistent international measurements for validation and monitoring work (GCOS, 1997). The strategy for implementing the plan is being developed in conjunction with the World Meteorological Organization (WMO) and the International GeosphereBiosphere Programme (IGBP). The plan will provide the necessary climate requirements for GTOS and the terrestrial requirements for GCOS. See http://www.wmo.ch/web/gcos/gcoshome.html.

Two core projects of IGBP have been instrumental in developing coordinated terrestrial systems. BAHC is the original project to suggest FLUXNET, and GCTE has led in designing the IGBP Terrestrial Transects. Both GAIM and IGAC now are supporting the continuing development of a global validation and monitoring system. Two internationally coordinated activities appear ready to implement FLUXNET and biospheric monitoring activities, the IGBP Transects, and the GTOS-NPP project.

The IGBP Terrestrial Transects, website at: http://gcte.org/LEMA-IGBP/LEMA-IGBP.html, are a set of integrated global change projects consisting of distributed observational studies and manipulative experiments, coupled with modeling and synthesis activities organized along existing gradients of underlying global change parameters, such as temperature, precipitation, and land use. The IGBP Terrestrial Transects consist of a set of study sites arranged along an underlying climatic gradient; of order 1000 km in length and wide enough to encompass the dimensions of remote sensing images. The initial set of IGBP Terrestrial Transects are located in four key regions, with three or four existing, planned or proposed transects contributing to the set in each region (Table 3).

The GTOS-NPP project (website at http://www.fao.org/GTOS/Home.htm) is being coordinated through the international U.S. Long Term Ecological Network (LTER) office, http://lternet.edu/ilter/. The goal of the GTOS-NPP project is to distribute the 1km EOS NPP and LAI products every 8 days to regional networks for evaluation, and after validation, translation of these standard products to regionally specific crop, range, and forest yield maps for land management applications. The project will also provide global validation points for land paramatrization in climate and carbon cycle models.

Databases and Archiving

Establishing data archiving centers is also important for international distribution and long-term availability of data. Several long-term databases are currently being compiled at the Oak Ridge, Tennessee, USA, DAAC facility. This data archive facility is home for data from FLUXNET, BigFoot, and GPPDI projects, all that have been summarized here (Olson et al., 1999, this issue). A centralized permanently funded data center such as the Oak Ridge DAAC insures continuity, consistency, and availability of data. However, the proliferation of Internet makes a more distributed array of data archive facilities equally useful if permanent commitments of support are made.

CONCLUSIONS

Each of the four monitoring scheme components described here—flux towers, flask sampling, ecosystem modeling, and EOS satellite data—are a source of consistency checks and validation to the other components. For example, if [as suggested in Fan et al. (1998)] the inverse modeling from the flask network suggested a C sink on the order of 1–2 Pg C y^{-1} in temperate North America, then results from a sample of flux tower sites in that region could confirm that specific sites were large carbon sinks, and results from a continental SVAT model initialized and driven by satellite data would support the presence of the carbon sink. The achievement of consistent agreement between the annual global NEE estimate from the flask network, and from a budget based on a spatially distributed SVAT model driven by satellite data, a spatially distributed model of marine sources and sinks driven by satellite data, and an inventory of anthropogenic sources, will be an important cross-check.

Accurate monitoring of global scale changes in the terrestrial biosphere are more critical than ever before. The Kyoto Protocol signals some of the huge socioeconomic and political decisions that lie ahead, and that will rely heavily on quantitatively accurate measures of global biospheric changes. The development of daily satellite earth observations, automated field measurement devices such as fluxtowers, powerful ecosystem models summarizing process interactions and high-speed computer networking makes a coordinated global biospheric monitoring program more attainable than ever before. All components of the program outlined in this article currently exist, and primarily need better coordination to become a global monitoring program. This article is designed to accelerate that coordination.

The primary sponsors of this work have been the U.S. Department of Energy, National Aeronautics and Space Administration Earth Science Enterprise, National Oceanic and Atmospheric Administration, and the National Science Foundation. International scientific organizations that have sponsored the evolution of this program include the International Geosphere–Biosphere Program, and the Global Climate and Terrestrial Observing Systems programs of the World Climate Research Program. An early version of this article was presented at the international FLUXNET meeting in Polson, Montana, USA on 3–5 June 1998.

REFERENCES

Bakwin, P. S., Tans, P. P., Hurst, D. F., and Zhao, C. (1998), Measurements of carbon dioxide on very tall towers: Results of the NOAA/CMDL program. *Tellus* 50B:401–415.

Baldocchi, D., Hicks, B. B., and Meyers, T. P. (1988), Measuring biosphere–atmosphere exchanges of biologically related gases with micrometeorological methods. *Ecology* 69:1331–1340.

Baldocchi, D., Valentini, R., Running, S., Oechel, W., and Dahlman, R. (1996), Strategies for measuring and modeling carbon dioxide and water vapour fluxes over terrestrial ecosystems. *Global Change Biol.* 2:159–168.

Baldocchi, D. D., Vogel, C. A., and Hall, B. (1997), Seasonal variation in carbon dioxide exchange rates above and below a boreal jack pine forest. *Agric. Forest Meteorol.* 83:147–170.

Benson, B. J., and MacKenzie, M. D. (1995), Effects of sensor spatial resolution on landscape structure parameters. *Landscape Ecol.* 10:113–120.

Black, T. A., den Hartog, G., Neumann, H. H., et al. (1996), Annual cycles of water vapor and carbon dioxide fluxes in and above a boreal aspen forest. *Global Change Biol.* 2:219–229.

Churkina, G., and Running, S. W. (1998), Contrasting climate controls on the estimated productivity of global terrestrial biomes. *Ecosystems* 1:206–215.

Ciais, P., Tans, P. P., Trolier, M., White, J. W. C., and Francey, R. J. (1995), A large northern hemisphere terrestrial CO_2 sink indicated by $^{13}C/^{12}C$ of atmospheric CO_2. *Science* 269:1098–1102.

Cohen, W. B., Fiorella, M., Gray, J., Helmer, E., and Anderson, K. (1998), An efficient and accurate method for mapping forest clearcuts in the Pacific Northwest using Landsat imagery. *Photogramm. Eng. Remote Sens.* 64:293–300.

Cohen, W. B., Spies, T. A., and Fiorella, M. (1995), Estimating the age and structure of forests in a multi-ownership landscape of western Oregon, U.S.A. *Int. J. Remote Sens.* 16:721–746.

Conway, T. J., Tans, P. P., Waterman, L. S., et al. (1994), Evidence for interannual variability of the carbon cycle from the National Oceanic and Atmospheric Administration/Climate Monitoring and Diagnostics Laboratory global air sampling network. *J. Geophys. Res.* 99:22,831–22,856.

Cramer, W., Kicklighter, D. W., Boned, A., et al., and Potsdam 95 (1999), Comparing global models of terrestrial net primary productivity (NPP): overview and key results. *Global Change Biol.* 5(Suppl. 1):1–15.

Crawford, T. L., Dobosy, R. J., McMillen, R. T., Vogel, C. A., and Hicks, B. B. (1996), Air–surface exchange measurement in heterogeneous regions: extending tower observations with spatial structure observed from small aircraft. *Global Change Biol.* 2:275–285.

Denning, A. S., Fung, I. Y., and Randall, D. (1995), Latitudinal gradient of atmospheric CO_2 due to seasonal exchange with land biota. *Nature* 376:240–243.

Dickinson, R. E. (1995), Land processes in climate models. *Remote Sensing Environ.* 51:27–38.

Denning, A. S., Collatz, G. J., Zhang, C., et al. (1996), Simulations of terrestrial carbon metabolism and atmospheric CO_2 in a general circulation model. Part 1: Surface carbon fluxes. *Tellus* 48B:521–542.

Fan, S.-M., Goulden, M., Munger, J., et al. (1995), Environmental controls on the photosynthesis and respiration of a boreal lichen woodland: a growing season of whole-ecosystem exchange measurements by eddy correlation. *Oecologia* 102:443–452.

Fan, S.-M., Gloor, M., Mahlman, J., et al. (1998), A large terrestrial carbon sink in North America implied by atmospheric and oceanic CO_2 data and models. *Science* 282:442–446.

Farquhar, G. D., Lloyd, J., Taylor, J. A., et al. (1993), Vegetation effects on the isotope composition of oxygen in atmospheric CO_2. *Nature* 363:439–443.

Field, C. B., Behrenfield, M. J., Randerson, J. T., and Falkowski, P. (1998), Primary production of the biosphere: Integrating terrestrial and oceanic components. *Science* 281:237–240.

Field, C. B., Randerson, J. T., and Malmstrom, C. M. (1995), Global net primary production: combining ecology and remote sensing. *Remote Sens. Environ.* 51:74–88.

Foley, J. A., Prentice, C., Namankutty, N., et al. (1996), An integrated biosphere model of land surface processes, terrestrial carbon balance and vegetation dynamics. *Global Biogeochem. Cycles* 10:603–628.

Frolking, S., Goulden, M. L., Wofsy, S. C., et al. (1996), Modeling temporal variability in the carbon balance of a spruce/moss boreal forest. *Global Change Biol.* 2:343–366.

Global Climate Observing System (GCOS) (1997), *GCOS/GTOS Plan for Terrestrial Climate-Related Observations, Version 2.0* GCOS-32, QMO/TD-No. 796, World Meteorological Organization, Geneva, Switzerland, 130 pp.

Goulden, M. L., Munger, J. W., Fan, S.-M., Daube, B. C., and Wofsy, S. C. (1996), Exchange of carbon dioxide by a deciduous forest: response to interannual climate variability. *Science* 271:1576–1578.

Gower, S. T., Kucharik, C. J., and Norman, J. M. (1999), Direct and indirect estimation of leaf area index, FAPAR and net primary production of terrestrial ecosystems. *Remote Sens. Environ.* 70:29–51.

Hollinger, D. Y., Kelliher, F. M., Byers, J. N., Hunt, J. E., McSeveny, T. M., and Weir, P. (1994), Carbon dioxide exchange between an undisturbed old-growth temperate forest and the atmosphere. *Ecology* 75:134–150.

Hunt, E. R., Jr., Piper, S. C., Nemani, R., Keeling, C. D., Otto, R. D., and Running, S. W. (1996), Global net carbon exchange and intra-annual atmospheric CO_2 concentrations predicted by an ecosystem process model and three-dimensional atmospheric transport model. *Global Biogeochem. Cycles* 10:431–456.

IGBP Terrestrial Carbon Working Group (1998), The terrestrial carbon cycle: implications for the Kyoto Protocol. *Science* 280:1393–1394.

Jarvis, P. G., Massheder, J. M., Hale, S. E., Moncreif, J. B., Payment, R., and Scott, S. L. (1997), Seasonal variation of carbon dioxide, water vapor and energy exchanges of a boreal black spruce forest. *J. Geophys. Res.* 102(D24) 28,953–28,966.

Justice, C. O., Vermote E., Townshend, J. R. G., et al. (1998), The Moderate Resolution Imaging Spectroradiometer (MODIS): land remote sensing for global change research. *IEEE Trans. Geosci. Remote Sens.* 36:1228–1249.

Keeling, C. D., Bacastow, R. B., Carter, A. F., et al. (1989), A three-dimensional model of atmospheric CO_2 transport based on observed winds, 1. Analysis of observational data. In *Aspects of Climate Variability in the Pacific and the Western Americas* (D. H. Peterson, Ed.), Geophys. Monogr., 55, American Geophysical Union, Washington, DC, 363 pp.

Keeling, C. D., Whorf, T. P., Wahlen, M., and v.d. Plicht, J. (1995), Interannual extremes in the rate of rise of atmospheric carbon dioxide since 1980. *Nature* 375:666–670.

Keeling, R. F., Piper, S. C., and Heimann, M. (1996), Global and hemispheric CO_2 sinks deduced from changes in atmospheric O_2 concentration. *Nature* 381:218–221.

Keeling, R. F., and Shertz, S. R. (1992), Seasonal and interannual variations in atmospheric oxygen and implications for the global carbon cycle. *Nature* 358:723–727.

Kern, J. S., Turner, D. P. and Dodson, R. F. (1998), Spatial patterns in soil organic carbon pool size in the Northwestern United States. In *Soil Processes and the Carbon Cycle* (R. Lal, J. M. Kimball, R. Follett, and B. A. Stewart, Eds.), CRC Press, Boca Raton, FL, pp 29–43.

Kimball, J. S., Thornton, P. E., White, M. A., and Running, S. W. (1997a), Simulating forest productivity and surface–atmosphere carbon exchange in the BOREAS study region. *Tree Physiol.* 17:589–599.

Kimball, J. S., White, M. A., and Running, S. W. (1997b), BIOME-BGC simulations of stand hydrologic processes for BOREAS. *J. Geophys. Res.* 102(D24):29,043–29,051.

Kimball, J. S. Running, S. W., and Saatchi, S. S. (1999), Sensitivity of boreal forest regional water flux and net primary production simulations to sub–grid scale landcover complexity. *J. Geophys. Res.*, in press.

Kittel, T. G. F, Rosenbloom, N. A., Painter, T. H., Schimel, D. S., and VEMAP Modeling Participants (1995), The VEMAP integrated database for modeling United States ecosystem/vegetation sensitivity to climate change. *J. Biogeogr.* 22 (4–5):857–862.

Landsberg, J. J., and Gower, S. T. (1997), *Applications of Physiological Ecology to Forest Management*, Physiological Ecology Series, Academic, San Diego, CA.

Lenschow, D. H. (1995), Micrometeorological techniques for measuring biosphere–atmosphere trace gas exchange. In *Trace Gases in Ecology* (P. Matson and B. Harris, Eds.) Blackwell Science Ltd., Oxford, pp. 126–163.

Melillo, J. M., McGuire, A. D., Kicklighter, A. D., Moore, B., III, Vorosmarty, C. J., and Schloss, A. L. (1993), Global climate change and terrestrial net primary production. *Nature* 363:234–240.

Moncrieff, J. B., Malhi, Y., and Leuning, R. (1996), The propagation of errors in long-term measurements of land–atmosphere fluxes of carbon and water. *Global Change Biol.* 2:231–240.

Moore, C. J. (1986), Frequency response corrections for eddy correlation systems. *Boundary Layer Meteorol.* 37:17–35.

Myneni, R. B., Keeling, C. D., Tucker, C. J., Asrar, G., and Nemani, R. R. (1997a), Increased plant growth in the northern high latitudes from 1981–1991. *Nature* 386:698–702.

Myneni, R. B., Nemani, R. R., and Running, S. W. (1997b), Estimation of global leaf area index and absorbed par using radiative transfer models. *IEEE Trans. Geosci. Remote Sens.* 35:1380–1393.

Oechel, W. C., Vourlitis, G. L., Brooks, S., Crawford, T. L., and Dumas, E. (1998), Intercomparison among chamber, tower, and aircraft net CO_2 and energy fluxes measured during the Arctic System Science Land–atmosphere–Ice Interactions (ARCSS-LAII) flux study. *J. Geophys. Res.* 103 (D22) 28,993–29,003.

Olson, R. J., Biggs, J. M., Porter, J. H., Mah, G. R., and Stafford, S. G. (1999), Managing data from multiple disciplines, scales and sites to support synthesis and modeling. *Remote Sens. Environ.* 70:99–107.

Pielke, R. A., Schimel, D. S., Lee, T. J., Kittel, T. G. F., and Zeng, X. (1993), Atmosphere–terrestrial ecosystem interactions: implications for coupled modeling. *Ecol. Model.* 67: 5–18.

Pierce, L. L., and Running, S. W. (1995), The effects of aggregating sub-grid land surface variation on large-scale estimates of net primary production. *Landscape Ecol.* 10: 239–253.

Potosnak, M. J., Wofsy, S. C., Denning, A. S., Conway, T. J., Novelli, P. C., and Barnes, D. H. (1998), Influence of biotic exchange and combustion sources on atmospheric CO_2 concentrations in New England from observations at a forest flux tower. *J. Geophys. Res.*, in press.

Prince, S. D. and Goward, S. T. (1995), Global primary production: a remote sensing approach. *J. Biogeogr.* 22: 815–835.

Prince, S. D., Olson, R. J., Dedieu, G., Esser, G., and Cramer, W. (1995), Global Primary Production Data Initiative Project description, IGBP-DIS Working Article No. 12, IGBP-DIS, Toulouse, France.

Randerson, J. T., Thompson, M. V., Conway, T. J., Fung, I. Y., and Field, C. B. (1997), The contribution of terrestrial sources and sinks to trends in the seasonal cycle of atmospheric carbon dioxide. *Global Biogeochem. Cycles* 11: 535–560.

Reich, P. B., Turner, D., and Bolstad, P. (1999), An approach to spatially-distributed modeling of net primary production (NPP) at the landscape scale and its application in validating EOS NPP products. *Remote Sens. Environ.* 70:69–81.

Ruimy, A., Saugier, B., and Dedieu, G. (1994), Methodology for the estimation of terrestrial net primary production from remotely sensed data. *J. Geophys. Res.* 99:5263–5283.

Running, S. W. (1998), A blueprint for improved global change monitoring of the terrestrial biosphere. *NASA Earth Obs.* 10(1):8–11.

Running, S. W., Justice, C. O., Salmonson, V., et al. (1994), Terrestrial remote sensing science and algorithms planned for EOS/MODIS. *Int. J. Remote Sens.* 15: 3587–3620.

Schimel, D. S. (1998), The carbon equation. *Nature* 393:208–209.

Schimel, D. S., VEMAP Participants, and Braswell, B. H. (1997), Continental scale variability in ecosystem processes: Models, data, and the role of disturbance. *Ecol. Monogr.* 67:251–271.

Tans, P. P. (1998), Oxygen isotopic equilibrium between carbon dioxide and water in soils. *Tellus* 50:163–178.

Tans, P. P., Bakwin, P. S., and Guenther, D. W. (1996), A feasible global carbon cycle observing system: a plan to decipher today's carbon cycle based on observations. *Global Change Biol.* 2:309–318.

Tans, P. P., Fung, I. Y., and Takahashi, T. (1990), Observational constraints on the global atmospheric CO_2 budget. *Science* 247:1431–1438.

Thomlinson, J. R., Bolstad, P. V., and Cohen, W. B. (1999), Coordinating methodologies for scaling landcover classifications from site-specific to global: steps toward validating global map products. *Remote Sens. Environ.* 70:16–28.

Townshend, J. R. C., and Justice, C. O. (1988), Selecting the spatial resolution of satellite sensors required for global monitoring of land transformations. *Int. J. Remote Sens.* 9:187–236.

Turner, D. P., Cohen, W. B., Kennedy, R. E., Fassnacht, K. S., and Briggs, J. M. (1999), Relationships between leaf area index and Landsat TM spectral vegetation indices across three temperate zone sites. *Remote Sens. Environ.* 70:52–68.

Turner, D. P., Dodson, R. D., and Marks, D. (1996), Comparison of alternative spatial resolutions in the application of a spatially distributed biogeochemical model over complex terrain. *Ecol. Model.* 90:53–67.

VEMAP (1995), Vegetation/Ecosystem Modeling and Analysis Project: comparing biogeography and biogeochemistry models in a continental-scale study of terrestrial ecosystem responses to climate change and CO_2 doubling. *Global Biogeochem. Cycling* 9:407–437.

Waring, R. H., and Running, S. W. (1998), *Forest Ecosystems: Analysis at Multiple Scales*, 2nd ed., Academic, San Diego, 370 pp.

Waring, R. H., Law, B. E., Goulden, M. L., et al. (1995), Scaling gross ecosystem production at Harvard Forest with remote sensing: a comparison of estimates from a constrained quantum-use efficiency model and eddy correlation. *Plant Cell Environ.* 18:1201–1213.

White, J. D., Running, S. W., Thornton, P. E., et al. (1998), Assessing simulated ecosystem processes for climate variability at Glacier National Park, USA. *Ecol. Appl.* 8:805–823.

Appendix: List of Acronyms

BAHC	Biospheric Aspects of the Hydrologic Cycle (IGBP)
BOREAS	Boreal Ecosystem Atmosphere Study
DAAC	Distributed Active Archive Center
EOS	Earth Observing System
ET	Evapotranspiration
ETM+	Enhanced Thematic Mapper
FPAR	Fraction photosynthetically active radiation
GAIM	Global Analysis and Modeling Project (IGBP)
GCM	General circulation model
GCOS	Global Climate Observing System (WMO)
GTOS	Global Terrestrial Observing System (WMO)
GCTE	Global Change Terrestrial Ecosystems (IGBP)
GPP	Gross Primary Production
GPPDI	Global Primary Production Data Initiative (IGBP)
IGAC	International Global Atmospheric Chemistry (IGBP)
IGBP	International Geosphere–Biosphere Program
IGBP-DIS	IGBP Data Information System
ILTER	International Long Term Ecological Research
LAI	Leaf area index
LTER	Long Term Ecological Research
MODIS	Moderate Resolution Imaging Spectroradiometer
NEE	Net ecosystem exchange
NPP	Net primary production
SVAT	Soil–Vegetation–Atmosphere transfer model
TOPC	Terrestrial Observing Panel for Climate (WMO)
VEMAP	Vegetation/Ecosystem Modeling and Analysis Program